Charles University in Prague

2nd Faculty of Medicine

Field of study: Medical Biophysics

Mgr. Andrea Míčková

Biodegradable Nanofibers for Tissue Engineering and Controlled Drug Delivery

Biodegradabilní nanovlákna pro tkáňové inženýrství a řízené dodávání léčiv

PhD Thesis

Supervisor: prof. RNDr. Evžen Amler, CSc.

Prague, 2015

Statement of originality:

I hereby declare that this thesis and the work reported herein was composed by and originated entirely from me. This thesis has not been submitted for any degree or other purposes. Information derived from the published and unpublished work of others has been acknowledged in the text and references are given in the list of sources.

I agree with prolonged accumulation of an electronic version of my work in the Theses.cz interuniversity database system project for the purposes of systematic checks on similarities among theses.

Prague, 31.03.2015

Andrea Míčková

Identifikační záznam:

Míčková, Andrea. *Biodegradabilní nanovlákna pro tkáňové inženýrství a řízené dodávání léčiv. [Biodegradable Nanofibers for Tissue Engineering and Controlled Drug Delivery]*. Praha, 2015. Počet stran 161, počet příloh 4. Disertační práce (Ph.D.). Univerzita Karlova v Praze, 2. Lékařská fakulta, Ústav biofyziky. Vedoucí práce Amler, Evžen.

Key words: Functionalization, Blend Electrospinning, Coaxial Electrospinning, Controlled Drug Delivery, Tissue Engineering, Liposomes, Platelets, α-granules.

Klíčová slova: Funkcionalizace, Směsné elektrostatické zvlákňování, Koaxiální elektrostatické zvlákňování, Řízené dodávání bioaktivních látek, Tkáňové inženýrství, Liposomy, Trombocyty, α-granule.

First of all, I would like to express my gratitude to my supervisor, prof. RNDr. Evžen Amler, CSc., for his kind and valuable advice, and for many suggestions concerning my experimental work and the writing of this manuscript.

I appreciate the kind help of my colleagues from the Institute of Experimental Medicine of the Academy of Sciences of the Czech Republic. I am also grateful to prof. RNDr. David Lukáš, CSc. and his research team from the Department of Nonwovens and Nanofibrous Materials, Technical University of Liberec, for their help and valuable advice on the preparation of nanofibers by electrospinning techniques. Mr. Robin Healey from the Czech Technical University in Prague is gratefully acknowledged for his language revision of the thesis.

I owe a great debt of gratitude to my family - especially to Erik and to grandpa - and to friends for their support throughout my studies.

List of Abbreviations

ACI	Autologous Chondrocyte Implantation
ANTS	8-Aminonaphthalene-1,3,6-trisulfonic acid
BrdU	5-bromo-2′’-deoxyuridine
CPP	Critical packing parameter
DiOC6	3,3´-diethyloxacarbocyanine iodide
DPX	*p*-xylene-bis-pyridinium bromide
dsDNA	double stranded Deoxyribonucleic acid
ECM	Extracellular matrix
EGF	Epidermal growth factor
ELISA	Enzyme-linked immunosorbent assay
ESC	Embryonic stem cells
FBS	Fetal bovine serum
FDA	Food and Drug Administration
FESEM	Field emission scanning electron microscopy
FGF	Fibroblast growth factor
FGF	Fibroblast growth factor
FITC	Fluorescein isothiocyanate
GF	Growth factor
HRP	Horseradish peroxidase
IGF	Insulin-like growth factor
LUV	Large unilamellar vesicles
MEM	Minimum essential media
MLV	Multilamellar vesicles
MPS	Mononuclear phagocyte system
MSCs	Mesenchymal stem cells

MTS	3-(4,5-dimethylthiazol-2-yl)-5-(3-carboxymethoxyphenyl)-2-(4-sulfophenyl)-2H-tetrazolium)
MTT	3-(4,5-Dimethylthiazol-2-yl)-2,5-Diphenyltetrazolium Bromide
PBS	Phosphate-buffered saline
PC	Phosphatidylcholine
PCL	Poly-ε-caprolactone
PDGF	Platelet-derived growth factor
PEG	Polyethylene glycol
PEO	Polyethylene oxide
PI	Propidium iodide
PS	Phosphatidylserine
PVA	Polyvinyl alcohol
PVA/PCL	Polyvinyl alcohol/Polycaprolactone
RPR	Platelet-rich plasma
SEM	Scanning electron microscopy
SUV	Small unilamellar vesicles
TBS	Tris-buffered saline
TGF-β	Transforming growth factor-beta
VEGF	Vascular endothelial growth factor
α-granule	Alpha granules

Contents

1 Indroduction

Regenerative medicine is one of the most dynamically developing medical fields, and its main goal is to promote tissue repair. One of the key issues in tissue engineering is the material design of scaffolds. Nanofibers formed by electrospinning have been shown to mimic the structure and the biological function of the extracellular matrix. Electrospun nanofibers have a small diameter that closely matches the size scale of the extracellular matrix, and the high surface area-to-volume ratio of nanofibers is ideal for cell attachment, proliferation and differentiation (Yarin et al. 2001). These unique properties of electrospun nanofibers make them suitable for various tissue engineering applications.

In addition to serving as scaffolds, nanofibrous meshes can be designed to serve as delivery vehicles for bioactive factors (Dahlin et al. 2011). The main considerations for the development of successful delivery systems for tissue engineering are the bioactivity of the biomolecules incorporated within the scaffolds and the controlled release of these biomolecules according to the time frame of tissue regeneration (Ji et al. 2011).

1.1 Electrospinning

In recent years, electrospinning has gained much attention as a highly efficient fiber-forming nanotechnology process that enables the creation of submicrometer fibers drawn from polymer solutions and melts (Cipitria et al. 2011; Garg and Bowlin 2011). The earliest theoretical work related to electrospinning phenomena was written in the 19th century by Lord Rayleigh (Rayleigh 1882). The principle of needle electrospinning originated through the work of Zeleny, who designed an apparatus for studying electrical discharges from liquid points (Zeleny 1914). The process of electrospinning was patented in 1934 by Formhals, who

outlined an experimental setup for the production of polymer filaments using electrostatic force (Formhals 1934). A theoretical investigation in the area of electrospinning was made by Taylor, who followed Zeleny's works (Zeleny 1914; Zeleny 1917) and formulated instability criteria for spherical drops of liquid when subjected to an external electrostatic field (Taylor 1964). Nowadays, a unique needleless electrospinning technology, Nanospider^{TM}, based on the patent of Jirsak et al. (2005), from the Technical University of Liberec, has been developed by Elmarco, a Czech company based in Liberec (Jirsak et al. 2005). Research in electrospinning started gaining popularity, especially after Doshi and Reneker spun various kinds of polymers to characterize their properties (Doshi and Reneker 1995). Since then, there have been many theoretical developments of the driving mechanism of the electrospinning process (Feng 2002; Lukas et al. 2008b; Reznik et al. 2004; Theron et al. 2005).

1.1.1 Principle of electrospinning

The basic configuration required for the process of electrospinning is a high-voltage source, a capillary tube with a spinneret, a metering pump that continuously supplies the polymer solution, a polymer and a collector (Figure 1.1). The principle of electrospinning is based on the application of strong electric fields either to polymer solutions or to melts. A charge is induced in the polymer, and charge repulsion occurs in the solution. Above a certain critical value of the applied electric field strength, the polymer liquid surface starts to self-organize on a mesoscopic scale due to the "fastest forming instability" mechanism. This instability is represented by the fastest growing stationary capillary wave with "Taylor cones" and electrospinning jets originating from the wave crests. As the jets move, the solvent evaporates and ultrafine fibers are produced on the collector (Lukas et al. 2009).

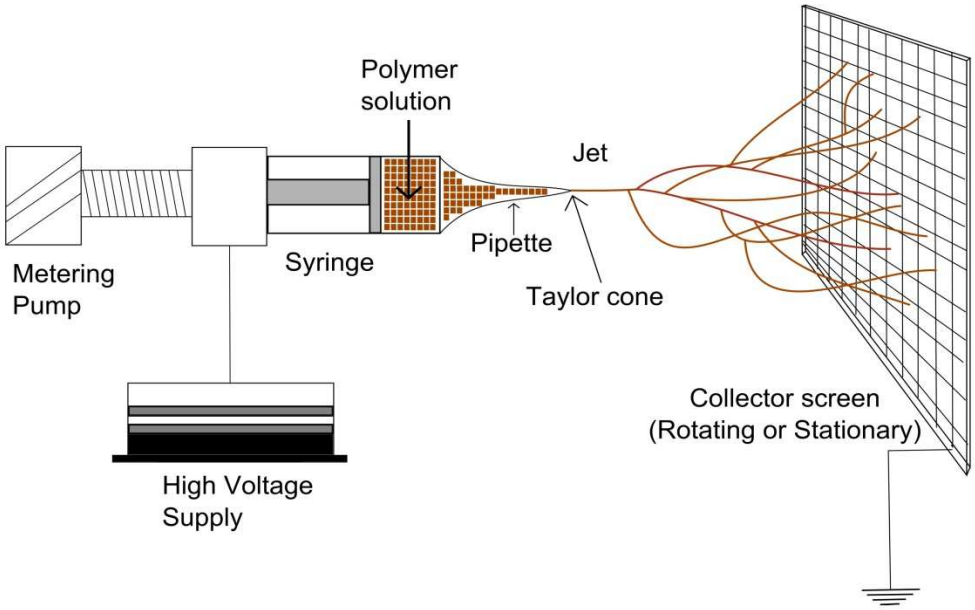

Figure 1.1 Schematic diagram of an electrospinning setup
*Adapted from Lukas D. et al., 2008 [Nonwoven Fabrics] (*Principles of Electrospinning, Lukas D., Sarkar A., Chaloupek J, (Chapter submitted), Nonwoven Fabrics, Edited by V. K. Kothari, IAFL Publications, New Delhi, India (Lukas et al. 2008a).

1.1.2 Working parameters and their effect on the electrospinning process

Solution parameters (e.g. concentration, molecular weight, viscosity, surface tension and conductivity/surface charge density), processing parameters (e.g. voltage, flow rate, distance between the collector and the tip of the syringe) and ambient parameters (e.g. humidity, temperature) have strong influence on the conversion of polymer solutions into nanofibers during the electrospinning process (Li and Wang 2013). Electrospun fibers with desired morphologies and diameters can be produced by modulating these parameters (Teo et al. 2011).

1.1.2.1 Solution parameters

The concentration of the polymer solution is one of the most effective parameters for controlling the structural morphology of electrospun nanofibers, e.g. when the concentration is very low, electrospraying occurs instead of electrospinning, resulting in the formation of

polymeric micro(nano)particles (Deitzel et al. 2001). When the concentration is increased, smooth fibers are obtained. However, if the concentration is very high, micro-ribbons are formed (Eda and Shivkumar 2007). Very high molecular weight of the polymer also favors the formation of micro-ribbons, even if the polymer concentration is low (Zhao et al. 2005). Surface tension, as a function of solvent composition, also plays an important role in the electrospinning process. Beaded fibers can be converted into smooth fibers by reducing the surface tension of a solution with a fixed concentration (Yang et al. 2004). The viscosity of the solution is the critical parameter for determining the fiber morphology. It has been confirmed that low viscosity solutions are unsuitable for the production of smooth and continuous fibers, while high viscosity causes hard ejection of jets from the solution (Sukigara et al. 2003). It is also very important to remember that viscosity, polymer concentration and polymeric molecular weight are related to each other (Li and Wang 2013). The conductivity of the solution is determined mainly by the type of polymer, the salt and the type of solvent. Published data indicates that increasing the conductivity of the solution leads to the formation of thinner fibers (Huang et al. 2006a).

1.1.2.2 Processing parameters

The voltage that is applied is another crucial factor in the process of electrospinning, due to its direct influence on the fluid flow dynamics. An increase in applied voltage has been found to affect the structural morphology of nanofibers (Jacobs et al. 2010). Some groups have observed that higher voltages facilitate the formation of bead fibers with a thick diameter (Deitzel et al. 2001; Rodoplu and Mutlu 2012). Thus, the level of influence on the fiber diameter is obvious, but the level of significance depends on the polymer concentration and on the distance between the tip and the collector (Yoerdem et al. 2008). It has also been confirmed that the effect of decreasing the tip-collector distance is almost the same as the effect of increasing the voltage (Homayoni et al. 2009). Greater distance may enhance the

evaporation of the solvent, leading to the formation of thinner fibers. A short distance between the tip and the collector could cause the formation of wet fibers with a flattened cross-section (Chowdhury and Stylios 2010). Flow rate is another important processing parameter. If the flow rate is too high, thicker fibers with higher occurrence of beads are formed, due to the short drying time prior to reaching the collector, and low stretching forces (Li and Wang 2013).

1.1.2.3 Ambient parameters

Several studies have examined the effect of ambient parameters on the electrospinning process. Reneker and Chun performed the electrospinning process under a vacuum in order to obtain higher electric fields for the production of large diameter fibers and yarns (Reneker and Chun 1996). Mituppatham et al. (2004) observed thinner electrospun polyamide-6 fibers at 60°C compared to fibers prepared by electrospinning below 30°C. They attributed the formation of thinner fibers to the decrease in the viscosity of the polymer solution at a higher temeparture (Mit-uppatham et al. 2004). The influence of humidity on the surface morphologies of the polystyrene fibers was observed by Casper et.al (2004). Their experiment showed that at 31–38% of humidity, pores started to form on the fiber surface, and increasing the humidity further to 60–72% led to fusion of the pores (Casper et al. 2004).

1.1.3 Collectors

Collectors have a significant impact on the productivity and on the resulting nanofiber mesh properties. Special collectors can be classified into 2 main groups: static and rotating collectors (Figure 1.2).

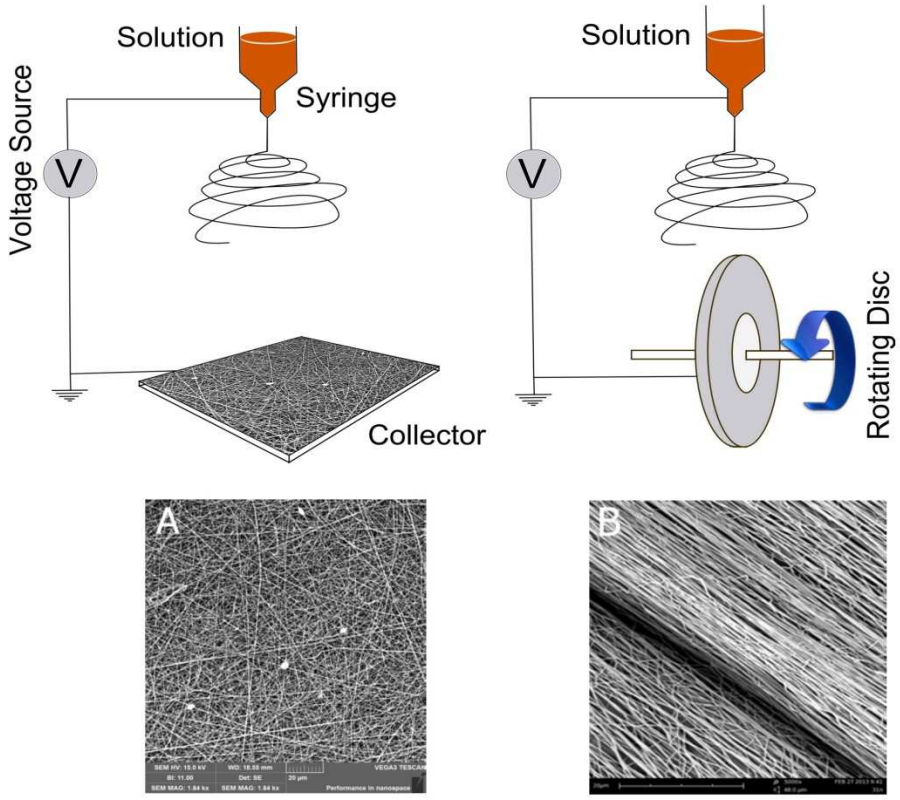

Figure 1.2 Schematic depiction of the electrospinning process
(A) A charged solution is drawn from the tip and the residual random fibers collect on a grounded plate. (B) A spinning disc technique commonly employed to create aligned electrospun fibers. Corresponding random and aligned fibers produced from the setup shown here (unpublished data). Adapted from Li et al., 2010 (*Biomimetics Learning from Nature, book edited by Amitava Mukherjee (Ed.), ISBN: 978-953-307-025-4, InTech, (2010), Chapter 24 Biomimetic Architectures for Tissue Engineering, Jianming Li, Sean Connell and Riyi Shi., DOI:10.5772/8773,*© (2010)
http://www.intechopen.com/books/biomimetics-learning-from-nature/biomimetic-architectures-for-tissueengineering (Li et al. 2010).

The design of the collector is always adapted to the product requirements. Various collectors are therefore used to collect nanofibers, e.g. static or rotating plate collectors (Ding et al. 2009); static or rotating patterned collectors and rotating drum collectors to achieve nanofibers with aligned structures (Neves et al. 2007; Niu et al. 2009); wire drum collectors (Sundaray et al. 2004); disk collectors (Huang et al. 2013); water bath collectors (Ki et al. 2007), etc. Jirsak et al. (2010) used a moving substrate to collect nanofibers in their system (Jirsak et al. 2010). The distance between the tip and the collector determines the way the

fibers arrive on the collector, and thus has a significant influence on the mesh properties (Gomes et al. 2007).

1.2 Improved electrospinning techniques

On the basis of the spinneret and the spinning mode, electrospinning can be broadly classified into needle electrospinning and needleless electrospinning.

1.2.1 Conventional needle electrospinning

In conventional needle electrospinning, also known as capillary electrospinning, a needle-like spinneret is used. A polymer solution is injected through a needle, which is charged with high voltage. The applied voltage induces a charge on the surface of the liquid droplet at the needle tip. If the applied voltage is high enough, the hemispherical surface of the fluid elongates and a Taylor cone is established. When the applied voltage is further increased, a charged liquid jet is ejected from the Taylor cone and is attracted to the collector, as shown in Figure 1 (Lukas et al. 2008a). The disadvantage of the conventional electrospinning technique based on the use of a syringe is that the nanofibers are produced at a low production rate (approximately 0.1–1 gram per hour), which is a disadvantage for commercialization (Jirsak et al. 2010). Multi-jet electrospinning systems based on multi-spinneret components were designed to increase fiber productivity and the covering area, and to prepare mixed fibers from various materials (Ding et al. 2004). However, the multi-jet electrospinning method has been shown to alter the electric field profile induced by adjacent jets, which may lead to reduced fiber production and decreased quality of the fibers (Theron et al. 2005). To overcome this problem, the usage of a secondary electrode connected to multiple nozzles has been proven to stabilize the initial spun jets (Kim et al. 2006). Varesano et al. (2009) studied the effect on nanofiber morphology of various multi-jet configurations (from 2 to 16 jets),

with positive and negative polarity respectively, and they estimated the inter-jet repulsion by measuring the divergence angles. Large area deposition with quality nanofibers was accomplished with a maximum collector dimension of 50 cm x 50 cm (Varesano et al. 2009). The main problem with the traditional needle electrospinning method, which may limit the continuous nanofiber production process, is polymer clogging at the spinneret nozzle. Clogging may occur when high solution concentration or composite blends (e.g. nanoparticles embedded in blends) are used for electrospinning (Persano et al. 2013).

1.2.2 Needleless electrospinning

A much more productive process, suitable for industrial-scale production of nanofibers, is needleless electrospinning. Yarin and Zussman reported a new approach for mass production of nanofibers based on a combination of normal magnetic and electric fields acting on a two-layer system. In their study, nanofibers were electrospun from numerous cones located at the free surface of the upper layer, a polymer solution, punched by the lower layer, a magnetic fluid. Steady vertical spikes were formed, perturbing the interlayer interface, when a normal magnetic field was applied during the spinning process. When in addition a high voltage was applied to the system, thousands of jets ejected upward, as in an ordinary electrospinning process (Yarin and Zussman 2004). However, this upward electrospinning system required a complicated setup, and the nanofibers that were obtained were large in diameter and had a wide diameter distribution.

Jirsak et al. (2009) invented and patented a needleless electrospinning nanofiber production technology, in which the polymer solution is delivered into the electrostatic field by the surface of a rotating charged electrode, while a spinning surface is formed on a part of the circumference of the charged electrode near to a counter elelctrode (Jirsak et al. 2009).

Under favourable conditions (appropriate viscosity of the polymer solution, appropriate surface tension, and an appropriate value of the electric conductivity of the solution) the polymer solution is able to generate multiple Taylor cones in the electric field, not only while being discharged from the spinning jet but also on the surface of the rotating electrode partly immersed in a container with this polymer solution (Figure 1.3). This setup has been commercialized by Elmarco Company, under with the brand name Nanospider^{TM}.

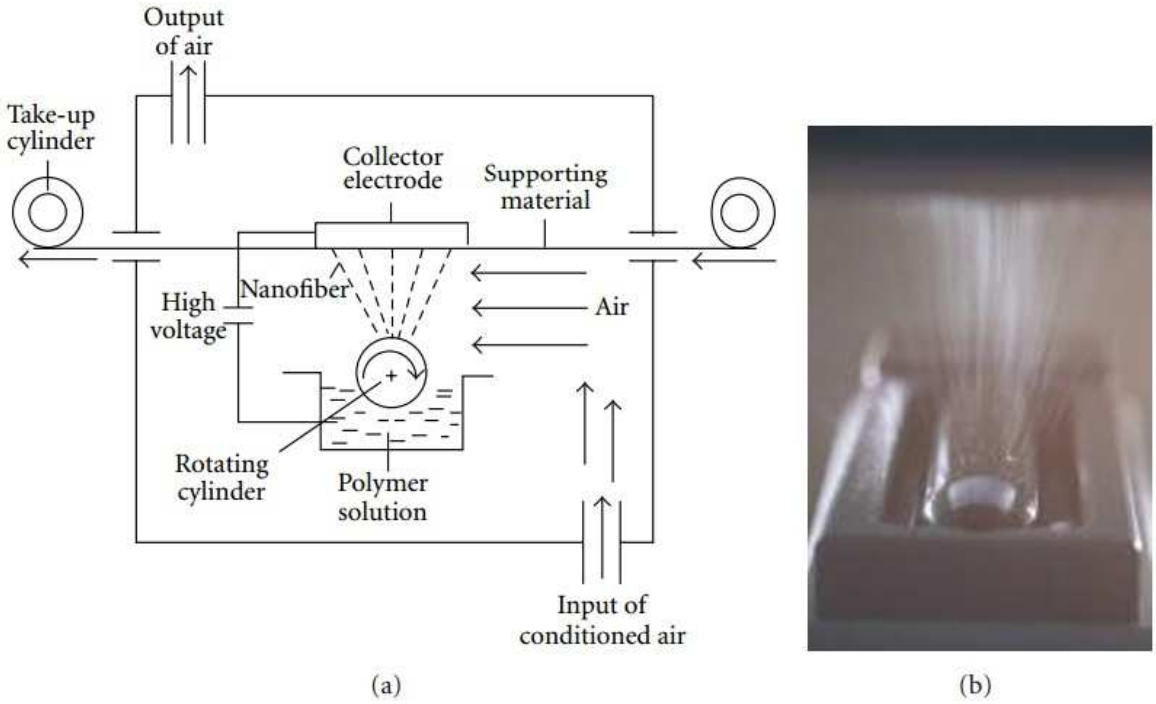

Figure 1.3 The principle of the needleless electrospinning device
(a) Schematic diagram (b) A photograph of the roller electrostatic spinner. Reprinted by kind permission of the first author from Hindawi Publishing Corporation [Journal of Nanomaterials] (*Polyamic acid nanofibers produced by needleless electrospinning, Jirsak O., Sysel P., Saneternik F., Hruza J. and Chalupek J., Journal of Nanomaterials, 1–7, (2010), doi:10.1155/2010/842831*), Copyright © (2010) (Jirsak et al 2010).

The Nanospider^{TM} system has undergone further development, and a new model has been created, where the rotating electrode is replaced by a wire spinning electrode. In the optimized system, the polymer is applied continuously on a wire electrode using a moving solution tank, thus preventing volatilization of the solvent and drying of the polymer solution on the electrode.

Lukas et al. described electrospinning from the free surface of conductive liquids and validated their hypothesis, which explained the self-organization of jets on one-dimensional free liquid surfaces in terms of the electro-hydrodynamic instability of surface waves (Lukas et al. 2008). During the electrospinning process from a free liquid surface, above the critical field intensity value, the liquid jet starts to be self-organized. Due to the electric force, the amplitude of one characteristic wavelength grew faster than the others. The fastest growing stationary wave marks the onset of electrospinning from a free liquid surface with polymer jets originating from the crests of the stationary wave (Lukas et al. 2008; Lukas et al. 2009). The self-organization of jets on the free liquid surface is illustrated in Figure 1.4, using the motion of a droplet of a viscous epoxy resin under increasing external field strength. The droplet is deposited on a bulky metallic rod approximately 1 cm in diameter, which serves as an electrode. A collector, which is not shown here, is placed above the electrode.

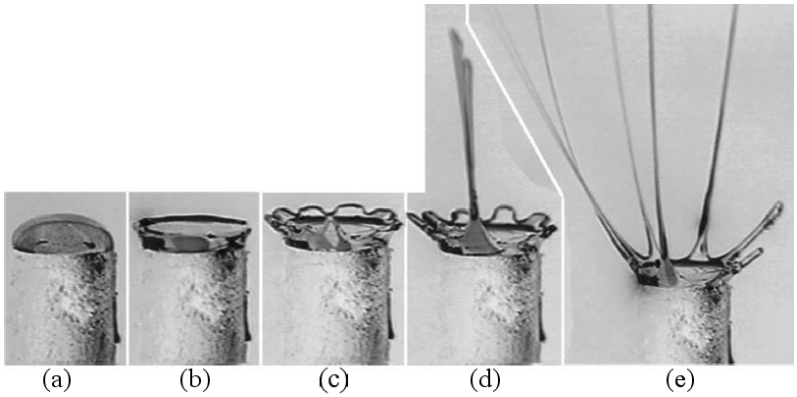

Figure 1.4 The self-organization of jets on a free liquid surface
(a) The hemispherical shape of a highly viscous epoxy resin droplet at zero field strength. (b) The shape of the droplet changes after the high voltage source is switched on. Attractive Coulombic forces between the net charge on the periphery of the droplet and the collector develop a swelling droplet rim and bring about a plate-like shape of the droplet. (c) On the previously smooth rim a stationary wave is organized with further field strength increment. (d), (e) If the field intensity is mounted even further, the jets appear simultaneously from the crests of the stationary wave. Reprinted from The Textile Institute, Taylor and Francis Group [Textile Progress] *(Physical principles of electrospinning. Electrospinning as a nano-scale technology of the twenty-first century, Lukas, D., Sarkar A., Martinova L., Vodsedalkova K., Lubasova D., Chaloupek J., Pokorny P., Mikes P., Chvojka J. and Komarek M. Textile Progress, 41(2):59-140, (2009), doi: 10.1080/00405160902904641)* Copyright © (2009) [The Textile Institute] Courtesy of Sandra Torres, Technical University of Liberec (Lukas et al. 2009).

Niu et al. compared needleless electrospinning using three rotating fiber generators (a cylinder, a disc and a spiral coil wire), and clarified the influence of spinneret shape on the electrospinning process, fiber diameter and productivity (Figure 1.5). They found that disc spinneret required the lowest voltage to initiate fiber formation, and finer fibers with narrower diameter distribution were produced from the disc spinneret and the coil spinneret than from the cylinder spinneret. It was also found that the spiral coil had a much larger polyacrylonitrile (PAN) fiber production rate than a cylinder spinneret of the same dimension. Electric field analysis indicated that higher intensity of the electric field was formed by the disc and coil spinnerets, which concentrated on the circumferential edge of the disc and coil wire surface respectively. The cylinder spinneret formed an unevenly distributed electric field, which concentrated mainly on the end and middle area (Niu et al. 2009; Niu et al. 2012).

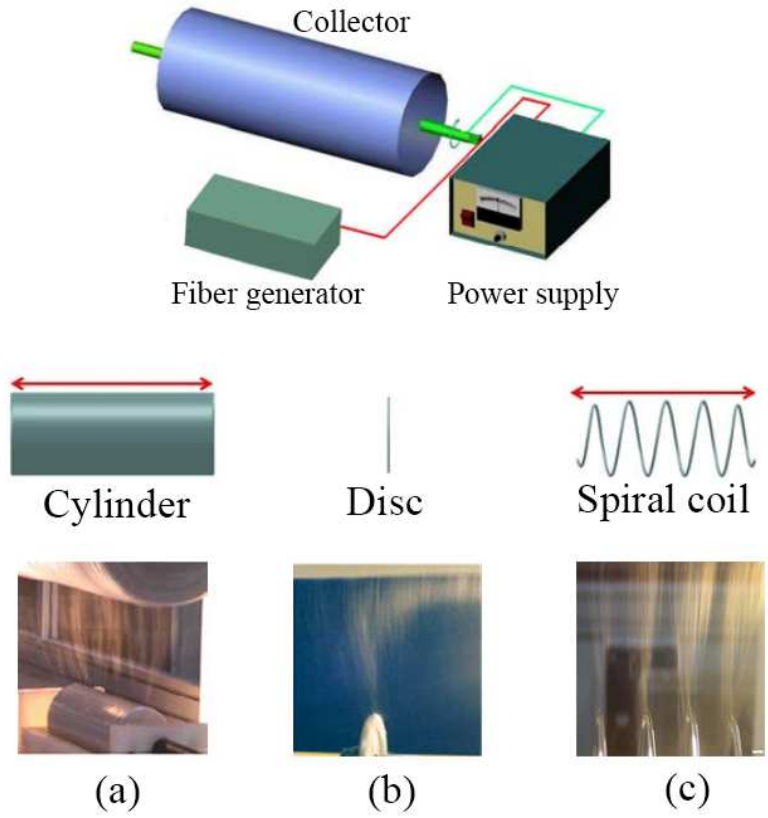

Figure 1.5 Schematic illustration of needleless electrospinning and cylinder, disk and spiral coil spinnerets; and photos of the three electrospinning processes.
A schematic illustration of needleless electrospinning and fiber generators, and a photo of a spiral coil (c) needleless electrospinning process reprinted and adapted from [Journal of Engineered Fibers and Fabrics] (*Upward Needleless Electrospinning of Nanofibers, Haitao Niu, Xungai Wang and Tong Lin, Journal of Engineered Fibers and Fabrics, SPECIAL ISSUE - July 2012 – FIBERS, (2012)*), Copyright © (2012). Reproduced courtesy of Journal of Engineered Fibers and Fabrics, P.O. Box 1288, Cary, North Carolina 27512-1288, USA. Tel: (919) 233- 1210 Fax: (919) 233-1282 Internet: www.jeffjournal.org. Photos of the cylinder (a) and disc (b) neddleless electrospinning processes reprinted by permission from Wiley Periodicals, Inc. [Journal of Applied Polymer Science] (*Needleless Electrospinning. I. A Comparison of Cylinder and Disk Nozzles, Haitao Niu, Tong Lin, Xungai Wang, Journal of Applied Polymer Science, 114, 3524-3530, (2009), doi:10.1002/app.30891*), Copyright © (2009), [Wiley Periodicals, Inc.], http://onlinelibrary.wiley.com/doi/10.1002/app.30891/pdf. (Niu et al. 2009; Niu et al. 2012).

All these findings indicate that a spinneret that can generate a narrowly distributed electric field overlapping the fiber generating area will lead to the development of large scale needleless electrospinning systems for the mass production of high quality nanofibers for advanced applications (Lin and Wang 2013).

1.2.3 Electrospinning of core/shell fibers

Several electrospinning techniques are available for producing nanofibers with a strictly organized core/shell structure, especially emulsion and coaxial electrospinning.

1.2.3.1 Emulsion electrospinning

Emulsion electrospinning is a simple technique for producing nanofibers with a core/shell structure from blends via a needle or needleless electrospinning technique. The emulsion electrospinning method depends on the immiscibility of the prepared solutions, in which one is present as a continuous phase and another one is present as droplets, distributed throughout the continuous phase. The major steps in emulsion electrospinning include the process for emulsifying the core materials, dissolving the fiber forming materials, and finally electrospinning the emulsion (Figure 1.6).

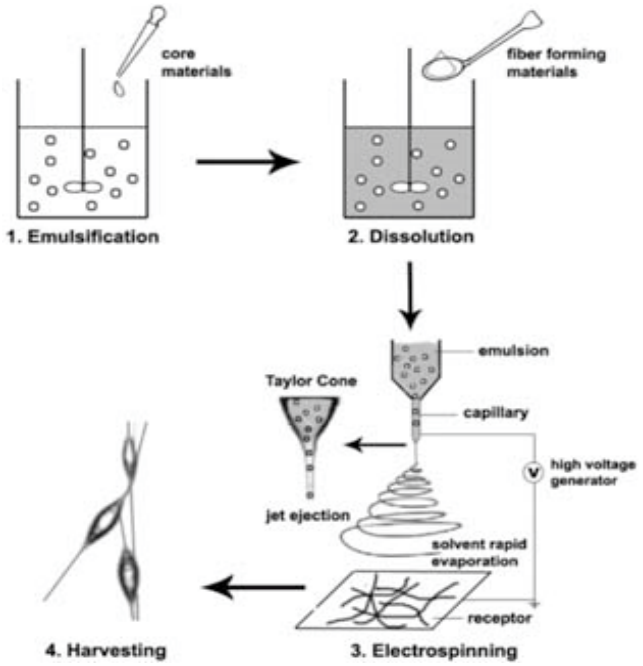

Figure 1.6 Schematic illustration of emulsion electrospinning
Schematic illustration of emulsion electrospinning, reprinted by permission from John Wiley & Sons, Ltd. [Polymers for Advanced Technologies] (*On the way to clean and safe electrospinning—green electrospinning: emulsion and suspension electrospinning, Seema Agarwal, Andreas Greiner, Special Issue: Selected topics in electrospinning, 22, 3, 372–378,(2011), DOI: 10.1002/pat.1883*), Copyright © (2011), [John Wiley & Sons, Ltd.], http://onlinelibrary.wiley.com.ezproxy.is.cuni.cz/doi/10.1002/pat.1883/epdf. (Agarwal and Greiner 2011).

As a result of emulsion electrospinning, composite fibers of sub-micrometer diameter with a core/shell morphology can be prepared by dispersion of water drops containing bioactive molecules in the organic phase comprising electrospun polymer solutions (Yarin 2011).

Because the drug is dispersed within the polar polymer during emulsion electrospinning, the process is suitable for encapsulating drugs that are sensitive to organic solvents. The feasibility of electrospinning an oil-in-water type emulsion was also evaluated. The emulsions contained an aqueous solution of poly(ethylene oxide) (PEO) as the continuous phase and either mineral oil or a polystyrene (PS) in a toluene solution as the drop phase (Angeles et al. 2008).

Though emulsion electrospinning is a very simple method for fabricating core shell nanofibers, the diameter of the fibers is hard to control and usually leaves some defects in the fiber mesh (Qu et al. 2013).

1.2.3.2 Coaxial electrospinning

Modifying the conventional needle electrospinning setup led to the preparation of nanofibers with unique structures and properties. Compound coaxial nozzles were designed to enforce the formation of composite functionalized nanofibers with a rather strictly organized core/shell structure (Song et al. 2005; Yarin 2011). Coaxial electrospinning of nanofibers was first demonstrated by Sun et al. (Sun et al. 2003). Hollow interior nanofibers were also fabricated using the coaxial electrospinning setup (Figure 1.7). Xia et al. demonstrated the coaxial morphology of nanofibers by producing TiO_2 hollow nanofibers with controllable dimensions, removing the oil phase as the core at the end of the process (Li and Xia 2004).

The spinning electrode of the coaxial electrospinning apparatus consists of two capillaries that are placed together coaxially. The shell solution, which most commonly consists of a spinnable polymeric material, is injected through the outer needle, while the core solution is injected through the inner needle and consists of other polymers or encapsulated masses,

including simple liquids (Bazilevsky et al. 2007; Yarin 2011). From the technological point of view, the core fluid may or may not be spinnable, since the physics of spinnability is governed mostly by the surface of the jet (Lukas et al. 2009). This finding opened up the possibility of creating composite fibers that can function as drug delivery vehicles for susceptible bioactive substances. Biomolecules such as antibiotics, drugs, DNA, proteins and living cells have been directly incorporated into the nanofiber core, affording protection from the environment by the shell (Reznik et al. 2006; Sill and von Recum 2008; Wenguo et al. 2010).

During the process of coaxial electrospinning, the shell and core fluids are drawn out from spinneret and form a compound Taylor cone from the tip of which a coaxial jet is emmited. The jet is subsequently elongated to form continuous ultrathin fibers. Evaporation of the solvents contained in the jet results in the formation of a core/shell structure fiber on the collector (Figure 1.7; Loscertales et al. 2004). The shell and the core may or may not be miscible, because the short duration of the process during which the jet solidifies in the fibers prevents fluids from mixing significantly (Yu et al. 2004; Lukas et al. 2009).

For successful coaxial electrospinning, the critical factors are the selection of the polymers and solvents, the applied electric field, the size of the core/shell capillaries, and the viscosity and conductivity of the core/shell fluids; and also the balance between the strength of the electric field and an appropriate injection rate of the inner and outer fluid (Khajavi and Abbasipour 2012). The effects of various processing parameters on coaxial electrospinning were evaluated by Saraf et al. (2009).

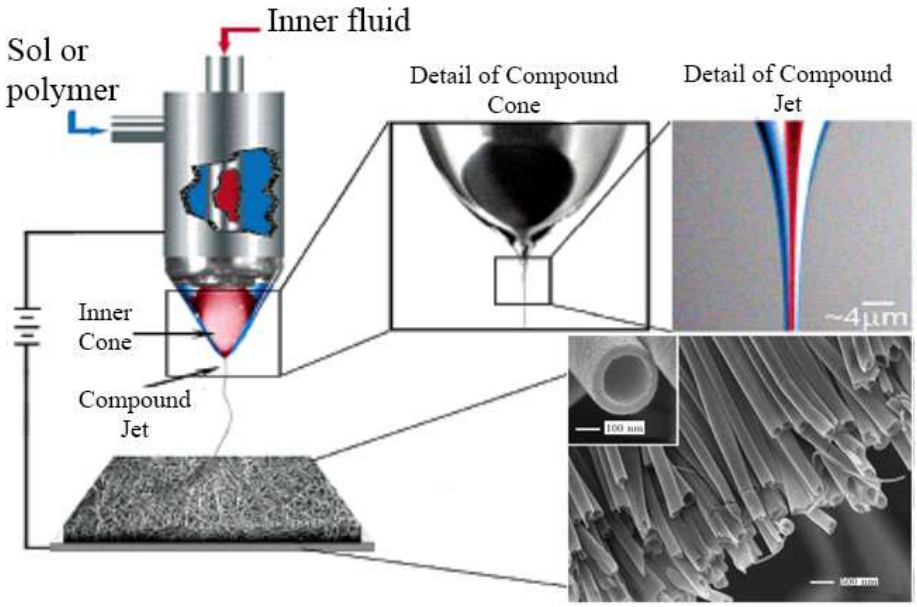

Figure 1.7 Coaxial electrospinning of nanofibers
Two immiscible (or poorly miscible) liquids (red and blue) are injected through two capillaries placed together coaxially. A compound Taylor cone is developed, from the tip of which a coaxial jet is emitted. Evaporation of the solvents contained in the jet results in the formation of a core/shell structure fiber (or a liquid-filled hollow fiber) on the collector.
The coaxial elelctrospinning setup sketch is reprinted and adapted with permission from [Journal of the American Chemical Society] (*Electrically Forced Coaxial Nanojets for One-Step Hollow Nanofiber Design, Ignacio G. Loscertales, Antonio Barrero, Manuel Marquez, Ruben Spretz, Raffet Velarde-Ortiz, and Gustavo Larsen, Journal of American Chemical Society, 126 (17), 5376–5377 (2004), DOI: 10.1021/ja049443j*). Copyright © 2004 American Chemical Society. SEM image of a uniaxially aligned array of TiO_2 (anatase) hollow fibers reprinted with permission from [Nano Letters] (*Direct fabrication of composite and ceramic hollow nanofibres by electrospinning, Dan Li and Younan Xia, Nano Letters, 4 , 933–938 Nano Letters, 4 (5), 933–938, (2004), DOI: 10.1021/nl049590*f). Copyright ©2004 American Chemical Society. (Loscertales et al. 2004; Li and Xia 2004).

In addition to the use of a coaxial setup, other approaches to the production of core shell nanofibers have also been presented. Blends of immiscible polymethylmetacrylate (PMMA) and polyactrilonitrile (PAN) polymers were dissolved separately in DMF to prepare nanofibers with a core/shell structure using a single nozzle approach. The authors claimed that the outer shell flow was strong enough to stretch the inner droplet into the Taylor cone, thus forming a core/shell jet (Bazilevsky et al. 2007).

Lee et al. used a single nozzle technique for preparing poly (ethylene oxide) (PEO) and chitosan (CS) coaxial nanofibers. They investigated the fraction effect of each component in the solution, and found that the core shell pattern transformation is caused by various phase separation mechanisms with a continuous decrease in the PEO fraction (Lee et al. 2010). The effectiveness of the technology and the coaxial structure of the nanofibers were also confirmed by Sun et al. (2003). Unfortunately, the fiber productivity of coaxial fibers utilizing a single nozzle technique was not suitable for mass production of nanofibers. A straightforward way to increase the electrospinning throughput was to use multi-jet spinnerets. The productivity of nanofibers could be increased simply by increasing the number of jets (Varesano et al. 2009). However, multi-jet electrospinning showed strong repulsion among the jets, and this may lead to reduced production of nanofibers. Moreover, poor quality nanofibers were prepared, which was an obstruction for practical applications. For the mass production of nanofibers, the jets should be set at an appropriate distance, in order to reduce jet repulsion (Niu et al. 2012).

The low productivity of needle-based coaxial processes led to the development of novel methods modified from free surface electrospinning to massive production of core/shell nanofibers. Forward et al. (2013) presented a novel coaxial electrospinning technology by developing coaxial jets directly from compound droplets of immiscible liquids entrained on wires. The authors declared that they had achieved control over mass transfer processes for the production of uniform, core/shell fibers (Forward et al. 2013). Jiang and Qin developed a novel stepped pyramid-shaped spinneret. A two-layer polymer system, with the lower layer consisting a core polymer solution and the upper layer consisting a sheath polymer solution, subjected to a sufficient electrical field, resulted in the formation of multiple coaxial jets from the edges of the spinneret. The authors claimed that they achieved more than 100 times greater productivity than for traditionally obtained core/shell nanofibers (Jiang and Qin 2014).

The proposed technologies create an opportunity to fabricate nanofibers with core/shell structures on an industrial scale for a wide variety of applications.

Electrospinning has proven to be the best fiber forming manufacturing process, due to its simplicity, material compatibility, and cost effectiveness. Moreover, the process is performed at atmospheric pressure and at room temperature. Thus, the electrospinning process affords the opportunity to prepare fibers with a micro-to-nanoscale topography, large surface area-to-volume ratios, tunable porosity and surface properties, high permeability, ability to retain electrostatic charges, flexibility and good mechanical properties. These remarkable features of electrospun nanofibers have made them into preferred materials for many biomedical applications, including tissue engineering applications and controlled drug delivery (Ma et al. 2005; Pham et al. 2006; Sill and von Recum 2008).

1.3 Applications of nanofibers in tissue engineering

The versatility of the material, combined with fibers within biologically relevant length scales makes electrospinning a highly attractive method for producing biodegradable and biocompatible scaffolds for tissue engineering applications (Ma et al. 2005; Pham et al. 2006).

1.3.1 Tissue engineering

The term tissue engineering was introduced at a meeting of the National Science Foundation in 1987. The first recorded use of the term tissue engineering, as it is applied today, was in a paper entitled, “Functional Organ Replacement: The New Technology of Tissue Engineering” in “Surgical Technology International” in 1991 (Vacanti and Vacanti 1991). The definition, as stated by Langer and Vacanti, is that “Tissue engineering is an interdisciplinary field that applies the principles and methods of engineering and life sciences toward the fundamental understanding of structure-function relationships in normal and pathological mammalian

tissue, and the development of biological substitutes to restore, maintain, or improve tissue function“ (Langer and Vacanti 1993).

The common principle of tissue engineering applications is the ability to exploit living cells in a variety of ways. The tissue could be grown inside or outside the patient and transplanted; or grown *in vitro* and tested for drug metabolism and uptake, toxicity and pathogenicity. Three main components, and combinations of these components, are required for optimal tissue engineering:

1. **Scaffolds** to provide temporary support for cells to regenerate new extracellular matrix (ECM) prepared from biodegradable and biocompatible materials.
2. An appropriate source of **cells** such as autologous cells, allogeneic cells, xenogeneic cells, stem cells, or genetically engineered cells. Emphasis on cell expansion *in vitro,* cell and tissue growth on scaffolds (cultivation in bioreactors), following possible implantation into the defect site to form new tissue.
3. **Stimulating factors**, including growth factors, angiogenic factors, differentiation factors, small molecules, etc., added to culture media *in vitro* or in combination with drug delivery vehicles (scaffolds and liposomes) to induce, accelerate, enhance and/or control cellular differentiation and tissue formation.

An example of the tissue engineering concept is represented in Figure 1.8

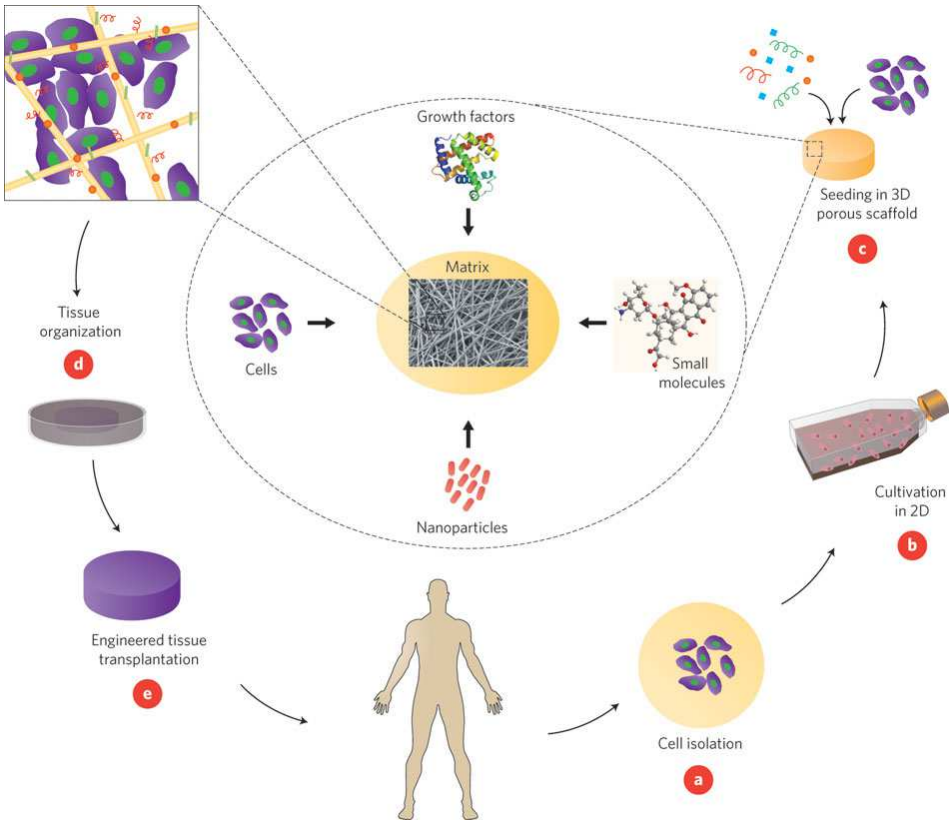

Figure 1.8 An example of a tissue engineering concept that involves seeding cells within porous biomaterial scaffolds
(a) Cells are isolated from the patient and may be cultivated **(b)** *in vitro* on two- or, three-dimensional surfaces for efficient expansion. **(c)** Next, the cells are seeded in porous scaffolds together with growth factors, small molecules, and micro- and/or nanoparticles. The scaffolds serve as a mechanical support and a shape-determining material, and their porous nature provides high mass transfer and waste removal. **(d)** The cell constructs are further cultivated in bioreactors to provide optimal conditions for organization into a functioning tissue. **(e)** Once a functioning tissue has been successfully engineered, the construct is transplanted on to the defect to restore function. Reprinted by permission from Macmillan Publishers Ltd: [Nature Nanotechnology] (*Nanotechnological strategies for engineering complex tissues Tal Dvir, Brian P. Timko, Daniel S. Kohane, and Robert Langer, Nature Nanotechnology, 6, 13–22, (2011) doi:10.1038/nnano.2010.246)*, Copyright © (2010) (Dvir et al. 2011).

1.3.1.1 Nanofiber scaffolds for tissue engineering

The development of nanofibers has greatly enhanced the scope for fabricating scaffolds that mimic the structure and the biological function of the extracellular matrix (ECM) in terms of chemical and physical structure. Various techniques are available for fabricating nanofibers: self-assembly, phase separation, drawing and electrospinning. Of these techniques, nanofiber

scaffolds prepared by electrospinning techniques have shown the most promising results in terms of applications in tissue engineering and in regenerative medicine (Filova et al. 2013; Rampichova et al. 2013). Nanofibers offer distinct advantages of biocompatibility and biodegradability, versatility of chemistry and mechanical properties. Nanofibers are characterized by a large surface area-to-volume-ratio, high porosity and a diameter of the nanofibers that closely matches the size scale of the ECM. They are therefore, ideal for cell attachment, proliferation, differentiation and drug loading (Keun Kwon et al. 2005). Typically, an electrospun matrix has porosity as high as 90% and a pore diameter of less than 100 nm. Cell infiltration depends strongly on the pore size and the porosity of the polymer mesh. The optimal pore size for cell attachment, proliferation and migration varies from 5 to 500 µm (Pham et al. 2006). The pore size of electrospun scaffolds can be adjusted by modifying the fiber diameter or the fiber alignment, or by introducing sacrificial components (Rnjak-Kovacina and Weiss 2011; Vaquette and Cooper-White 2011).

The availability of a wide range of natural and synthetic polymers has broadened the framework for developing and fabricating nanofibrous scaffolds, using the electrospinning technique (Vasita and Katti 2006).

1.3.1.1.1 Natural and synthetic polymers

Owing to their bioactive properties, naturally derived materials have the advantage of biological recognition, which may positively support cell adhesion, proliferation and function. However, they may exhibit immunogenicity and can contain pathogenic impurities. There is also less control over their mechanical properties and biodegradability (Liu and Ma 2004). Natural polymers can be classified as proteins (e.g. collagen, gelatin, silk, fibrinogen, elastin etc.), polysaccharides (cellulose, dextran, chitin, glycosaminoglycans, hyaluronan etc.), or polynucleotides (DNA, RNA) (Dhandayuthapani et al. 2011).

Natural polymers often lack the desired physical properties or are difficult to electrospin on their own. Natural polymers are therefore often blended with synthetic polymers (Shalumon et al. 2010; Zhou et al. 2007) in order to enhance the mechanical properties, the degradation stability, and to provide enhanced affinity to cellular components. Huang et al. fabricated a hybrid, chitosan/polyvinyl alcohol (CS/PVA) nanofibrous membrane by the electrospinning technique. The stabilized chitosan nanofibrous membrane supported enzyme immobilization and improved the pH and the thermal stabilities of lipase on the chitosan nanofibrous membrane (Huang et al. 2007). Ultrafine nanofibrous scaffolds were fabricated using a natural polymer, chitosan (CS) and the synthetic polymer, poly-ε-caprolactone (PCL). CS/PCL nanofibers were blended in various concentrations and compositions using a formic acid/acetone solvent mixture. The author revealed that fibers obtained from 1% chitosan and 8% PCL in 1:3 compositions resulted in the formation of fine nanofibers 102 ± 24 nm in diameter (Shalumon et al. 2010).

A wide variety of synthetic polymers have been used to form biodegradable or non-degradable scaffolds. Biodegradable scaffolds have been particularly popular, because they eliminate the need to remove the implanted scaffold surgically (Hammouche et al. 2012). Synthetic polymers offer the advantage of reproducible mass production with controlled degradation rate properties, microstructure, tensile strength and elastic modulus; synthetic polymers are also often cheaper than biological scaffolds (Gunatillake et al. 2006). Synthetic polymers also show physicochemical and mechanical properties comparable to those of biological tissues. A wide variety of synthetic polymers have therefore been used to form nanofibers for various tissue engineering applications and for controlled drug delivery. A biocompatible and biodegradable poly-lactic acid (PLA), poly-glycolic acid (PGA), poly-ε-caprolactone (PCL), poly(lactic-co-glycolic acid) (PLGA), polyurethane (PU), polyethylenglycol (PEG), pluronic (PEO-PPO-PEO) and polyvinylalcohol (PVA) are the

most commonly used synthetic polymers for drug delivery and tissue engineering applications (Park et al. 2010; Patel et al. 2011; Yeganegi et al. 2010; Karuppuswamy et al. 2015).

Poly-ε-caprolactone (PCL) is a semi-crystalline, FDA approved polymer. It is a rather hydrophobic, relatively inexpensive, non-toxic, tissue compatible, chemically stable, highly elastic polyester with good mechanical properties and a slow degradation rate (approximately 1–2 years) resulting from the hydrolysis of its ester linkages (Figure 1.9). During the degradation process, the ester groups undergo non-enzymatic hydrolytic cleavage followed by rapid intracellular degradation in phagosomes of macrophages and giant cells when the molecular weight of the polymer is reduced (Woodward et al. 1985). PCL nanofibers are widely used as scaffolding materials for cell-based, neural, bone and cartilage tissue engineering (Gomes et al. 2015; Rampichova et al. 2013). PCL electrospun nanofibers have been formed for a tissue-engineered cardiac graft (Yoshimoto et al. 2003). The interconnected structure of electrospun nanofibers has been shown to provide efficient encapsulation of various chemical agents, such as drugs, siRNA, antibiotics, proteins, and growth factors (Hu et al. 2014; Cao et al. 2010; Dave et al. 2013; Matlock-Colangelo and Baeumner 2014; Wenguo and et al. 2010).

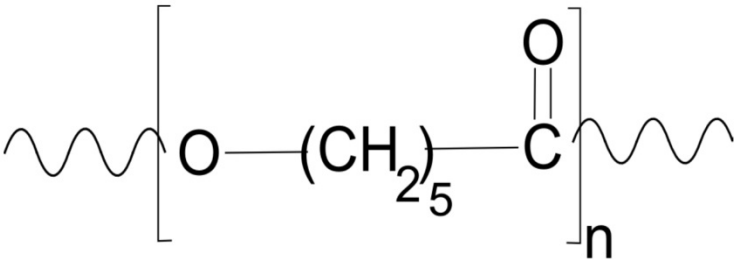

Figure 1.9 Chemical structure of poly-ε-caprolactone (PCL)

Polyvinylalcohol (PVA) is an important water-soluble, highly hydrophilic, nontoxic, and biocompatible, semicrystalline polymer obtained by controlled hydrolysis (or alcoholysis) of

polyvinyl acetate (PVAc) (Figure 1.10**)**. Electrospun PVA nanofibers find use in a broad range of applications, such as filtration materials, optics, protective clothing, enzyme immobilization, drug delivery vehicles, anti-adhesive membranes, and scaffolds for tissue engineering, due to their excellent properties such as strength, elasticity, gas permeability and thermal characteristics (Peresin et al. 2010). The free hydroxyl groups in the chemical structure of PVA provide easy water solubility, so the use of organic solvents for nanofiber preparation via electrospinning is eliminated. Moreover, the –OH side groups are accessible for further chemical modifications (Lin et al. 2012).

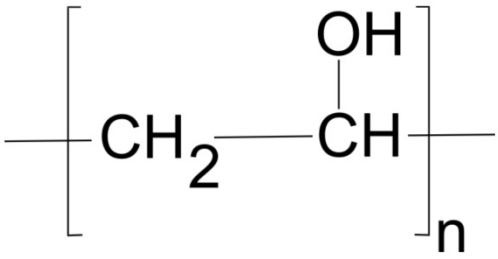

Figure 1.10 Chemical structure of polyvinylalcohol (PVA)

However, excessive hydrophilicity is limiting for tissue engineering applications, due to limited adhesion of cells to the surface of PVA nanofibers. Various alternatives have therefore been triggered to improve the hydrophilicity and the mechanical properties of PVA nanofibers, such as post-treatment (e.g. cold-plasma modification, gamma irradiation) physical or chemical cross-linking and blending (Jeun et al. 2009; Blanes et al. 2010; Kim et al. 2007; Santos et al. 2014). Asran et al. (2010) prepared biocompatible and degradable polyvinyl alcohol/polyhydroxybutyrate (PVA/PHB) blend nanofibers of various compositions for skin tissue engineering applications. Their results indicated the possibility of fabricating bilayered nanofiber scaffolds. They suggested creating the top layer from PVA/PHB (50/50) blend fibers, which could promote adhesion and growth of human keratinocyte cell line

(HaCaT) but inhibit fibroblasts generating an epidermal layer. The dermal equivalent could be prepared from pure PHB or PVA/PHB (10/90) to promote fibroblast adhesion and growth only (Asran et al. 2010). The solubility of PVA electrospun nanofibers in water is an advantage preferably used for targeted delivery of bioactive substances (Scott et al. 2013).

1.3.1.2 Source of cells for tissue engineering applications

The source of the cells is an important choice to consider, when applying tissue engineering strategies to restore lost tissues and their function (Laurencin and Nair 2008). A range of cell types, as discussed below, can be combined with scaffolds to produce tissue-engineered constructs. Conventional tissue engineering approaches usually utilize the fully differentiated adult cell types that make up the target organ or tissue, e.g. chondrocytes for cartilage repair and regeneration, etc. However, the proliferation capacity of fully differentiated cells is very limited. Moreover, differentiated adult cells tend to lose their phenotype or to dedifferentiate during *in vitro* cultivation (Schulze-Tanzil et al. 2004). Attention has therefore become focused on the use of stem cells, including embryonic stem (ES) cells and bone marrow mesenchymal stem cells (MSCs), etc. (Howard et al. 2008).

1.3.1.2.1 Chondrocytes

Chondrocytes are the only mature cell type found in healthy human cartilage (Figure 1.11), their use in cartilage tissue engineering is therefore evident. These spherical cells, originating from chondroblasts and located in cartilaginous tissue, are characterized by their special ability to produce cartilage matrix and their highly developed cytoskeleton of actin filaments. The extracellular matrix that is produced consists primarily of collagen type II, which is responsible for the structure, and cartilage-specific proteoglycans (aggrecan), which make up 5% to 10% of the wet weight of the cartilage (Brittberg and Gersoff 2010). Actin filaments provide biomechanical support and also connect the chondrocyte to the articular matrix. The

interactions are important both, for the development and for the maintenance of the cartilage (Guilak 1995). Chondrocytes originate from mesenchymal stem cells (MSCs) found in the bone marrow in mature individuals. During embryogenesis, MSCs start to differentiate into chondrocytes and secrete a cartilaginous matrix. Mature articular chondrocytes embedded in cartilage appear rounded and are not capable of cell division *in vivo* (Temenoff and Mikos 2000). With an advanced Golgi apparatus and plenty of rough endoplasmic reticulum, chondrocytes are scattered in cartilage cavities, also called lacunae (Muir 1995). The blood supply of chondrocytes is facilitated through the perichondrium and the synovial fluid (Brittberg and Gersoff 2010).

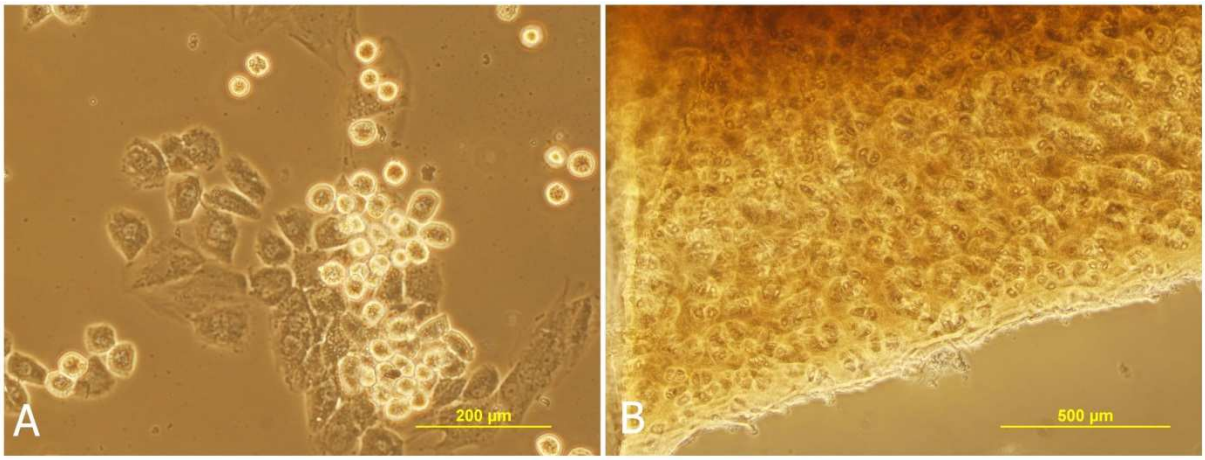

Figure 1.11 Spherical chondrocytes
(A) Spherical chondrocytes from cartilage spread on tissue culture flasks after 7 day culture. (B) A cross section of native pig cartilage shows spherical chondrocytes in lacunae. Magnification (A) 200x; (B) 100x.

Since cartilage is avascular, mature chondrocytes do not proliferate and cartilage lesions do not have the capacity to heal (Schulze-Tanzil et al. 2002). The limited self-repair capacity of cartilage forced researchers to find methods to induce cartilage repair. Driven by urgent medical needs, a variety of surgical techniques have been used for cartilage repair, including bone-marrow stimulation (e.g. abrasion, drilling and microfracturing), osteochondral autograft transfer and autologous chondrocyte implantation (ACI) (Makris et al. 2014). ACI can also be

used in combination with scaffolds (Cole et al. 2009). The most suitable treatment options have to be chosen individually, according to the type (defect size, depth, location, etc.) of defect that is to be regenerated. For small defects, osteochondral autograft transplantation or bone-marrow stimulation is suitable (Steadman et al. 2003). Two-step ACI has been developed to treat large full-thickness chondral articular defects. This approach is based on implanting *in vitro* cultured autologous chondrocytes into the defect site (Knutsen et al. 2007). Recently, matrix-assisted autologous chondrocyte implantation has become the most widely used scaffold-plus-cell-based two-step cartilage repair technique in present day clinical practice (Makris et al. 2014).

Articular chondrocytes are responsible for the unique properties of articular cartilage. Committed chondrocytes are therefore used to engineer cartilage *in vitro* or *in vivo* in order to repair a cartilaginous defect (De Boer et al. 2008). Chondrocytes can be isolated by enzymatic digestion from pieces of cartilage. Pieces of cartilage pieces can be harvested arthroscopically from a healthy part of the joint. As was mentioned above, articular cartilage contains only a limited number of cells (only about 1%), so *in vitro* expansion of the cells is necessary before implantation. However, cells grown as a monolayer tend to lose their chondrogenic phenotype with type II collagen production or dedifferentiate during *in vitro* cultivation (Schnabel et al. 2002). The use of specific growth factors (GFs), such as basic fibroblast growth factor (FGF-2) or transforming growth factor (TGF-β1) stimulates cell proliferation. Moreover, these specific growth factors maintained the capability of cells to re-differentiate when transferred to a 3D environment (Jakob et al. 2001). 3D cultures imitate physiological conditions, so chondrocytes are able to maintain their morphology. Cells could be cultured on natural polymeric substrates such as aggrecan, collagen (Darling and Athanasiou 2005) or fibrinogen (Brodkin et al. 2004). Chondrocytes have also been found to maintain their phenotype for a longer period when seeded at higher density (Watt 1988).

Other sources of human autologous chondrocytes (e.g. nose, rib, and ear) have also been considered for nonarticular reconstructive surgery. Their regeneration potential can be enhanced by using a combination of various growth factors (Tay et al. 2004).

1.3.1.2.2 Stem cells

Stem cells provide alternative cell sources for tissue engineering applications. Stem cells are unspecialized cells capable of long term self-renewal. They maintain their capacity to differentiate into multiple specialized cell types under the right conditions or given the right signals (Figure 1.12).

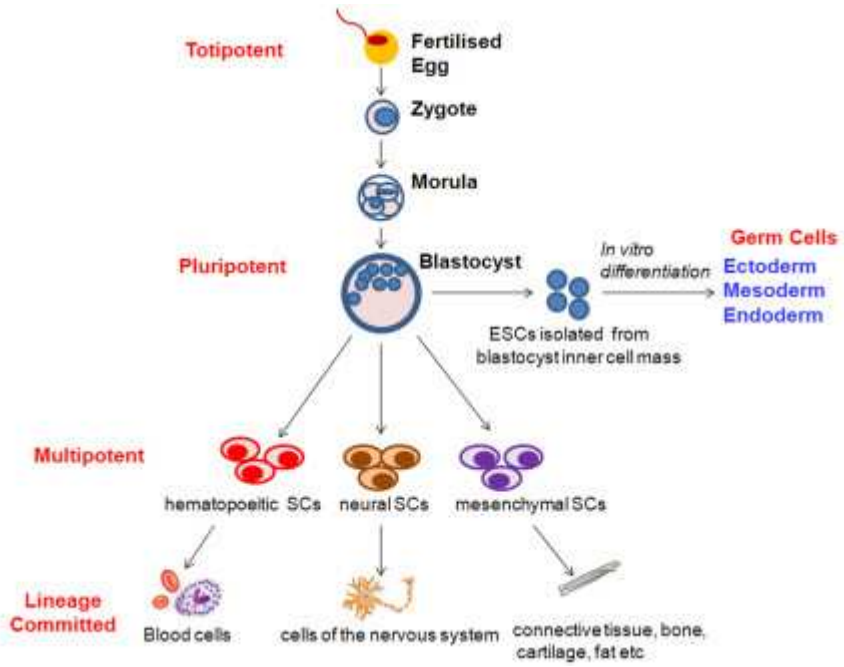

Figure 1.12 Schematic diagram illustrating the stem cell hierarchy
Adult stem cells are multipotent, and have a more restricted ability to differentiate, being committed to a specific lineage. Embryonic stem cells (ESCs) are pluripotent, and have the capacity to differentiate into cells of all three germ layers (endoderm, mesoderm and ectoderm). Reprinted from BioMed Central Ltd: [Critical Care] *(Clinical review: Stem cell therapies for acute lung injury/acute respiratory distress syndrome - hope or hype?, Mairead Hayes, Gerard Curley, Bilal Ansari and John G. Laffey, Critical Care, 16:205 (2012) doi:10.1186/cc10570),* copyright © 2012 BioMed Central Ltd. (Hayes et al. 2012).

Depending on the development stage of the tissue from which the stem cells are isolated, stem cells can be divided into adult stem cells and embryonic stem cells (Thomson et al. 1998). Adult stem cells are considered to be multipotent, having the potential to differentiate into a more limited range of mature cell types. An exception is induced pluripotent stem cells (iPSCs), which are derived from adult cells that have been reprogrammed to de-differentiate following transduction with transcription factors (Weiss et al. 2011). Adult stem cells can be found and isolated from many adult tissue types, including bone marrow, peripheral blood, adipose tissue, neural tissue, muscle, dermis, etc. After isolation, stem cells can be cultivated *in vitro* for several passages without loss of differentiation potential, and then differentiated into a desired cell phenotype (Uccelli et al. 2008).

Among adult stem cells, mesenchymal stem cells from bone-marrow (MSCs) have attracted great interest in tissue engineering applications (Prosecka et al. 2011; Prosecká et al. 2015). MSCs are cells of stromal origin that are capable of self-renewal and differentiation into cells of mesodermal origin, including chondrocytes, osteocytes and adipocytes (Weiss et al. 2011). The ability to differentiate into multiple tissue types is also dependent on growth factors, chemical composition, and the physical and biomechanical properties of the scaffolds, as well as different biomechanical loading of the material (Jelen et al. 2008; Pittenger et al. 1999). MSCs have been shown to have great potential for autologous cell-based therapy (Pittenger et al. 1999). Their potential allogenic use without immunosuppressive therapy in regenerative medicine has also been considered (Aggarwal and Pittenger 2005).

An interesting source of mesenchymal stem cells is the adipose tissue. The advantage of using adipose tissue as a source of cells is the relatively easy isolation procedure, and the large number of cells that can be obtained (Danisovic et al. 2009). Adipose tissue-derived mesenchymal stem cells (and also MSCs) may, under appropriate culture conditions, differentiate into cells and tissues of mesodermal origin, including adipocytes, chondrocytes,

osteoblasts, and skeletal myocytes, and can be used to generate the respective tissue, including fat, muscle, bone, and cartilage (Masuoka et al. 2006; Zuk et al. 2002).

Stem cells have been found not only in the adult tissues mentioned above, but also in fetal tissues such as umbilical cord blood and Wharton's jelly (Trivanović et al. 2013). Other sources of stem cells include muscles, synovium and the periosteum (Bueno et al. 2008; Kim et al. 2014; Ferretti and Mattioli-Belmonte 2014).

Embryonic stem cells (ES) or embryonic germ cells (EG) can self-renew without differentiation for much longer time than MSCs. These pluripotent cells have high proliferative potential and the capacity to differentiate into cells of all three germ layers, i.e. endoderm, mesoderm and ectoderm (Kramer et al. 2000). Embryonic stem cells are therefore attractive cell sources for tissue engineering applications, where a large number of cells are needed. ES cells are derived from the inner cell mass of blastocysts, and EG cells are isolated from the developing gonadal ridge. In 1998, an ethical controversy surrounding stem cells erupted with the creation of human ES cells derived from discarded human embryos (Thomson et al. 1998). Although significant ethical concerns have been raised, ES cells may hold the secret to multiple cures and groundbreaking developments in regenerative medicine (Laurencin and Nair 2008).

1.3.1.3 Stimulating factors for tissue engineering and drug delivery

As the third component of the tissue engineering triad, stimulating factors have been employed to induce, accelerate, and/or enhance tissue formation. For example, synthetic GFs, natural sources of GFs, such as platelet derivatives, and other additives may be added to culture media *in vitro* or incorporated into drug delivery vehicles such as scaffolds, liposomes etc. to control cell differentiation and tissue formation.

1.3.1.3.1 Natural source of growth factors

Tissue engineering and regenerative medicine require the development of regulated drug delivery and growth factors. The delivery of multiple growth factors in optimized ratios is desirable in order to mimic physiological microenvironments, and this can be achieved by using natural sources of growth factors, such as platelet derivatives (Chen et al. 2010).

1.3.1.3.1.1 Platelet derived growth factors

Platelets are blood cells that play a primary role in hemostasis (White 1987). They also initiate wound repair by releasing locally-acting growth factors via α-granule degranulation. Platelets also contribute directly to matrix synthesis, and they induce cell proliferation and differentiation and the formation of new tissue (Lana et al. 2014). Platelet bioactive substances are entrapped within α-granules, dense granules, or lysosomal granules, or are present in the cytoplasm. Alpha granules contain vast amounts of platelet bioactive substances (Blair and Flaumenhaft 2009). They are essential for normal platelet activity and are released when activated. Interestingly, recent findings have shown that multiple alpha granule subpopulations are sensitive to different activation pathways (Italiano et al. 2008). Polypeptide GFs entrapped within platelet alpha granules are the key factors orchestrating tissue regeneration (Burnouf et al. 2013). Regulating the synthesis of specific adhesion molecules, growth factors regulate differentiation, proliferation, migration and metabolism in target cells. Each GF can have either one or several essential functions for a specific cell, depending on the specific conditions in the cell environment (Ramos-Torrecillas et al. 2014).

Platelet-derived growth factor (PDGF) was the original growth factor found in alpha granules. It is released by platelets, macrophages, keratinocytes, fibroblasts, and endothelial cells. Platelet-derived growth factor (PDGF) comprises a group of homodimeric (PDGF-AA,

PDGF-BB, PDGF-CC, and PDGF-DD) and heterodimeric (PDGF-AB) polypeptide dimers linked with disulfide bonds. PDGF plays an important role in wound healing of hard and soft tissues and in CNS development. It is a major mitogen for osteoblasts and undifferentiated osteoprogenitor cells, fibroblasts, smooth muscle cells, and glial cells (Burnouf et al. 2013).

The transforming growth factor (TGF)-β family includes three isoforms of 25 kDa. TGF-β is an important factor in cell proliferation inhibition. TGF-β has been observed to promote synthesis and preservation of the extracellular matrix (Luttenberger et al. 2000). TGF-β family members have a major role in cartilage development; they induce chondrogenesis in embryonic and adult MSCs, and enhance proliferation of chondrocytes (Chung and Burdick 2008). TGF-β1 induces initial chondrogenic differentiation and increases the synthesis of aggrecan and collagen II (Tuli et al. 2003). TGF-β family members also play regulatory roles in modulating wound healing responses and scarring (Beanes et al. 2003). This growth factor is crucial in bone formation and healing, enhancing the chemotaxis and mitogenesis functions of osteoblast precursors, and stimulating osteoblast deposition on the bone collagen matrix (Burnouf et al. 2013). TGF-β family member bone morphogenetic protein (BMP)-2 plays a crucial role in the repair of bone and of epidermis in more superficial layers of the skin (Ramos-Torrecillas et al. 2014).

Insulin-like growth factor (IGF)-I, is involved in cell proliferation, differentiation, and migration. IGF-I favors reepithelization and production of granulation tissue. The presence of the growth factor at the site of a vascular injury has been found to be essential for wound healing. IGF-1, acts in an anabolic manner to increase the production of proteoglycans and type II collagen (Gooch et al. 2001). IGF-1 is also responsible for the bone formation-bone resorption interaction (Zhang et al. 2013).

The epidermal growth factor (EGF) family plays a crucial role in wound healing and in re-epithelization by acting as a potent mitogen for keratinocytes and enhancing their migration in acute wounds (Barrientos et al. 2008).

The fibroblast growth factor (FGF) family includes 23 members. Fibroblast growth factors 1, 2, 7, 10 and 22 are expressed after dermal injury. FGF-1 and FGF-2 are produced by inflammatory cells, vascular endothelial cells, keratinocytes and fibroblasts, and they play roles in re-epithelization, angiogenesis, and granulation tissue formation. FGF-2, also known as basic FGF, contributes to matrix synthesis and remodeling (Demidova-Rice et al. 2012). FGF-2 stimulates DNA and RNA synthesis, and has a mitogenic effect on most types of cells. It has been shown that FGF increased cell proliferation and contributed to maintaining the chondrogenic character of *in vitro* cultivated cells (Miot et al. 2006).

Other proteins involved in the regulation of angiogenesis are vascular endothelial growth factor (VEGF), and thrombospondin-1. Platelets also contain proteins involved in MSC and epithelial cell migration (SDF-1, FGF-2) inflammation (IL-8, CLXL-4, RANTES, CLXL-7) cell adhesion (vWF, fibrinogen, fibronectin), and antimicrobial defense (Blair and Flaumenhaft 2009; Italiano et al. 2008; von Hundelshausen and Weber 2007).

1.3.1.3.1.2 Platelet-rich plasma

Platelet growth factors are currently used for the purposes of regenerative medicine in platelet-rich plasmas (PRPs). PRP is defined as a volume of the plasma fraction of autologous blood with a platelet concentration above a certain value (Marx et al. 1998). PRP offers several advantages, since it is neither toxic nor immunoreactive, and it can be obtained inexpensively and readily from the patient (Ramos-Torrecillas et al. 2014).

PRP and platelet derivatives are nowadays used in cartilage, bone, tendon and ligament, skin, and nerve tissue engineering and regeneration (Alsousou et al. 2009; Lacci and Dardik 2010; Lana et al. 2014). PRP has been shown to enhance chondrocyte proliferation and, most importantly, matrix production (Akeda et al. 2006). PRP has been reported to provide healing of complex wounds (Lacci et al. 2010). Recently, PRP has been used to treat musculoskeletal injuries both in people and in horses, where it is applied via a percutaneous injection or an open surgical approach (Lana et al. 2014; Taylor et al. 2011).

The positive role of PRP in tissue regeneration and wound healing is undeniable. The major advantage of autologous PRP is that PRP has no adverse effects. However, there are number of variables involved in therapeutic use that make it difficult to standardize PRP as a product. Preparation methods, activation, platelet concentration, and the effect of the individual and physical form of the PRP are factors that have to be considered (Anitua et al. 2009). Production methods for platelet preparation differ greatly according to the metabolic state of the platelets and the presence of extracellular proteins such as fibrinogen (Ehrenfest et al. 2009). Because of the autologous nature of PRP, standardized results may not be obtained in all patients. In “personalized medicine”, each of the variables may be viewed as an opportunity to tailor the PRP according to the specific requirements of a particular individual or a certain tissue. However, further experimental research is required to optimize each of the variables and to establish the role of PRP in the treatment of tissue regeneration (Lana et al. 2014).

1.3.1.3.2 Synthetic growth factors

Numbers of promising *in vitro* cell culture studies and *in vivo* studies in animal models have shown enhanced healing when variety of synthetic growth factors is added. However, their clinical use remains limited due to their high cost, and mainly because methods for delivering

these synthetic growth factors are still under investigation or need further development (Demidova-Rice et al. 2012). Until now, the only FDA approved growth factors are osteogenic growth factor bone morphogenetic proteins (BMP-2 and BMP-7), and recombinant human platelet derived growth factor (PDGF-BB) - becaplermin. PDGF-BB, supplied in a gel form with sodium carboxymethylcellulose acting as a drug delivery vehicle, is relatively effecient in wound treatment (Beenken and Mohammadi 2009). However, the remaining problem is rapid degradation of the growth factor due to the proteolytic wound environment. Therefore there is insufficient concentration of the PDGF in the site of action (Tomic-Canic et al. 2008). Further development of effective drug delivery systems is therefore required to protect the labile growth factor, extend its presence at the injury site and minimize the systemic absorption of the growth factor not just in wound healing but also in other tissue engineering applications (Demidova-Rice et al. 2012).

1.4 Controlled drug delivery

The development of new drug delivery systems has been employed to tune release kinetics, to regulate biodistribution and to minimize toxic side effects, thereby enhancing the therapeutic potential of susceptible bioactive molecules or drugs.

An effective drug delivery system consists of a formulation or a device that enables growth factors, supplements or drugs to be delivered safely in a sustained and controlled manner to the required site. The drug delivery system is aimed at delivering and retaining a sufficient concentration of bioactive substances or drugs for an adequate period of time, thus significantly enhancing the treatment efficacy, and also minimizing potential adverse effects associated with undesired fluctuations in drug concentration or ineffectiveness of damaged drug molecules and toxicity of drugs (Zamani et al. 2013).

During the past few decades, various methods have been employed for fabricating effective drug delivery systems. Numerous nanotechnology-based drug delivery systems have been prepared, such as micro/nanoparticles (e.g. lipid or polymeric particles, nanoemulsions, liposomes) and electrospun nanofibers (Lima et al. 2012; Sill and von Recum 2008).

1.4.1 Micro/nanopraticles

Micro/nanoparticles, such as lipid or polymeric particles, nanoemulsions and liposomes, have been used as carriers for controlled delivery applications due to their ability to encapsulate variety of bioactive substances (e.g. low and high molecular mass therapeutics, antigens or DNA). Thus nanoparticles outperform conventional delivery of free drugs in terms of delivery of an encapsulated drug and its sustained release. Each system has its advantages and disadvantages. Polymeric drug-delivery systems can be synthesized to generate specific molecular weights and compositions, but their drug-carrying capacity is relatively low. In contrast, liposomes have a high drug-carrying capacity, but their release profiles are more difficult to regulate (Duncan 2003). Liposomes belonged to the first generation of nanocarriers approved by the US FDA, and they currently remain among the most widely used nanoparticles as carriers of drugs, small interference RNA (siRNA), peptides, proteins, viruses and bacteria, etc. (Ignatius et al. 2000; Lowery et al. 2011; Mufamadi et al. 2013).

1.4.1.1 Liposomes

Liposomes may be defined simply as spherical vesicles in which an aqueous volume is entirely enclosed by a membrane composed of lipid molecules (Figure 1.13). They were first described by British hematologist, A.D. Bangham, in 1965. His work led to the use of liposomes as the main model system for studying the physicochemical and other properties of biological membranes (Bangham et al. 1965).

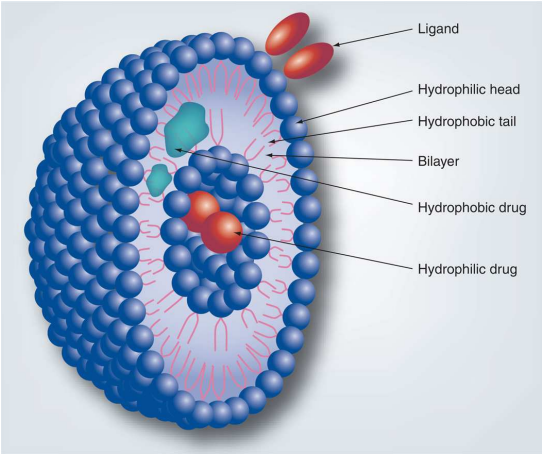

Figure 1.13 Schematic illustration of a liposome and its various drug-loading and surface functionalization modalities
Reprinted by permission from Future Medicine Ltd. [Nanomedicine] (Engineering nanomedicines for improved melanoma therapy: progress and promises, Di Bei, Jianing Meng and Bi-Botti C Youan, Nanomedicine, 5, 9, 1385-1399 (2010), DOI 10.2217/nnm.10.117), Copyright © (2010) [Future Medicine Ltd] (Bei et al. 2010).

1.4.1.1.1 Critical packing parameter (CPP)

Lipids that form liposomes are mainly those that have a critical packing parameter (CPP) in the range of 0.74-1.0 (Kumar 1991). The CPP is defined as the ratio of the cross-sectional area of the apolar to polar regions of the amphiphile,

$$CPP = \frac{V}{(l \times A_0)},$$

where V and l are the volume and the length of the hydrophobic tails respectively, and A_0 is the effective area of the hydrophilic head group (Figure 1.14).

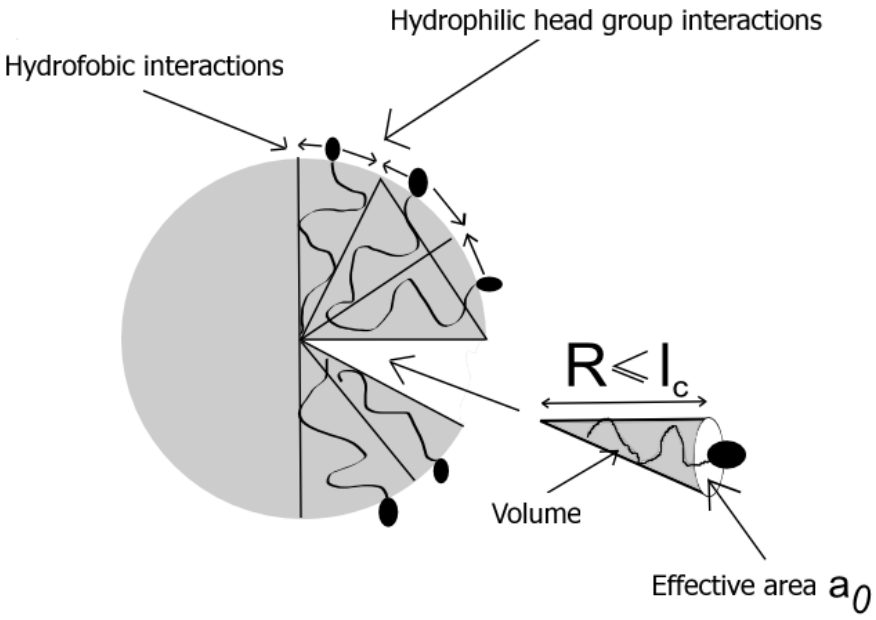

Figure 1.14 Parameters of the amphipathic molecule
Adapted from Kiraly Z., 2011 [Online] [Citacion 1.4.2011] (*koll1.chem.u-szeged.hu/colloids/staff/zoli/Pharmacy/Lecture%209.pdf. Király, Zoltán. University of Szeged, Department of Colloid Chemistry, Colloid Stability)* (Kiraly 2011).

This correlation predicts a range of structures according to the following conditions (Table 1.1) (Balazs and Godbey 2010).

Table 1.1 Structures predicted by the packing parameter

Critical Packing Parameter	Predicted structures	Examples
$CPP < \frac{1}{3}$	Spherical micelle	SDS (sodium dodecyl sulphate)
$\frac{1}{3} < CPP < \frac{1}{2}$	Cylindrical micelle	Lysophospholipids Phosphatidylinositol
$\frac{1}{2} < CPP < 1$	Flexible bilayers, vesicles	Phosphatidylcholine
$CPP = 1$	Planar bilayers	Phosphatidylcholine Sphingomyelin
$CPP > 1$	Inverted micelles, (Hexagonal (H_2) phase)	Diacylglycerol Phosphatidylethanolamine

1.4.1.1.2 Phase transitions and membrane permeability

The lipid bilayer of liposomes can be either in the solid-ordered (SO, also called the crystalline, solid, or gel phase), or liquid-disordered (LD, also called the liquid crystalline, fluid, or liquid phase), or liquid-ordered (LO) intermediate phase, based mainly on the packing of the lipid hydrocarbon chains (Mouritsen 2005).

One consequence of the packing of the fatty acyl chains within the center of a phospholipid bilayer is an abrupt change in its physical properties over a very narrow temperature range. The most consistently observed of these phase transitions is the transition occurring at the highest temperature, in which the membrane passes from a highly ordered gel or solid phase to a more mobile liquid-crystal phase. There is a considerable influence of hydrocarbon chain length and unsaturation, and of the ionic strength of the suspension medium and the type of polar head group, on the transition temperature (T_m) value for bilayer membranes composed of different phospholipids. The phase behavior of the lipid bilayer is determined by the van der Waals interactions between adjacent lipid molecules. In general, lipids with short or unsaturated fatty acyl chains undergo the phase transition at lower temperatures than do lipids with long or saturated chains. Lipids with a longer tail usually form more rigid structures, as the tails have more area to interact. An unsaturated double bond can produce a kink in the alkane chain. This kink will create extra free space within the bilayer which allows additional flexibility in the adjacent chains. Membranes with a large number of unsaturated hydrocarbon chains are therefore more fluid than bilayer membranes with a low number of double bonds in the hydrocarbon chains (Alberts et al.).

Most phospholipids have a phase transition of their lipid bilayer, from the SO phase to the LD phase, and vice versa. The LO phase only occurs when a membrane-active sterol, such as cholesterol, is included in the phospholipid bilayer (Barenholz 2002). Bilayers in the LO

phase are less sensitive to temperature changes, and are therefore more rigid, less permeable and more stable than bilayers in the LD phase (Mouritsen 2005).

The phase behavior of a liposome membrane determines such properties as permeability, fusion, aggregation, and protein binding, all of which can markedly affect the stability of liposomes and their behavior in biological systems - especially the stability of drug loading and the rate of drug release (Barenholz 2003).

1.4.1.1.3 Characterization of liposomes by size, morphology and charge

When pure lipids or lipid mixtures suspended in an aqueous solution are assembled, liposomes can exhibit a range of sizes and morphologies (Jesorka and Orwar 2008). They can range in size from the smallest vesicle (diameter~20 nm) to liposomes with a diameter of a micrometer or greater, equal to the dimensions of living cells. They can be characterized by a single bilayer membrane, or may be composed of multiple concentric membrane lamellae stacked one on top of the other (Samad et al. 2007).

Due to their large aqueous core, Unilamellar vesicles are preferentially used for encapsulation of hydrophilic drugs. Due to their high lipid content, multilamellar vesicles (MLV, > 0.5 µm in diameter) are preferentially used to passively entrap hydrophobic drugs. MLV can then be downsized by various methods to form either large unilamellar vesicles (LUV, >100 nm in diameter) or small unilamellar vesicles (SUV, 20–100 nm in diameter). Routine methods for downsizing liposomes include high-intensity low-frequency ultrasound (LFUS) and extrusion (New 1990). SUVs have a longer half-life than MLVs. They are therefore not eliminated from the blood circulation as rapidly as large liposomes. It is therefore evident that the enhanced mononuclear phagocyte system (MPS) uptake of liposomes by the liver is size-dependent (Harashima et al. 1994).

Several approaches have also involved modulating the liposome charge to reduce MPS uptake. The overall charge is characterized by the hydrophilic parts of the lipid molecules,

and has a relevant influence on the stability of the liposome in the biological environment. In general, anionic liposomes (such as phosphatidyl serine, phosphatidyl glycerol, and phosphatidyl inositol) have a shorter half-life in the blood than do neutral liposomes (phosphatidyl choline molecule, sphyngomyelin and phosphatidyl ethanolamine). The negatively charged head group prevents efficient DNA compaction; gene delivery by anionic lipids is therefore not very efficient (Nishikawa et al. 1990). Cationic liposomes have been widely used as efficient transfecting vectors in gene delivery applications (Li et al. 2011). A solution of cationic lipids, often formed with neutral helper lipids, can be mixed with DNA to form a positively charged complex reffered to as a lipoplex (Wasungu and Hoekstra 2006). However, positively charged liposomes (such as ethylphosphocholine) are unstable when stored, exhibit some cytotoxicity both *in vitro* and *in vivo*, and are quickly removed from blood circulation (Senior 1986).

1.4.1.1.4 Stabilized liposomes

Many methods have been sought to stabilize liposomes, because of the stability problem, rapid clearance from the blood, restricted control of encapsulated molecule release, and low or non-reproducible drug loading with conventional liposomes. The use of synthetic polymers for steric stabilization of liposomes led to the development of “stealth liposomes”. The surface of sterically stabilized liposomes is protected by polyethylene glycol (PEG) or by other polar surface ligands, such as carbohydrates. These PEG-liposomes, which are invisible to the immune system, showed decreased uptake into the MPS, increased circulation half-lives, increased stability to content leakage, and dose-independent pharmacokinetics (Immordino et al. 2006).

Immunoliposomes can be prepared by conjugating antibodies either directly to the lipid bilayer of liposomes in the absence (type 1) or in the presence (type 2) of PEG chains, or to the distal end of the PEG chain (type 3) (Figure 1.15).

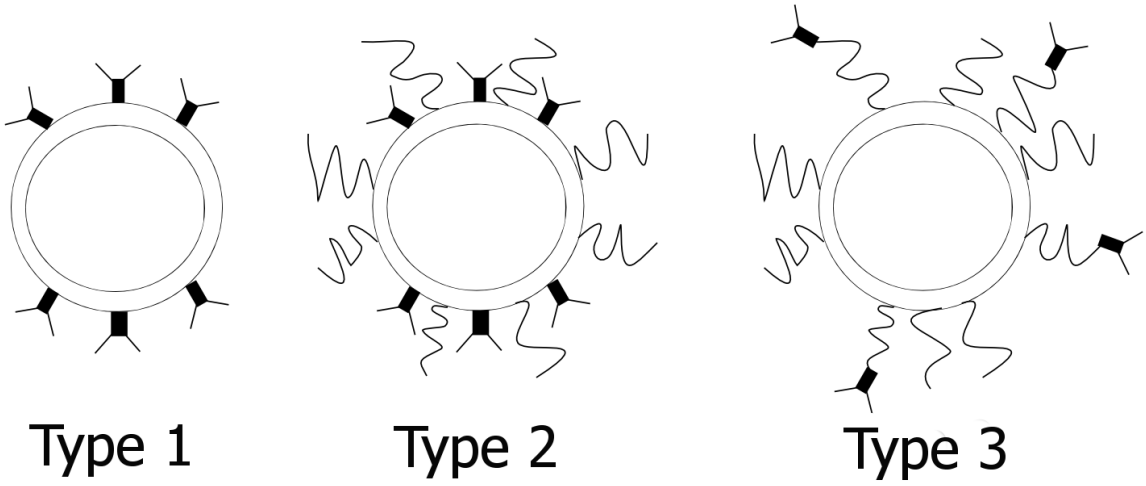

Figure 1.15 Schematic representation of the three types of immunoliposomes
(**Type 1**) Immunoliposome with the antibody covalently attached to the bilayer in the absence of PEG chains. (**Type 2**) PEG-liposome with antibodies attached to the liposomal bilayer in the presence of PEG chains. (**Type 3**) PEG-liposome with antibodies attached at the distal end of the PEG chain in a site specific manner. Adapted from Greplova J., 2009 (*Greplová, Jarmila. Využití imunoliposomů pro tansport a řízené uvolňování léčiv [Bachelor project] Prague, Charles University, Faculty of Natural Sciences, p.30*) (2009) (Greplova 2009).

However, whole monoclonal antibodies (MAb) coupled to liposomes are highly immunogenic. This disadvantage can be circumvented by the use of fragment antigen-binding (Fab-fragments) or single chain fragment variable (scFv). Other targeting moieties include peptides, growth factors, glycoproteins, carbohydrates, or receptor ligands (Sapra and Allen 2004). In addition, the number of ligand molecules exposed on the carrier surface can be increased, enhancing ligand avidity and the degree of uptake.

1.4.1.1.5 Application of liposomes

Liposome technologies have made considerable progress and several important formulations for the treatment of various diseases are now available commercially or in advanced clinical trials. Commercial vaccines based on virosome technology such as surface antigens derived from the hepatitis A virus (Epaxal® [Berna Biotech Ltd.] or from the influenza virus Inflexal® V [Berna Biotech España SA] have been developed (Copland et al. 2005). As a result of extensive research on liposomes, several antitumor liposome delivery systems have

been commerionalized, such as the doxorubicin–liposome system (Doxil®, Myocet® or Lipo-dox®), and the camptothecin–liposome and daunorubicin–liposome systems (DaunoXome) (Bei et al. 2010; Mross et al. 2004; O'Byrne et al. 2002). However, PEGylated liposomes (Doxil and Lipo-dox) displayed significant incidence of stomatitis in clinical trials, which may be related to PEGylation (Chang and Yeh 2012). Many anti-angiogenic and anticancer formulations based on cationic liposomes able to release their contents into the cytoplasm following endocytosis have been developed (Uwe and Heinrich 2006). Thermosensitive Thermodox® liposomes have found applications in the treatment of benign prostatic hyperplasia and clinical treatment of hepatocellular carcinoma (Wang et al. 2005). PH-sensitive, light-activated and ultrasound-induced drug release systems have been widely investigated (Kocer 2007; Puri 2014; Schroeder et al. 2009). NOVC-DOPE is an example of applying caged compounds in biological studies in the design of light-sensitive lipids (Bochet 2002). Liposomes are also used in diagnostic imaging as they can incorporate multiple contrast moieties, and they can specifically deliver the agent to the target area and enhance the contrasting signal (Immordino 2006).

High drug-carrying capacity is one of the most impressive advantages of liposomes. However, there are still many barriers to overcome before the full therapeutic potential of liposomes can be reached (Wang et al. 2005). The main reason for the limited success is that there are many design and application problems with drug delivery systems. These include drug accumulation in tissues, short half-life, low stability, and poor interaction with certain drugs. In addition poor control of drug release over a prolonged period limit their use for long-term drug delivery (Sharma and Sharma 1997). Combining liposomes with polymeric scaffolds could overcome the limitations of conventional liposomes and extend their use in biomedical engineering.

1.4.2 Elelctrospun nanofibers for drug delivery of bioactive molecules

In addition to serving as scaffolds, nanofibrous meshes can be designed to serve as bioactive delivery vehicles to induce a desired cellular or tissue response (Dahlin et al. 2011). Bioactive agents can either be immobilized or adsorbed on the surface of nanofibers (e.g. proteins (Huang et al. 2006b) or incorporated into the nanofiber mesh e.g. drugs (Martins et al. 2010) and proteins (Zeng et al. 2005). The main consideration for the development of successful delivery systems for tissue engineering are the bioactivity of the biomolecules adsorbed on the scaffolds or incorporated within the scaffolds, and the controlled release of these biomolecules according to the time frame of tissue regeneration (Ji et al. 2011).

1.4.2.1 Functionalization of the nanofiber surface

Electrospun nanofiber surfaces have been functionalized to achieve sustained delivery of various bioactive substances, just by physical adsorption (Mattanavee et al. 2009). Nie et al. loaded bone morphogenic protein-2 (BMP-2) into electrospun PLGA scaffolds by dipping the scaffold into an aqueous phase containing biomolecules. They showed that bone morphogenic protein-2 (BMP-2) adsorbed to PLGA scaffolds reached over 75% release within 5 days and almost complete release within 20 days (Nie et al. 2008). Simple physical adsorption of proteins on nanofiber surfaces has therefore seldom been used, due to the uncontrolled release profiles (Ji et al. 2011). Moreover, surface characteristics such as hydrophilicity/ hydrophobicity arising from the chemical composition of nanofibers may not be satisfactory for inducing selective cell adhesion, migration, and proliferation (Chung and Park 2007). The surface chemistry can be modified for optimal tissue engineering by cold plasma treatments, surface graft polymerization UV-ozone treatments, wet chemical methods and with co-electrospinning of bioactive agents and polymers (Mori et al. 1994; Darain et al. 2011; Mattanavee et al. 2009; He et al. 2005). Naturally derived biomolecules and specific cell

ligands on nanofiber surfaces were immobilized to modulate cell-matrix interactions, thus achieving improved cell adhesion, proliferation and differentiation (Wang et al. 2010). Functionalized nanofibers have also been prepared by adhesion of bioactive factor-loaded nanoparticles (Ruggeri et al. 2013). Immobilized nanoparticles interact with the targeted cells and also with the nanofiber scaffold on which the cells are cultured, thus creating a combined sustained and local release system (Santo et al. 2012). These combined release systems may be used for delivering therapeutically active compounds to the intended injury site (Anitua et al. 2008). The main disadvantages of using scaffolds of this kind are high burst release and poor control over the release profile of the loaded biomolecules (Ji et al. 2011).

1.4.2.2 Blend elelctrospinning for drug delivery of bioactive substances

Fibers prepared by blend electrospinning have been used as drug delivery vehicles with the ability to incorporate a wide range of bioactive molecules (Cui et al. 2010). Functionalized nanofibers have been produced directly by electrospinning polymer blends/mixtures with various chemical agents such as antibiotics, cytostatics, proteins, DNA, and small interfering RNA (Sill and von Recum 2008; Wenguo et al. 2010). Successful encapsulation of bacterial cells and viruses into blend nanofibers was recently reported (Zussman 2011). However, a common problem in this process is loss of the activity of the incorporated biomolecules (e.g., enzymes and growth factors) due to conformational changes in the organic solution environment. This problem was overcome by incorporating proteins with precipitously degradable polymers dissolved in polar solvents. Their ability to maintain enzyme activity was demonstrated by the incorporation of natural proteins, such as lipase and casein, horseradish peroxidase (HRP), alkaline phosphatase, and β-galactosidase (Xie and Hsieh 2003; Patel et al. 2006; Dror et al. 2008). The disadvantages of using these scaffolds are the

low aqueous stability of the nanofibers, and also burst release and low adhesion of cells to the hydrophilic polymer surface (Ji et al. 2011).

1.4.2.3 Coaxial electrospinning for drug delivery of susceptible biomolecules

Coaxial electrospinning is an attractive strategy for delivering susceptible biomolecules, because the core/shell fibers that are produced have great potential to preserve proteins during the electrospinning process. The hydrophilic core polymer facilitates the loading and preservation of protein bioactivity, while the hydrophobic shell allows fiber formation (Saraf et al. 2009). Nanofiber cores have been employed for encapsulating diverse bioactive substances such as antibiotics, drugs, DNA and proteins (Sill and von Recum 2008; Wenguo and et al. 2010).

Preparation of protein-compatible nanofibers has improved the preservation of protein activity, and has allowed prolonged release of proteins from nanofibers. Electrospun nanofibers have been used for delivering various growth factors. Sahoo et al. prepared nanofibrous scaffolds for the controlled delivery of basic fibroblast growth factor (bFGF), and showed greater mesenchymal stem cell (MSC) proliferation on coaxial nanofibers than is afforded by classical blend electrospun nanofibers (Sahoo et al. 2010). In addition, other proteins such as lysozyme; platelet-derived growth factor-bb (PDGF-bb) and nerve growth factor (NGF) have been successfully incorporated into nanofibers by coaxial electrospinning (Yang et al. 2008; Liao et al. 2006; Wang et al. 2012).

Successful preservation of molecular bioactivity requires a lesser amount of delivered molecules to promote optimized tissue regeneration. In addition, coaxial electrospinning provides homogeneous protein distribution throughout the fibers, and proteins can be delivered in a controlled manner (Ji et al. 2011). Reduced doses of biomolecules enable safe and cost-effective strategies for tissue engineering applications.

Development of biodegradable and biocompatible nanofibers with prolonged and controlled release of bioactive molecules prepared by electrospinning techniques, are therefore believed to be an important tool for modern regenerative medicine.

2 Aims of the study

1. Develop functionalized nanofibers as a simple delivery system for growth factors, and make nanofiber cell seeded scaffold implants a one-step intervention.
2. Develop a novel drug delivery system based on liposome-enriched nanofibers, concentrating on efficient delivery and on preserving the enzymatic activity of the delivered proteins. Demonstrate the potential of this system for tissue engineering applications by testing it *in vitro*.
3. Develop a novel drug delivery system for preserving and delivering platelet derivatives, and demonstrate the potential of the system for tissue engineering applications in an *in vitro* study.

3 Experimental part

The experimental part of this manuscript consists of 5 experiments divided into 3 sections.

In the first section of the experiments, a platelet functionalized scaffold was prepared by adhering washed platelets to PCL biodegradable nanofibers prepared by the blend electrospinning technique. The morphology of the system was examined by cryo-FESEM, and the adhered platelets exhibited strong interactions with the PCL nanofibers even after two hours of incubation with the nanofibers. The potential of the platelet immobilized functionalized scaffold as a nanoscale delivery system for natural growth factors was evaluated by a chondrocyte cell culture study *in vitro,* and a significant stimulation effect on chondrocyte viability was revealed. In addition, the production of chondrocyte-specific ECM, and thus the stimulation capacity of the functionalized nanofiber scaffold to induce type II collagen production, was confirmed using indirect immunofluorescence staining. The main advantage of a nanofiber system is the ability to immobilize the platelets, so that the release of the growth factors from the nanofibers is more stable and more sustained. A locally higher concentration of natural growth factors appropriate for cells can form promising functionalized scaffolds in a useful drug delivery system with comparatively short time scales.

In the preliminary study, functionalized PCL nanofibers were prepared with synthetic growth factors encapsulated in liposomes adhering to them. The interaction of the liposomes with the PCL nanofibers was visualized by FESEM. Quantitative analyses showed that around 29% of the liposomes remained tightly attached to the nanofiber mesh after overnight washing. The potential of the liposome immobilized scaffold as a delivery system for synthetic growth factors, and as a suitable system for MSCs adhesion and proliferation, was evaluated by confocal microscopy and dsDNA amount determination. The results showed that

the growth factors adhered to the surface of the PCL nanofibers stimulated cell proliferation mainly up to day 7, and that subsequently their effect was significantly lower. By contrast, the release of growth factors from liposomes resulted in gradual proliferation of MSCs throughout the study period. Moreover, both systems stimulated type II collagen production, which was confirmed by immunohistochemical staining using monoclonal antibody against type II collagen. The results of the preliminary study indicate that growth-factor enriched liposomes adhered to PCL nanofiber system could be useful as a drug delivery tool for application in short time scales, and could find broader use in tissue engineering.

In the second section of the experiments, the blend electrospinning technique was employed to encapsulate liposomes into hydrophilic PVA nanofibers. The incorporation ratio and the preservation of the enzyme activity of HRP were tested in nanofibers prepared by blend electrospinning. The effect of the PVA polymer solution on liposome stability was also tested. The results revealed by SEM and confocal microscopy indicated that blend electrospinning caused the liposomes to break and release their encapsulated material. HRP was encapsulated very effectively into the nanofibers. However, the incorporation ratio of the free enzyme into the nanofibers was almost twice as high as the ratio of incorporated liposomes with embedded HRP. Moreover, the biological activity of the encapsulated protein was greatly depressed in both samples. The results also confirmed that the PVA polymer concentration has a significant effect on the stability of the liposomes. Thus there are several key challenges to be overcome before these nanofibers can be implemented as a sustained delivery system for bioactive agents in practical tissue engineering applications.

To overcome the problem with blend electrospinning of conventional liposomes, a coaxial electrospinning technique was employed to prepare PVA-core/PCL-shell nanofibers with liposomes embedded in the 5% PVA core in the third section of the experiments. The study concentrated on delivery efficiency, and on preserving the enzymatic activity of the

delivered model protein (HRP). The water content in dry nanofibers was measured in order to examine whether liposomes are able to maintain their internal aqueous environment. Finally, the potential of the system was evaluated in a cultivation study using mesenchymal stem cells (MSCs). Visualization of nanofibers by FESEM and by confocal microscopy confirmed that the liposomes were embedded into the coaxial nanofibers and remained intact during and after the process of coaxial electrospinning. The cumulative release profile of FITC-dextran from PVA/PCL coaxial nanofibers with or without encapsulated liposomes was evaluated in a drug release experiment. The results showed the protective activity of the liposomes and the sustained release of encapsulated FITC-dextran. The protective effect of liposomes in the nanofiber core on enzymatic activity was verified. Enzymes encapsulated in liposomes can better survive the electrospinning process, probably because of the shielding effect of the lipid sphere. Interestingly, coaxial electrospinning enabled the retention of an aqueous environment inside intact liposomes embedded in nanofibers for several weeks of shelf storage. Finally, nanofibrous scaffolds containing embedded liposomes with encapsulated recombinant growth factors were more potent for stimulating MSC proliferation than coaxial nanofibers without liposomes. The results presented here show the potential of this drug delivery system using intact liposomes embedded for application in various fields of tissue engineering and regenerative medicine.

In the last study presented here, a novel drug delivery system was developed, based on nanofibers containing encapsulated platelet α-granules as a source of natural growth factors. α-granules contain most of the platelet secreted growth factors, and are therefore an ideal source for tissue engineering applications. The first task was therefore to isolate α-granules from platelets. The second task was focused on successful incorporation of isolated α-granules into the core of PVA/PCL coaxial nanofibers. This system should combine the benefits of natural growth factors with sustained release of the growth factor. Finally, a simple

demonstration of the performance of the system in stimulating the viability and chondrogenic differentiation of MSCs was evaluated. α-granules were introduced as an autologous source of growth factors. The isolated α-granules were small enough to be encapsulated into the nanofiber core, and were successfully incorporated into PVA/PCL coaxial nanofibers. Incorporation of α-granules into the 5% PVA was visualized by means of confocal microscopy, and the encapsulation efficiency was determined using overall protein quantification. The system preserved the biological activity of the growth factors that were delivered, and also stimulated the viability and the chondrogenic differentiation of MSCs *in vitro*. The results showed that coaxial nanofibers with embedded α-granules are a promising system for tissue engineering applications with comparatively prolonged time scales.

4 Methods

4.1 Preparation and characterization of platelet derivatives as natural source of growth factors

4.1.1 Preparation of washed platelets

Platelet rich plasma (PRP) prepared by the buffy coat method (2 x 10^{11} platelets in 250 ml of T-SOL buffer) was obtained from the Hematology Service of the General Teaching Hospital (Prague, Czech Republic). First, the PRP was washed to deplte the blood plasma and contaminating blood cells. Then, the PRP (volume 400 ml, platelet concentration 225 x 10^{9}) was centrifuged (2250 g, 15 min), supernatant was discarded and resulting platelets were washed in washing buffer (pH 6.5, 113 mM NaCl, 4.3 mM K2HPO4, 4.3 mM Na2HPO4, 24.4 mM NaH2PO4 and 5.5 mM glucose) as described by (Baenziger et al. 1971). Platelet washing was repeated three to four times. Contaminating leukocytes and erythrocytes were removed by further centrifugation (120 g, 7 min). Platelets were then resuspended in 40 ml of washing buffer and centrifuged at 120 g for 7 min to recover platelets that sedimented in the first 120 g spin. Platelets were pelleted by centrifugation (2000 g, 15 min) and washed once and finally resuspended in buffer pH 7.5 (109 mM NaCl, 4.3 mM K2HPO4, 16 mM Na2HPO4, 8.3 mM NaH2PO4 and 5.5 mM glucose). Manipulation of platelets and platelet-rich solution (TRS) was carried out in a sterile tissue culture hood in a clean room. TRS was stored in centrifuge tubes in a clean room until use. Temperature in the clean room was set at 22°C.

4.1.2 α-granule isolation

The washed platelets were sonicated using a Microson XL-2000 sonicator (Misonix Inc., NY, USA; output power 3 W, 3 cycles, 1 min. sonication, and 1 min. cooling) and then stored at -70°C. α-granules were isolated by 30-50% (w/v) sucrose gradient ultracentrifugation using an Optima L-90K ultracentrifuge (Beckman Coulter, CA, USA, rotor SW32Ti; 175 000 x g, 12h, 4°C). The resulting granules were separated. The resulting granules were separated into three fractions (lowest: α-granule rich fraction (ALPHA); middle: fraction one (FR1); and upper: fraction two (FR2), diluted in a washing buffer (volume ratio 1:1), and ultracentrifuged again (175 000 x g, 4 h, 4°C). The resulting pellets were resuspended in the washing buffer and stored at -70°C.

4.1.3 Dot Blot

The isolated gradient fractions (ALPHA, FR1 and FR2) and control sample (sonicated platelets) were characterized by the dot blot technique. A nitrocellulose membrane (Protran™, Whatman) was incubated with 2 µl of each sample (total protein concentration of samples: 0.3 mg/ml, assayed in duplicate) and blocked by 5% bovine serum albumin (BSA) in TBS with 0.05% (v/v) Tween 20 (TBS-T; pH 7.5; Sigma-Aldrich) for 1 h. The blocked membrane was washed twice with TBS-T and stained with a primary antibody against P-selectin (1:1000 dilutions, 4 h, 4°C; Exbio). The membrane was washed twice with TBS-T and then stained with a horseradish peroxidase-conjugated secondary antibody (1:2000 dilution, 2 h, 4°C; Promega). Finally, the membrane was washed in TBS and incubated with a tetramethylbenzidine substrate solution (Promega). The reaction was stopped after 10 min by rinsing the membrane with distilled water. The stained membrane was carefully scanned and densitometric analysis was performed using a Dot Blot Analyzer for ImageJ. The data are represented as an integration of the area density.

4.1.4 Fluorescent labeling of α-granules

The isolated α-granules were labelled with fluorescent carboxyfluorescein succinimidyl ester (CFSE) molecular probes. The reaction mixture, prepared from 1 ml of α-granule solution (total protein concentration: 1 mg/ml) and 100 µl of CFSE (1.5 mg/ml), was incubated for 90 min. in the dark at RT. The labeled α-granules were separated by gel chromatography (Sephacryl HR-500, GE Healthcare). Prepared, fluorescently labeled α-granules were electrospun by coaxial electrospinning and dry samples of nanofiber mesh were further analysed by confocal microscopy.

4.2 Liposome preparation and characterization

4.2.1 Liposome preparation

Unilamellar liposomes were prepared from soybean-derived L-α-phosphatidylcholine or L-α-phosphatidylcholine from egg yolk (PC; Avanti Polar Lipids, Inc.) using the extrusion method (Mayer et al. 1986). Briefly, 25 mg of soybean or egg yolk PC were dissolved in chloroform (1 mL); to prepare fluorescently labeled liposomes (FITC-LIP, FITC – labeled phospahtidylcholine purchased from Molecular Probes (FITC–PC: PC from soybean in a 1:1,000 molar ratio) was added and subsequently evaporated under a flow of N_2 at 4°C to form a thin lipid film. The dried lipid films prepared from PC were then resuspended in 1 mL of Tris-buffered saline (TBS; 150 mM NaCl and 50 mM Tris, pH 7.4) for the preparation of empty liposomes (LIP). For fluorescent spectroscopy measurements lipid films were resuspended in a 8-Aminonaphthalene-1,3,6-trisulfonic acid (ANTS) + *p*-xylene-bis-pyridinium bromide (DPX) system (1.5 ml of solution containing 15 mM ANTS, 45 mM DPX in TBS, pH = 7.4; Molecular Probe). Liposomes with encapsulated substances

were prepared by resuspending the dry lipid films in 1ml of TBS with 2 mg/mL HRP or 25 mg/mL fluorescein or 5 mg/mL FITC-dextran (10,000 MW; purchased from Sigma-Aldrich) or with a mixture of recombinant growth factors (0.1 µg/ml TGF-β; 5 µg/ml bFGF, 10 µg/ml IGF-I in phosphate-buffered saline (PBS), LIPGF). To create unilamellar liposomes, the obtained multilamellar liposomes were extruded several times through polycarbonate filters with a well-defined pore-size (1 µm diameter) using an Avanti® Mini-extruder (Avanti Polar Lipids Inc.). Unencapsulated fluorescein and ANTS + DPX system was separated on a Sephadex G-25 column (Sigma-Aldrich). Unencapsulated FITC-dextran, HRP and a mixture of growth factors were separated from the encapsulated liposomes using a Sephacryl HR-500 column (GE Healthcare).

4.2.2 Measurement of liposome size

The average diameter and size distribution of the liposomes were measured using dynamic light scattering on a Zetasizer Nano ZS (model ZEN3601, Malvern Instruments Ltd). Experiments were carried out at 18ºC with a detection angle of 90°. The data were prepared using the Contin mode, and the results were given in average mean diameters reported as function of the size distribution and intensity.

4.3 Preparation and characterization of functionalized nanofiber scaffolds

4.3.1 Blend electrospinning of nanofibers

10% (w/v) solutions of poly-ε-caprolactone (PCL) with a molecular weight (MW PCL) of 40 000 (Sigma-Aldrich) dissolved in chloroform:ethanol (9:1) were prepared for platelet adhesion studies. 24% (w/v) solutions of PCL with a molecular weight (MW PCL) of 45 000

(Sigma-Aldrich) dissolved in chloroform:ethanol (8:2) were prepared for liposome and growth factor adhesion studies.

A mixture of 12% (w/v) polyvinyl alcohol (PVA, Sloviol®) with empty liposomes or TBS buffer was prepared for the quantification of lipid incorporation and water content. A mixture of 12% (w/v) PVA with 271 µg/mL HRP or 253 µg/mL HRP encapsulated into liposomes was prepared for enzymatic activity studies. A mixture of 12% (w/v) PVA with 5 mg/mL FITC-dextran (Sigma-Aldrich) encapsulated into liposomes was prepared for visualization by confocal microscopy. Electrospinning was carried out on a Nanospider^{TM} device as described previously in detail (Lukas et al. 2008). A high-voltage source generated voltages of up to 56 kV, and the polymer solutions were connected with the high-voltage electrode. The electrospun nanofibers were deposited on a grounded collector electrode. The distance between the tip of the syringe needle and the collecting plate was 12 cm. All electrospinning processes were performed at room temperature (RT; ~24°C) and a humidity of ~50%.

4.3.2 Coaxial electrospinning of PVA/PCLnanofibers

A 10% (w/v) poly-ε-caprolacton (PCL) solution was used as the shell solution for all prepared samples. For confocal microscopy the core solution consisted of 5% (w/v) PVA with fluorescein (25 mg/mL) or liposomes containing encapsulated fluorescein (25 mg/mL) (Fluka, Sigma-Aldrich), or FITC-dextran (5 mg/mL) or liposomes (25 mg/mL) containing encapsulated FITC-dextran (5 mg/mL) (Sigma-Aldrich), or α-granules (total protein content: 0.3mg/ml). For the cell proliferation studies the core solution contained either a mixture of growth factors (0.1 µg/ml TGF-β; 5 µg/ml bFGF, 10 µg/ml IGF-I in PBS; GF) or liposomes containing an encapsulated mixture of growth factors (0,03 µg /ml TGF-β, 0,7 µg /ml bFGF, 3 µg/ml IGF-I; LIP-GF) dissolved in 5% (w/v) PVA.

The coaxial spinneret apparatus consisted of 2 needles placed together coaxially (Lukas et al. 2009). Two syringe pumps were utilized to deliver the core and shell solutions, respectively. The flow rate was 5 mL/h for the core polymer and 2 mL/h for the shell polymer in case of liposomes, fluorescein, FITC-dextran and growth factors. For the preparation of coaxial nanofibers with incorporated α-granules, 12 ml of shell PCL solution and 4 ml of core PVA solution containing α-granules (total concentration of inserted proteins: 1.2 mg/fiber mesh) were used. Additionally, PVA/PCL nanofibers without α-granules were used as a control using similar parameters. A high-voltage power supply was used to generate voltages of up to 55 kV, and an aluminium plate collector was used as the receiving plate to collect the electrospun nanofibers. The distance between the tip of the syringe needle and the collecting plate was 12 cm. All electrospinning processes were performed at room temperature (~24°C) and a humidity of ~50%.

4.3.3 Coaxial electrospinning of PVA/PVA nanofibers

Readily dissolvable coaxial PVA/PVA nanofibers were prepared for studies on water content and enzymatic activity. A 12% (w/v) PVA (Sloviol R) solution was prepared as the shell solution for all prepared samples. For water content determination, the core solution contained empty liposomes or TBS buffer dissolved in 5% (w/v) PVA. For determination of enzymatic activity the core solution consisted of HRP (2 mg/mL) dissolved in 5% (w/v) PVA or liposomes with encapsulated HRP (888 µg/mL) dissolved in 5% (w/v) PVA. The coaxial spinneret apparatus consisted of 2 needles placed together coaxially (Lukas et al. 2009). Two syringe pumps were used to deliver the core and shell solutions, respectively. A high-voltage power supply was used to generate voltages of up to 55 kV, and an aluminum plate collector was used as the receiving plate to collect the electrospun nanofibers. The distance between the

tip of the syringe needle and the collecting plate was 12 cm. All electrospinning processes were performed at room temperature (~24°C) and a humidity of ~50%.

4.3.4 Scaffold composite preparation

Before cell seeding, PCL nanofibers were cut into round patches of 6 mm diameter. Scaffolds for adhesion of recombinant growth factor mixture (GF), liposomes with encapsulated mixture of recombinant growth factors (LIPGF) and fluorescently labeled liposomes (FITC-LIP) prepared for confocal microscopy analysis were sterilized using ethylene oxide at 37°C. Scaffolds for platelet adhesion were sterilized by immersing in 70 % ethanol for 30 min and then washed three times in PBS (pH 7.4). To enable adhesion, PCL nanofibers were immersed in: 6 ml of GF (0.1 µg/ml TGF-β; 5 µg/ml bFGF, 10 µg/ml IGF-I in PBS; GF); 6 ml of LIPGF (0,03 µg/ml TGF-β; 0,7 µg/ml bFGF, 3 µg/ml IGF-I in PBS; determined by ELISA; LIPGF) and incubated for 2 hours; 1 ml of FITC-LIP (25 mg/ml of FITC–PC: PC from soybean in a 1:1,000 molar ratio) or immersed into a liposome solution of ANTS + DPX for 60 seconds and rinsed with TBS (pH 7.4) overnight. PCL nanofibers were immersed in a platelet rich solution (380 x 10^6 platelets/ml) for either 14 h (PCL14) or 2h (PCL2). After the incubation time, scaffolds were rinsed in TBS repeatedly to remove non-adhered GF, LIPGF and FITC-LIP and in PBS to remove non adhered platelets. Additionally, pure PCL nanofibers were used as control samples.

4.3.5 Fluorescent spectroscopy measurements of liposome-nanofiber interactions

Nanofibers with adhered liposomes containing ANTS + DPX after rinsed and washed with TBS solution overnight, were subsequently dissolved in ethanol to release the ANTS + DPX system. Fluorescence measurement were performed as described in (Fiser and Konopasek 2009) on a FluoroMax-3 JY-Horiba spectrofluorimeter. Excitation and emission wavelengths

were 370 and 505 nm, respectively (both with bandwidths of 4 nm). A suspension (1.5 ml) was placed into a 1 x 1 cm quartz cuvette, and the recorded fluorescence intensities were corrected for the background (vesicles without ANTS and DPX, about 2% of total intensity) and for the effect of dilution due the addition of DPX and Triton X-100.

4.3.6 Cryo-field emission scanning electron microscopy

Cryo-field emission scanning electron microscopy (FESEM) was used to visualize nanofiber morphology, liposomes and platelets. Briefly, the sample was frozen rapidly in liquid N2 (-210°C). The sample was then transferred to the cryo-stage of the preparation chamber (ALTO2500), where it was freeze-fractured at −140°C, freeze-etched by raising the sample temperature until the sublimation of water started at −95°C for 10 min, and then coated with gold at −135°C for 60 s. After this preparation, the sample was placed on a cold-stage microscope and examined in the frozen state at a temperature of approximately −135°C. The specimen was observed at 1 kV in the GB-high mode and at 3 kV in the GB-low mode on a Jeol 7401-FE microscope.

Electrospun scaffolds were characterized in terms of fiber diameter pore size and porosity using mathematical stereological methods, as described in detail by (Pan and Phil 2006). Briefly, stereological parameters were measured from arbitrarily selected sections of the FESEM images in LUCIA software (Laboratory Imaging s.r.o., CZ). The distribution of fiber diameters was determined quantitatively from 200 measurements. The most probable void space radius, *r*p, that is the most probable radius of a spherical pore, was estimated using the method of Masounave et al. (1981).

$$r_p = \frac{1}{\sqrt{2\pi N_S}},$$

where N_S is the number density of fiber hits in a random cross section of the specimen.

The probability density of a void space radius, *r*, was estimated using a Masounave's formula (Masounave et al. 1981).

$$\rho(r) = 2\pi N_S r e^{-N_s \pi r^2}$$

Additionally, the size of the liposomes embedded in coaxial nanofibers was also evaluated from SEM micrographs using Ellipse software (Version 2, 0, 7, 1, ViDiTo).

4.3.7 Scanning electron microscopy

Air-dried samples of blend electrospun PVA nanofibers were mounted on aluminum stubs and sputter-coated with a layer of gold (~60 nm thick) using a Polaron Sputter-coater (SC510; Now Quorum Technologies Ltd.). The samples were examined in an Aquasem (Tescan) scanning electron microscope in the secondary electron mode at 15 kV.

4.3.8 Confocal microscopy

Visualization of fluorescently labeled liposomes adhered to PCL nanofibers, prepared by the addition of FITC-labeled phosphatidylcholine to L-α-phosphatidylcholine from soybeans, and the distribution of encapsulated FITC-dextran and fluorescein within the prepared nanofibers was observed using a Zeiss LSM 5 DUO (FITC fluorescence, λ_{ex} = 488 nm, λ_{em} = 520 nm) confocal laser scanning microscope.

Visualization of platelets adhered to PCL nanofibers (Adher) were performed using P-selectin and actin staining. Platelets were incubated in 4% paraformaldehyde solution (pH 7.2) in TBS (50 mM Tris–HCl, 150 mM NaCl, pH 7.4) for 20 min at 4°C, then washed twice in TBS (pH 7.4). To permeabilize and block nonspecific binding, the platelet solution was incubated with 5% BSA and 0.5% Triton X-100 for 1 h. at RT and washed twice again in TBS (pH 7.4). Phalloidin (phalloidin–tetramethylrhodamine B isothiocyanate;

Sigma-Aldrich) and anti-P-selectin (CD62P antibody (C2) (FITC); Abcam) were added to the platelet-rich solution and incubated overnight at 4°C. Phalloidin–tetramethylrhodamine B isocyanate (1:50) and anti-P-selectin–FITC (1:500) in 1% BSA and 0.05% Triton X-100 solution were used to visualize the proteins. After washing twice in TBS, platelets were resuspended in TBS (pH 7.4) solution (5 ml) before being observed using a Zeiss LSM 5 DUO confocal microscope (phalloidin–tetramethylrhodamine B isothiocyanate λ_{ex} = 540–545 nm and λ_{em} = 570–573 nm, anti-P-selectin-FITC λ_{ex} = 494 nm and λ_{em}= 518 nm).

The dry samples of fluorescently labeled α-granules encapsulated into coaxial nanofiber mesh were analysed by confocal microscopy using a Zeiss LSM 5 DUO (CFSE fluorescence, λ_{ex} = 494 nm, λ_{em} = 515 nm).

4.3.9 Stability of liposomes in PVA solution

To quantify the degradation rate, unilamellar liposomes with the encapsulated fluorescent probe 8-aminonaphthalene-1,3,6-trisulfonic acid, disodium salt (ANTS) and quencher *p*-xylene-bis-pyridinium bromide (DPX; Invitrogen) dissolved in TBS were prepared by the extrusion method an separated, as described in Liposome Preparation.

The liposomal suspension (1.25 mL) was mixed with 16% (w/v) PVA solution and TBS to obtain 5 mL of liposome-PVA suspension with a PVA concentration ranging from 1–12% (w/v). Liposomes diluted with TBS buffer without the addition of PVA were used as a control sample. The solution was incubated for 30 min and the degradation ratio was calculated using fluorescence spectroscopy on a microplate reader (Synergy HT; λ_{ex}. 360–500 nm, λem. 520–540 nm). First, 100 μL of the samples were diluted with 100 μL TBS in order to lower the viscosity and fluorescence intensity of the liposomes in buffer (background intensity ***Io***), and the liposomes diluted in PVA (***I***) were measured. The intact liposomes in the diluted samples were lysed by the addition of 20 μL of 2% Triton X-100, and the ***IoTX*** for the control sample

and ***ITX*** for the liposomes diluted in PVA were determined. The degradation ratio was calculated as:

$$DR\ (\%) = \frac{I - (I_0 \times C)}{I_{TX} - I_0},$$

where C represents the background correction factor calculated as:

$$C = \frac{I_{0TX}}{I_{TX}}$$

All values represent the mean ± standard deviation (SD) of at least four independent experiments.

4.3.10 Phosphorus determination

To quantify the incorporation of phospholipids into PVA nanofibers prepared by blend electrospinning, we measured the amount of phosphorus in the nanofiber mesh. The nanofiber samples containing empty liposomes were first weighed and cut into four small pieces to determine the total amount of incorporated phospholipids. The samples were placed into calibrated tubes containing 0.3 mL of 70% perchloric acid. For combustion, the tubes were placed in a sand bath heated to 180°C for 60 min (the standards did not require combustion). The resulting metaphosphates were converted to orthophosphate by adding 2 mL of redistilled water to the cooled samples and mixing thoroughly. Subsequently, 0.25 mL of 2.5% ammonium molybdate solution followed by 0.25 mL of 10% ascorbic acid solution (freshly prepared) were added, mixed thoroughly, and heated for 5 min in a boiling water bath. After cooling the samples in a cold water bath for 5 min, the optical density at 820 nm was measured using a Unicam SP1700 UV/VIS spectrophotometer. In each series of measurements, parallel determinations were made of the blank values of the reagent solution and a standard preparation. The weight of the incorporated phospholipids ($m_{incorporated}$ =

$mg_{phospholipids}/mg_{sample}$) was calculated from the amount of measured phosphorus (1 mol of phospholipids = 1 mol of phosphorus):

$$m_{incorporated} = \frac{n \times M}{m_{sample}},$$

where *n* represents the amount of detected phosphorus, *M* represents the molecular weight of phosphatidylcholine (760.09 g/mol), and m_{sample} represents the weight of sample used for the analysis.

The incorporation of phospholipids (*IR*) was calculated as a ratio between the measured weight of phospholipids in the samples ($m_{incorporated} = mg_{phospholipids}/mg_{sample}$) and the weight of the total added phospholipids in the samples ($m_{total} = mg_{phospholipids}/mg_{total\ sample}$):

$$IR\ (\%) = \frac{m_{\ incorporated}}{m_{total}} \times 100$$

4.3.11 Measurement of the FITC-dextran release profile

To study the release profile of FITC-dextran, nanofiber meshes with or without liposomes were cut into round patches (6 mm diameter) and incubated with 1 mL of TBS at RT. At specific intervals, the TBS was withdrawn and replaced with fresh buffer. The time interval was determined according to the balance between the release of a detectable amount of FITC-dextran and the maintenance of the sink condition. Drug release was quantified using fluorescence spectroscopy. Briefly, 200 µL of samples and blank samples were measured on a multiplate fluorescence reader (Synergy HT; $\lambda_{ex.}$ 480–500 nm, $\lambda_{em.}$ 520–540 nm) and a background subtraction was performed. All values represent the mean ± SD of at least three independent experiments. The cumulative release profile of FITC-dextran was obtained, and the release half-time was determined as the time at which the initial fluorescence intensity (I_0) decreased to $I = I_0 \cdot e^{-1}$.

4.3.12 Determination of HRP activity

Nanofiber samples prepared either by blend electrospinning (PVA/HRP, PVA/liposomes with encapsulated HRP) or by coaxial electrospinning (PVA/PVA with HRP, PVA/PVA with HRP encapsulated in liposomes) were dissolved in dH2O, vortexed, and incubated overnight at 4ºC. The total protein concentration was determined by the Bradford assay (Bradford QuickStart; BioRad) using an enzyme-linked immunosorbent assay (ELISA) reader at 590 nm (Biotec, Synergy HT). Enzyme activity was measured colorimetrically using tetramethylbenzidine (TMB) as the substrate. The enzyme substrate reaction was terminated by the addition of 50 μL of 2M H2SO4 after 30 s. Enzyme activity was measured at 450 nm using an ELISA reader (Biotec, Synergy HT). All values represent the mean ± SD of at least 3 independent experiments.

4.3.13 Water Content Determination

To determine residual water content inside embedded liposomes, coulometric Karl-Fisher titration was performed. Dry PVA nanofiber meshes with empty liposomes were prepared by coaxial or blend electrospinning, whereas the control samples were prepared without liposomes, simply with TBS buffer. All samples were cut into small pieces of equal size and weighed (~20 mg/sample). Subsequently, the samples were wrapped in filter paper and measured. Blind samples prepared without nanofibers consisted simply of filter paper. Water content was determined by coulometric Karl Fisher titration on an 831 KF Coulometer (Methrom AG) with a diaphragm-free cell and HYDRANAL-Coulomat AG (Sigma-Aldrich) as the anolyte. All samples were measured in triplicate and the background was subtracted. The water content corresponding to liposomes in nanofibers was calculated as the difference between the values measured in the samples with and without liposomes. Overall water

retention (%) was calculated as a ratio of the measured water content (mg) to the theoretical overall water content in the liposomes (mg).

4.3.14 Determination of α-granule content

Another batch of coaxial nanofibers was produced to determine the α-granule content. The nanofiber mesh containing α-granules (overall protein concentration: 1.2 mg/nanofiber mesh) was incubated in 1 ml of chloroform for 4 h to dissolve the PCL shell. The proteins were denatured during chloroform extraction, which could have resulted in some protein loss. We used the same protocol for all samples. The nanofiber mesh was dried by chloroform evaporation, and 1 ml of distilled water was added to dissolve the PVA core and solubilize the proteins. Protein concentration was measured using the Quick Start Bradford protein assay (BioRad). Briefly, 200 µl of the sample or control (α-granule isolate) was mixed with 1 ml of Quick Start Bradford protein assay reagent and monitored at 450 nm using an ELISA reader (Synergy 2, BioTek), and the protein concentration was determined using a five-point standard curve. The α-granule incorporation efficiency was calculated from the ratio of proteins in the fiber mesh to the overall proteins in the α-granules used for electrospinning (1.2 mg/nanofiber mesh).

4.3.15 Enzyme-Linked Immunosorbent Assay

In order to determine the cumulative release profile of growth factors from nanofiber meshes with (LIP-GF) and without liposomes (GF) were cut into round patches (6mm in diameter) and time dependent release study was performed. Samples were incubated with 1mL of sterile PBS at 37°C. At specific intervals, the PBS was withdrawn and replaced with fresh buffer. The concentration of TGF-β, IGF-I and bFGF in the medium was determined by sandwich Enzyme-Linked Immunosorbent Assay (ELISA; DuoSet, R&D Systems) following the

manufacturer's instructions. Briefly, the samples were prepared by acidification of the collected medium with 1 M HCl for 10 min and neutralized by the addition of 1.2 M NaOH with 0.5 M HEPES. Captured antibodies were pre-coated onto 96-well plates and blocked by 5% (w/v) BSA dissolved in PBS-T overnight and washed twice with PBS-T. Then, 100 μl of samples or standards were added to each of the wells in triplicate, and the plates were incubated for 2 h at 4°C and washed twice with PBS-T, which was followed by the addition of 100 μl of biotinylated primary antibodies and the plates were incubated for 2 h at 4°C. The plates were washed twice with PBS-T, and each well was incubated with 100 μl streptavidin-conjugated HRP (20 min, 4°C) and again washed twice with PBS-T. The antigen-antibody complex was detected by colorimetric reactions initiated by the addition of 100 μl of TMB substrate solution (R &D Systems) to each well and the reaction was stopped after 20 min with 50 μl of 2 N H2SO4. The absorbance of the samples was measured at 470 nm with ELISA reader (SynergyHT, Biotek) and the concentration was determined by a six-point calibration curve. The cumulative release profile is represented as mass of released growth factor per scaffold in time. All values represent the mean ± SD of at least three independent experiments.

4.4 *In vitro* cell culture studies

4.4.1 Chondrocyte isolation, culture, and seeding on nanofiber scaffolds

Chondrocytes were isolated and cultures as previously described, with slight modifications (Filova et al. 2007). Briefly, thin slices of articular cartilage were aseptically removed from the left femoral trochlea of mature pigs (Slaughter House; Cesky Brod, Czech Republic) within 2 h of sacrifice. The cartilage was then sectioned into approximately 1 x 1 mm, placed in a collagenase solution (0.9 mg/ml, collagenase NJB, SERVA) and incubated in a

humidified incubator (37°C, 5% CO2) for 14 h. The cells were then centrifuged (300 x g, 5 min) and seeded in culture flasks. The chondrocytes were then cultured in Iscove's modified Dulbecco's medium supplemented with 10% foetal bovine serum, penicillin/streptomycin (100 IU/ml and 100 µg/ml), 400 mM L-glutamine, 100 nM dexamethasone, 40 µg/ml ascorbic acid-2-phosphate and ITS – X (10 µg/ml insulin, 5.5 mg/l transferrin, 6.7 µg/l sodium selenite and 2 mg/l ethanolamine) at 37°C in a humidified atmosphere with 5% CO2.

Three ethanol-sterilized scaffolds from each sample (i.e. PCL nanofibers with adhered samples (Adher) and control PCL nanofibers (PCL) were distributed on a 96-well plate. Chondrocytes were seeded on the scaffolds with a cell density of 20×10^3 cells/cm^2. The medium was not changed during the cultivation. After 1,5,10 and 15 days, cell viability and immunofluorescence staining were determined.

4.4.2 Mesenchymal stem cells isolation, culture, and seeding on nanofiber scaffolds

Bone marrow was aspirated from the iliac wing of a minipig into a 5 mL-syringe containing 1 mL PBS and 25 IU heparin under general anaesthesia. The mononuclear cells were isolated using gradient separation with the plasma substitute Gelofusine®. Briefly, bone marrow was mixed with 1.25 mL Gelofusine®. After 30 min, the upper and medium layers containing plasma, mononuclear cells, and erythrocytes were aspirated, and centrifuged at $270 \times g$ for 15 min. Subsequently, the medium layer with mononuclear cells was aspirated and seeded in tissue culture flasks. Adherent cells were cultured in Minimum Essential Medium (MEM) (with L-glutamine, PAA) containing 10% fetal bovine serum (Mycoplex, PAA), 100 IU/mL penicillin, and 100 µg/mL streptomycin. The cells were passaged using the trypsin–EDTA method before confluence was reached. The cells from the second or third passage were used for the cell culture study.

PCL scaffolds with adhered GF, LIPGF were prepared for the cell culture studies as described in the *4.3.4 Scaffold composite preparation.* PVA/PCL scaffolds with coaxially encapsulated GF or LIP-GF were prepared for the cell culture studies as described in the *4.3.2 Coaxial electrospinning of PVA/PCL nanofibers* section. Three scaffolds of each sample were cut into circles with a diameter of 6 mm, sterilized using ethylene oxide at 37°C, and put in a 96-well plate. The scaffolds were seeded with MSCs (37×10^3 cells/cm^2) and cultured in 200 μL MEM (Sigma-Aldrich), 1% fetal bovine serum, and penicillin/streptomycin for 14 days. The medium was not changed during cultivation. After 1, 3, 7, or 14 days, cell viability, proliferation, and DNA content were determined on coaxial samples. DNA content was determined and immunofluorescence staining analysis was performed on GF and LIPGF samples adhered on PCL nanofibers.

PVA/PCL scaffolds with coaxially encapsulated α-granules (ALF) and pure coaxial PVA/PCL scaffolds used as control samples were prepared as described in the *4.3.2 Coaxial electrospinning of PVA/PCL nanofibers section.* Three ethanol sterilized scaffolds from each sample were distributed in a 96-well plate. The scaffolds were seeded with MSCs (37×10^3 cells/cm^2) and cultured in 200 μL MEM (Sigma-Aldrich), 1% fetal bovine serum, and penicillin/streptomycin for 15 days. The medium was not changed during cultivation. Following 1, 7 or 15 days of cell seeding, cell viability and immunofluorescence staining analysis was performed.

4.4.3 Viability of seeded chondrocytes and MSCs

Cell viability of MSCs on PVA/PCL coaxial nanofiber scaffolds (GF, LIP-GF) was determined using the CellTiter 96® Aqueous One Solution Cell Proliferation Assay (MTS; Promega). At 1, 3, 7, and 14 days of cultivation the scaffolds, were transferred to a new 96-well plate containing 100 μL of fresh medium per well and 20 μL of CellTiter 96®

Aqueous One Solution Reagent. The formazan absorbance in 100 μL of the solution was measured (λ_{sample} = 490 nm, $\lambda_{reference}$ = 690 nm) after a 2-h incubation at 37°C and 5% CO2 using an ELISA reader (EL800; BioTek). The absorbance of the samples without cells was deducted from the cell-seeded samples.

Cell viability of chondrocytes on PCL scaffolds (Adher and pure PCL as a control), and MSCs on PVA/PCL coaxial nanofiber scaffolds (ALF and PVA/PCL as a control) was analysed using the 3-(4,5-dimethylthiazol-2-yl)-2,5-diphenyltetrazolium bromide (MTT) assay. 50 μL of MTT (1 mg/mL in PBS, pH 7.4) were added to 150 μL of the sample medium and incubated for 4 h at 37°C. The MTT component was reduced by mitochondrial dehydrogenase of metabolizing cells, to purple formazan. Formazan crystals were solubilized with 100 μL of 50% N,N-dimethylformamide in 20% sodium dodecyl sulphate (pH 4.7) were added. The results were examined by spectrophotometry in an ELISA reader at 570 nm (reference wavelength, 690 nm).

4.4.4 Cell proliferation evaluation

The proliferation of MSCs seeded on the PVA/PCL coaxial nanofibrous scaffolds (GF and LIP-GF) was determined using a colorimetric immunoassay based on the measurement of 5-bromo-2′’-deoxyuridine (BrdU), which is incorporated during DNA synthesis (Cell proliferation ELISA, BrdU, colorimetric; Roche Diagnostics GmbH, Germany). The assay was performed according to the manufacturer`s instructions. Briefly, on days 3 and 7, 120 μL BrdU labeling solution was added to each well, containing a scaffold and was allowed to incorporate into the cells in a CO2-incubator at 37°C for 2 h. Subsequently, the supernatant in each well was removed, and the scaffolds were incubated with FixDenat solution to fix the cells and denature the DNA at RT for 30 min. The supernatant was removed and, subsequently, 100 μL anti-BrdU-peroxidase (dilution ratio = 1:100) was added and kept at RT

for 60 min. After removing the unbound antibody conjugate, 100 µL of substrate solution were added, allowed to stand for 6 min, and the reaction was completed by adding 25 µL H2SO4 solution (1 M). Then, 100 µL of solution was transferred to a 96-well plate and measured within 5 min at 450 nm with a reference wavelength of 690 nm using an ELISA plate reader (EL 800; BioTek). The blank corresponded to scaffolds without cells, with or without BrdU.

4.4.5 DNA measurement

DNA content was determined using the PicoGreen Assay Kit (Invitrogen Ltd.) at 1, 3, 7, and 14 days on PCL scaffolds with adhered GF and LIPGF and PVA/PCL coaxial scaffolds (GF, LIP-GF) with cultivated MSCs. To process the samples for the analysis of DNA content, 250 µL of cell lysis solution (0.2% (v/v) Triton X-100, 10 mM Tris (pH 7.0), 1 mM EDTA) was added to each well containing a scaffold sample. To prepare the cell lysate, the samples were processed through a total of 3 freeze/thaw cycles, i.e., the scaffold sample was first frozen at −70°C and then thawed at RT. Between each freeze/thaw cycle, the scaffolds were roughly vortexed. The prepared samples were stored at −70°C until analysis. To quantify the number of cells on the scaffolds, a cell-based standard curve was prepared using samples with known cell numbers (range 100–106 cells). DNA content was determined by mixing 100 µL PicoGreen reagent and 100 µL DNA sample. Samples were loaded in triplicate and florescence intensity was measured on a multiplate fluorescence reader (Synergy HT, λ_{ex} = 480–500 nm, λ_{em} = 520–540 nm).

4.4.6 Fluorescence confocal microscopy

DiOC6 (3,3´-diethyloxacarbocyanine iodide) was used to detect adhesion of chondrocytes to PCL scaffolds (Adher, PCL) on day 1; and MSCs cells to scaffolds on day 1 after seeding on

PCL scaffolds with adhered GF and LIPGF and PVA/PCL coaxial nanofibers (ALF, PCL as control). 1 day after seeding of chondrocytes and MSCs on PCL functionalized scaffolds and after 1, 7 and 14 days of cultivation on PVA/PCL coaxial nanofibers (GF, LIPGF), the scaffolds seeded with cells were fixed with frozen methanol (-20°C), rinsed twice with PBS, incubated in 10 μg/mL 3,3′-dihexyloxacarbocyanine iodide (DiOC6; Invitrogen) for 45 min at RT, and then incubated in 5 μg/mL propidium iodide in PBS for 10 min. The scaffold was rinsed twice with PBS and scanned the same day. DiOC6 staining was used to visualize mitochondria and inner membranes, while propidium iodide staining was used to visualize cell nuclei. A Zeiss LSM 5 DUO confocal microscope at λ_{ex} = 488 and 560 nm and λ_{em} = 505–550 and 575–650 nm was used for DiOC6 and propidium iodide detection respectively.

4.4.7 Detection of chondrogenic markers using indirect immunofluorescence staining

The presence of type II collagen as a marker of chondrogenic differentiation in PCL samples (GF, LIPGF) on day 7 and 14; PCL samples (Adher, PCL) and PVA/PCL coaxial samples (ALF, PVA/PCL) on day 7 and 15 was confirmed using indirect immunofluorescence staining as described previously (Filova et al. 2010). Briefly, samples were fixed with 10% formaldehyde/PBS for 10 min and permeabilized by PBS with 1% BSA/0.1% Triton X for 30 min at RT. The samples were incubated with the primary antibody against type II precollagen (1:20 dilution, 1 h incubation at RT; Developmental Studies Hybridoma Bank). Following three washes with PBS/0.05% Tween 20 after 3, 10 and 15 min., samples were incubated with a secondary antibody (Alexa Fluor 488-conjugated goat anti-mouse IgG (H+L);Invitrogen), diluted 1:300 and incubated for 45 min at RT. The cell nuclei was counterstained by incubating with Hoechst stain for 15 min and subsequently washed three times with PBS/0.05% Tween 20. The stain was visualized using a Zeiss LSM 5 DUO confocal

microscope λ_{ex} = 488 and 560 nm and λ_{em} = 505–550 and 575–650 nm was used for Alexa Flour 488 and propidium iodide detection respectively

4.4.8 Statistical analysis

The results were evaluated statistically using One Way Analysis of the Variance (ANOVA) and the Student-Newman-Keuls method. The level of significance was set at 0.05. The data was presented as the mean ± SD (standard deviation).

5 Results and discussion

5.1 Functionalized nanofibers as a simple delivery system for growth factors

5.1.1 Functionalization of PCL nanofibers with adhesion of platelets

5.1.1.1 Results

5.1.1.1.1 Adhesion of platelets to PCL nanofibers

The development of functionalized nanofibers seems to be the major obstacle to their broader application in tissue engineering. PCL nanofibers were prepared by needleless electrospinning. The surfaces of the PCL nanofibers were functionalized by adhering platelets to the scaffold. In order to immobilize the platelets, the nanofibrous scaffolds were pre-incubated with a platelet-rich solution for 2 hours (PCL2) and for 14 hours (PCL14) (Jakubova et al. 2011). Cryo-FESEM microscopy was applied to demonstrate the interaction of the platelets with the PCL nanofibers. The adhered platelets exhibited strong interactions with the PCL nanofibers, even after 2 hours of incubation (Figure 5.1). The fiber morphology was not apparent due to residual frozen water. Two hours of incubation of PCL nanofibers with a platelet-rich solution was therefore sufficient for adhesion of the platelets, and there was no significant increase in the samples incubated for 14 hours. The interactions were directly visualized by confocal microscopy. The platelets were stained for actin and P-selectin expression. P-selectin is expressed in the alpha-granules of the platelets and granules of endothelial cells, and has previously been used as a marker for platelet visualization (Yang et al. 2009). As a major dynamic protein, actin is highly abundant in platelets. Staining of these

two markers provided evidence of the presence of platelets on the scaffolding system (Figure 5.1).

Figure 5.1 Platelet visualization on nanofibers
FESEM of immobilized platelet on the PCL nanofiber scaffold. The spherical element adhering to the surface of the fibers typically around 2-3 µm in diameter is platelet. The thickness of the gold sputter coat used for visualization increased the observed dimension of the platelet slightly. The non-fibrous morphology of the scaffold is caused by residual frozen water. The scale bar indicates 1µm.

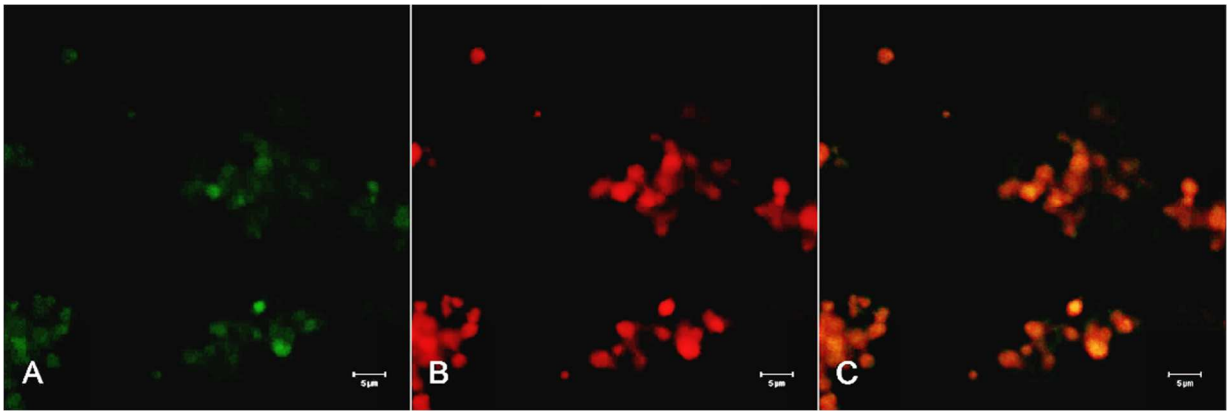

Figure 5.2 Confocal microscopy of platelets on PCL scaffolds
Visualization of platelets detected by anti-P-selectin immunostaining, with FITC, green (A), and anti-CD62 antibody, with tetramethylrhodamine B isocyanate (B), red. Part (C) represents the superposition of (A) and (B), which resulted in an orange tint (a less intense red tint) due to the high actin/P-selectin signal ratio. The scale bars indicate 5 µm.

5.1.1.1.2 Chondrocyte cell culture studies on PCL nanofibers with immobilized platelets

The biological effect of functionalized PCL nanofibers was tested in a chondrocyte cultivation study. A platelet-functionalized scaffold was prepared by the adhesion of washed platelets on PCL nanofiber scaffolds (Adher). A PCL scaffold without platelets served as a control. Chondrocytes were seeded on both scaffolds, and an MTT assay was performed on days 1, 5, 10 and 15 (Figure 5.3).

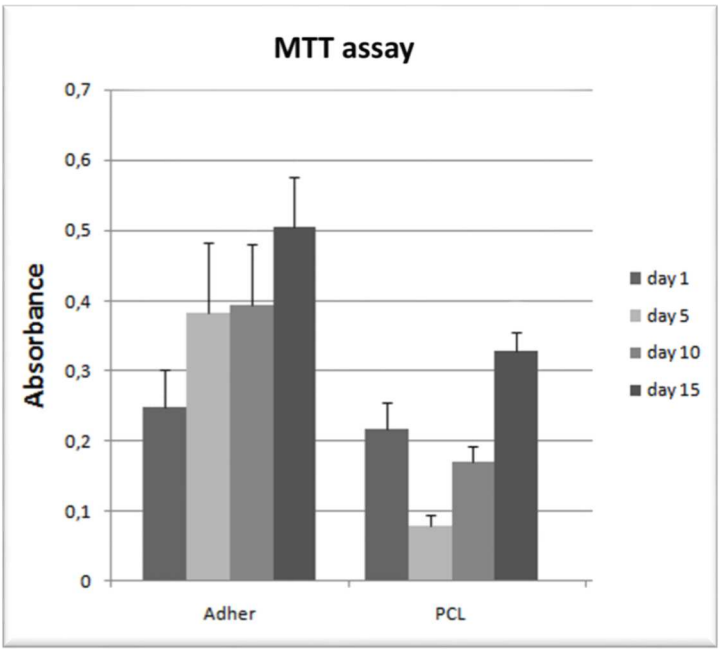

Figure 5.3 Cell viability of chondrocytes on PCL nanofibers with adhered platelets
The cell viability was measured by a 3-(4,5-Dimethylthiazol-2-yl)-2,5-Diphenyltetrazolium Bromide (MTT) Assay. The chondrocytes were cultivated on PCL scaffolds with adhered platelets (Adher) and pure PCL nanofibers, without the addition of platelets (PCL).

The Adher sample stimulated cell viability linearly from day 1 to 15. On day 1, there was no difference in cell viability among the samples. The MTT assay showed higher viability of chondrocytes on PCL scaffolds with adhered platelets (Adher) than on pure PCL nanofibers (PCL) on days 5, 10 and 15 (Figure 5.3), indicating positive stimuli of the growth factors released from the platelets.

Cell adhesion on day 1 was visualized using confocal microscopy (Figure 5.4). The cell membranes were stained with DiOC6 (green), and the nuclei were counterstained with propidium iodide (red). Cells adhered to both samples and were well spread. However, the adhesion to the PCL nanofibers containing adhered platelets was higher (Adher) than on the pure PCL nanofibers (PCL). Interestingly, micrographs of the Adher samples revealed that not only chondrocytes, but also platelets were detected by DiOC6 staining. Chondrocytes exhibited co-localization with platelets adhered to the scaffold.

In order to visualize matrix synthesis, immunostaining with an antibody against procollagen and immature type II collagen was performed on days 7 and 15. On the Adher samples, it was apparent that the cells formed large aggregates and produced a large amount of new type II collagen. However, the chondrocytes on the PCL scaffolds formed small cellular aggregates with moderate type II collagen production, indicating lower metabolic activity. Interestingly, the production of new collagen was lower on day 15 than on day 7 on both samples. The results were in accordance with the results from the MTT assay.

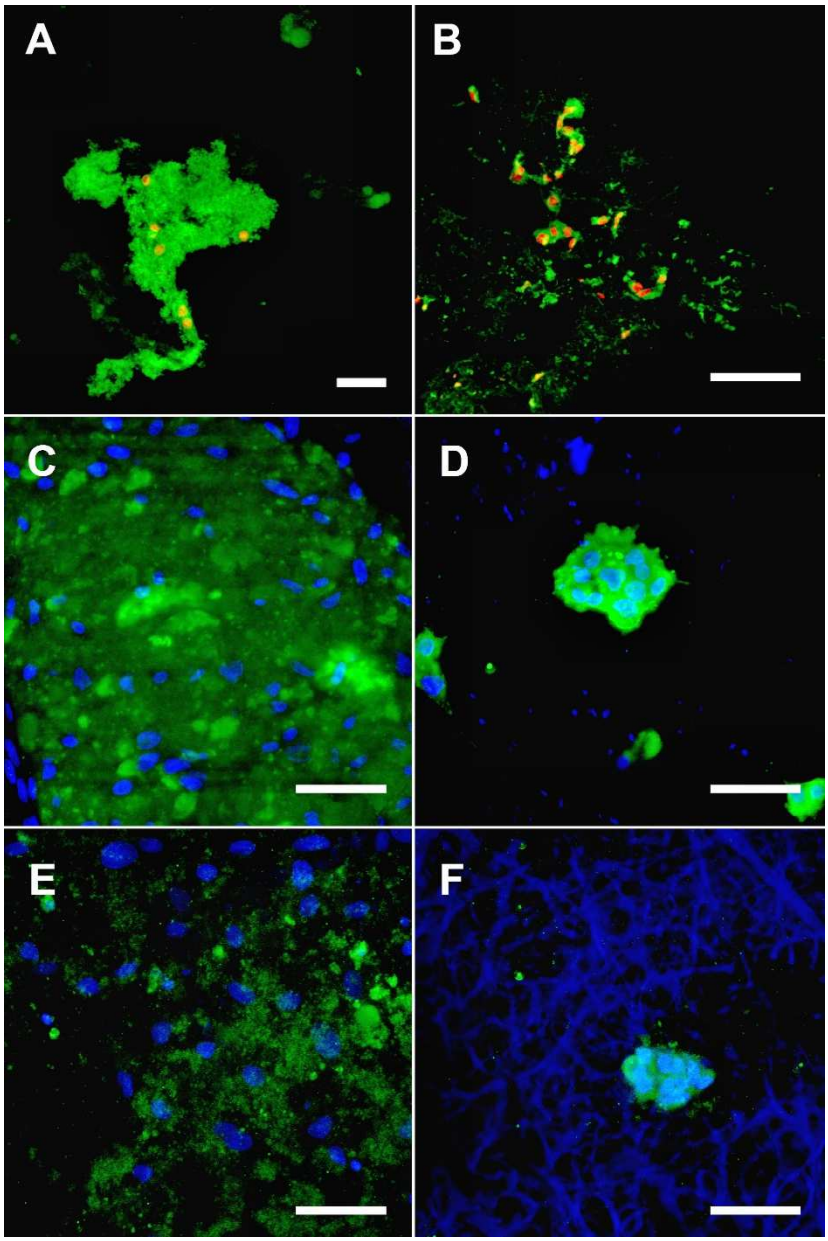

Figure 5.4 Confocal microscopy of chondrocytes on Adher and PCL scaffolds
Adhesion of chondrocytes on day 1 (A) to PCL scaffolds with adhered platelets (Adher) and (B) pure PCL nanofibers without the addition of platelets (PCL). Nuclei were stained using propidium iodide (red) and membranes were detected using DIOC6 staining (green). Synthesis of type II collagen on day 7 on (C) the Adher samples and (D) the PCL samples, and on day 15 (E) Adher and (F) PCL samples. Type II collagen was visualized by immunofluorescence (green) and cell nuclei were counterstained with Hoechst stain (blue). The scale bars indicate (A, B) 100 µm and (C-F) 50 µm.

5.1.1.2 Discussion

5.1.1.2.1 A platelet-functionalized scaffold was prepared by adhering washed platelets to PCL biodegradable nanofibers

Tissue engineering and regenerative medicine require the development of regulated delivery of growth factors. Delivery of native autologous growth factors, e.g. platelet derivatives, in optimized ratios is desired for tissue repair and tissue healing. Platelets are a natural source of growth factors for TGF-β, IGF-I, PDGF, FGF2, and EGF (Blair and Flaumenhaft 2009). Cells of blood origin play a primary role in hemostasis, initiate wound repair, and stimulate proliferation and differentiation of cells *in vitro* (White 1987; Mishra et al. 2009). The disadvantages of platelet-rich preparations are platelet delocalization, short-term retention and rapid washout from the application site (Isogai et al. 2005). A suitable scaffolding system for platelet immobilization would overcome these obstacles. Platelets have previously been immobilized on various gels, e.g. gelatin or fibrin (Anitua et al. 2007; Hokugo et al. 2005). In this study, platelets were immobilized on the surface of PCL nanofiber scaffolds for tissue engineering applications. Biocompatible and biodegradable PCL nanofiber scaffolds prepared by the electrospinning technique immobilized platelets efficiently after only 2 hours of pre-incubation in a platelet-rich solution. The platelets were not removed even after intensive rinsing with PBS buffer. A locally higher concentration of natural growth factors appropriate for cells can create promising functionalized scaffolds in a useful drug delivery system.

5.1.1.2.2 Platelet-functionalized scaffold enhanced chondrocyte proliferation *in vitro*

The potential of a platelet-functionalized nanofiber scaffold for cartilage tissue engineering applications was evaluated by simple cell culture studies. A study using porcine chondrocytes was performed to characterize the response of differentiated cells. In accordance with

previous reports (Drengk et al. 2009), a proliferative effect of platelet-functionalized nanofibers on chondrocytes was demonstrated in the experiments *in vitro*.

After an initial decrease, even the control PCL scaffolds exhibited good proliferation of chondrocytes. This result proved that PCL nanofibers provide a suitable matrix for chondrocyte cultivation. The result showed that the Adher sample stimulated cell viability linearly throughout the experiment. Improved adhesion of chondrocytes to platelet-functionalized scaffolds on day 1 was also confirmed by confocal microscopy. Additionally, the production of chondrocyte-specific ECM was characterized by immunostaining type II collagen. As has been mentioned above, the antibody that was used was specific for immature forms of type II collagen; the fluorescence signal was therefore proportional to the production of ECM, and reflected the stimulation capacity of the samples to induce type II collagen production. The results showed that the Adher samples induced cell proliferation from the beginning. However, there was lower matrix production on day 15 than on day 7. It is assumed that the decrease in type II collagen production in the Adher samples is associated with the higher numbers of cells.

The role of platelets in tissue engineering applications is growing rapidly (Tonti and Mannello 2008). A serum-free medium without the addition of growth factors cannot cause cell numbers to expand *in vitro*, so it is necessary to add growth factors. Numerous *in vitro* studies on cell growth and differentiation with the use of a variety of growth factors have been reported (Schuldiner et al. 2000; Drengk et al. 2009). However, the application of recombinant growth factors in human medicine is rather restricted. Blood derivatives such as platelets offer an acceptable solution, because they are a natural source of growth factors. The main advantage of a nanofiber system is the ability to immobilize the platelets, and as a result the release of growth factors from the nanofibers is more stable and more sustained. Another advantage of nanofibers with adhered platelets is that the cells are located in the close vicinity

of the source of the growth factors. It is hypothesized that the growth factors released from immobilized platelets on the scaffold can directly affect the cells. In a time-dependent study of bioactive factors in the culture medium, where the concentration of TGF-β was used to monitor the release of the growth factors from samples with adhered platelets, Buzgo et al. (2012) revealed that the half-time of TGF-β release was approximately 7 days. This system therefore appears suitable for drug delivery of growth factors for tissue engineering applications with comparatively short time scales. In order to improve the system, however, a more complex study is needed, involving the detailed effect of dose and release kinetics from platelet-derived growth factors and their effect on cell proliferation and differentiation.

5.1.2 Functionalization of PCL nanofibers with synthetic growth factor-enriched liposomes

5.1.2.1 Results

5.1.2.1.1 Interaction of liposomes with the PCL nanofiber scaffold

Liposomes may be combined with nanofiber scaffolds to promote local and sustained delivery of loaded bioactive agents. PCL nanofibers prepared by needleless electrospinning were employed as a model for fiber functionalization by liposomes. Functionalization was achieved by proper nanofiber incubation with liposomes, which immobilized the liposomes on the surface of the PCL mesh. The liposomes were prepared from a fluorescent phospholipid mixture (FITC–PC:PC in a 1:1 000 molar ratio), and were visualized by confocal microscopy (Figure 5.5). Clearly, the liposomes adhered very well to the PCL nanofibers and remained tightly attached to them, even after intensive rinsing with TBS buffer. Adhesion of the liposomes was also confirmed quantitatively by fluorescence measurements of liposomes containing DPX and ANTS, as described in the section on methods (*4.3.5. Fluorescent*

spectroscopy measurements of liposome-nanofiber interactions). Consequently, around 29% of the liposomes remained tightly bound to the nanofibers after they had been rinsed and washed with TBS solution overnight.

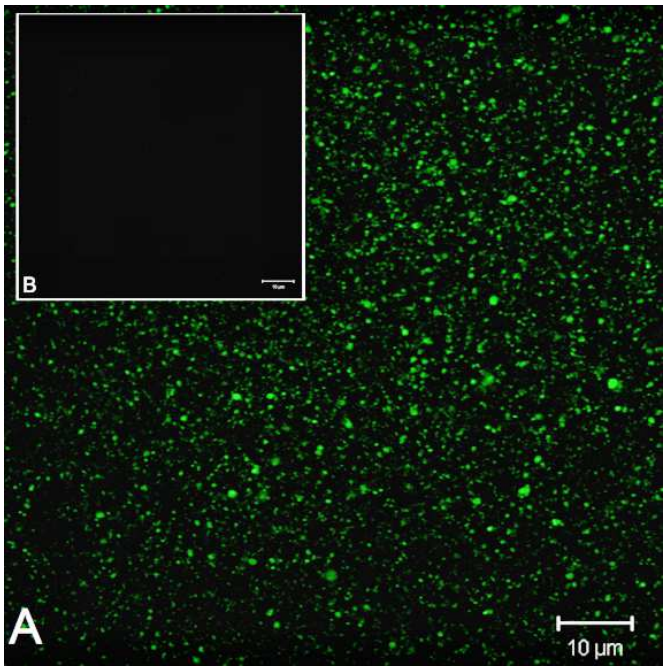

Figure 5.5 Confocal microscopy of fluorescently labeled liposomes adhered to a PCL nanofiber scaffold
Visualization of fluorescently labeled liposomes prepared by the addition of FITC-labeled phosphatidylcholine to L-α-phosphatidylcholine from soybeans using confocal microscopy. (B) A pure PCL nanofiber mesh without liposomes as a control. The scale bars indicate (A, B) 10 µm.

In additional, cryo-FESEM was applied to visualize the interactions of liposomes with PCL nanofibers. Tight interaction of the liposomes with the nanofiber surface was observed (Figure 5.6).

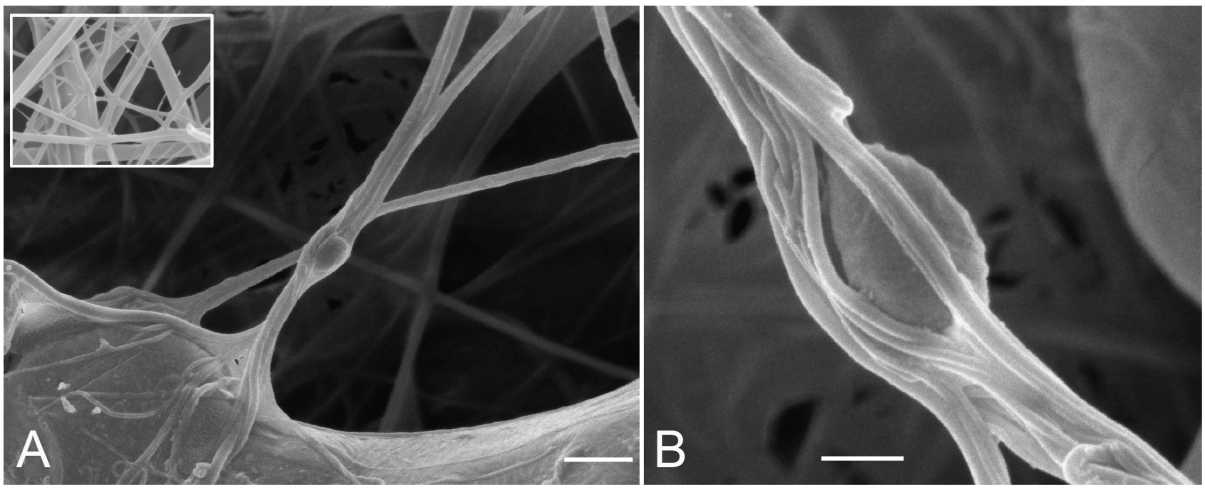

Figure 5.6 FESEM of adhered liposomes on PCL nanofibers
(A) FESEM of liposome adhered to PCL nanofibers. (Insert) A pure PCL nanofiber mesh without liposomes, as a control. (B) Details of an intact liposome tightly adhered to PCL nanofibers. The scale bars indicate (A, Insert) 1 µm and (B) 500 nm.

5.1.2.1.2 *In vitro* testing of PCL nanofibers with adhered liposomes (preliminary study)

In the preliminary study, a PCL nanofibrous scaffold with adhered liposomes was prepared and tested as a possible drug delivery system for various growth factors. TGF-β, bFGF and IGF-I have been shown to increase MSC proliferation (Shanmugarajan et al. 2011). A mixture of these growth factors was therefore either simply adhered to the surface of the PCL nanofibrous scaffold (GF) or was encapsulated in liposomes (LIP-GF) in order to have a positive influence on MSC adhesion and proliferation. The PCL nanofibers were functionalized by incubating the scaffolds with a GF and LIPG solution for 2 hours. To increase the effect of the growth factors that were delivered, the cells were cultivated in a medium containing only 1% FBS, and the medium was not refreshed during the cultivation period.

The number of cells on the scaffolds was quantified using a dsDNA-specific assay on days 1, 3, 7 and 14 (Figure 5.7).

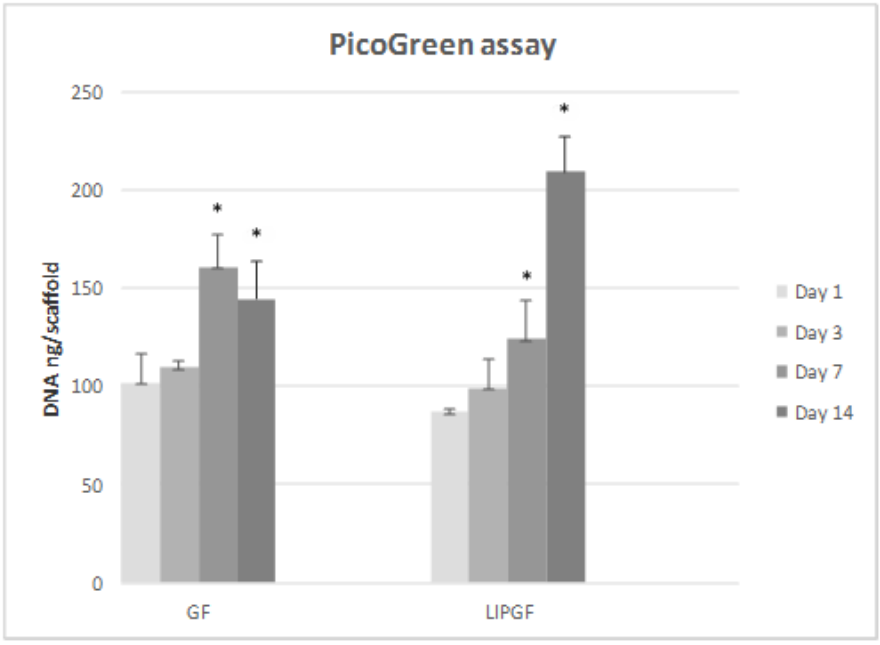

Figure 5.7 Determining the amount of dsDNA using the PicoGreen method
MSCs were cultivated on PCL scaffolds functionalized with growth factors (GF) and growth factors embedded in liposomes (LIPGF). This method showed a lower number of cells on the LIPGF scaffolds than on the GF scaffolds on day 7, and an increased number of cells on day 14. The level of statistical significance for the assay is indicated above the mean values (*$p<0.05$).

Statistically significant differences were detected from the third day of cultivation. On day 7, the number of cells on the GF scaffolds was significantly higher than on the LIPGF scaffolds. This suggested that the free GF adhered to the nanofiber scaffold enhanced the proliferation of MSCs in the 1% FBS medium from the early stages of the experiment until day 7. Interestingly, the concentration of DNA in the LIPGF samples was significantly higher on day 14 than on the GF samples. It is assumed that there is slower release of growth factors from the liposomes. The proliferation of MSCs graduated on the PCL scaffold with liposomes throughout the cultivation period, even in the medium with 1% FBS with a lower concentration of initial growth factors encpasulated into the liposomes.

The cell adhesion was visualized using confocal microscopy (Figure 5.8a, b) on day 1. The cell membranes were stained with DiOC6 (green), and the nuclei were counterstained

using propidium iodide (red). The cells were well adhered and were randomly distributed on both scaffolds.

In order to visualize the matrix synthesis, immunohistochemical staining using monoclonal antibody against type II collagen was performed on day 7 (Figure 5.8c,d) and on day 14 (Figure 5.8e,f). Secondary anti-mouse antibody was conjugated with AlexaFluor® 488, and was counterstained with propidium iodide. The scaffolds were visualized using confocal microscopy.

On day 7, moderate type II collagen was produced in the GF samples, and a larger amount of new type II collagen was produced in the LIPGF samples. A greater amount of type II collagen in the LIPGF samples indicates that growth factor release from the liposomes was sustained, and that it stimulated type II collagen production in a controlled manner (Figure 5.8c,d). Smaller cellular aggregates of cells were formed due to the unfavorable environment caused by the addition of 1% FBS to the medium, i.e. 10 times lower FBS concentration than in a standard cell culture. The production of collagen was higher in big groups of cells, which stimulated chondrogenic differentiation of MSCs.

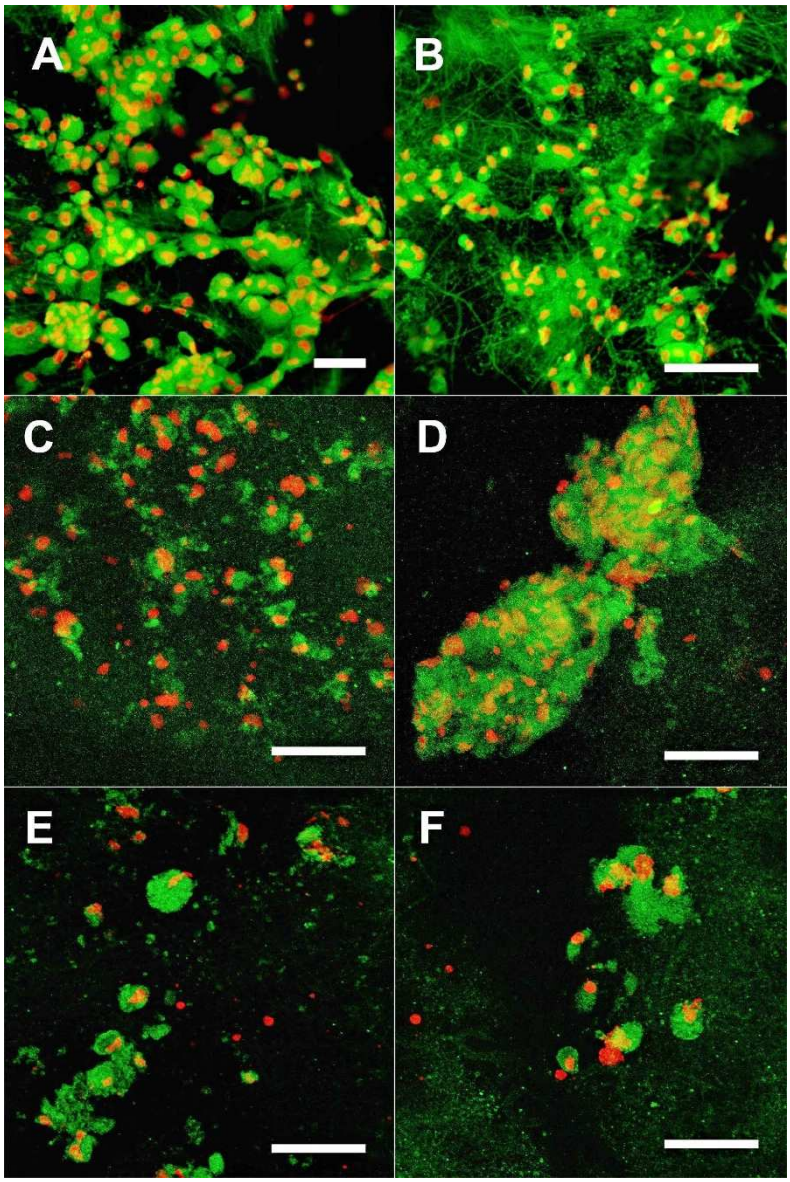

Figure 5.8 Confocal microscopy of MSCs on GF and LIPG scaffolds
Adhesion of cells on day 1 (A) to growth factors (GF) adhered to PCL scaffolds, and (B) to PCL scaffolds functionalized with growth factors embedded in liposomes (LIPGF). The nuclei were stained with propidium iodide (red) and the membranes were stained with DiOC6 (green). Synthesis of type II collagen on day 7 on (C) GF and (D) LIPGF. Synthesis of type II collagen on day 14 on (E) GF and (F) LIPGF. The scale bars indicate (A,B) 50 µm and (C-F) 20 µm. Type II collagen was visualized by immunofluorescence (green) and the cell nuclei were stained with propidium iodide (red).

5.1.2.2 Discussion

5.1.2.2.1 Liposomes adhere tightly to PCL nanofiber scaffolds

PCL nanofibers were used as a system for functionalization with liposomes. A tight interaction between liposomes and PCL nanofibers was clearly demonstrated by cryo-FESEM. Quantitative analysis showed that around 29% of the liposomes remained tightly attached to the nanofiber mesh after being rinsed with TBS overnight. These results were in accordance with the results of Rampichova et al., and reflected the large surface-to-volume ratio of the nanofibers (Rampichova et al. 2012). Nanofibers are extensively proposed for tissue engineering applications, and also as drug delivery systems (Dahlin et al. 2011). A unique advantage of liposomes is that the substances they encapsulate are protected from the environment. Thus, liposomes can serve as convenient delivery vehicles for a variety of biologically active compounds (Matteucci and Thrall 2000). A disadvantage of conventional liposomes is their short-term retention and fast washout from the site of application. Combining liposomes with nanofiber scaffolds could overcome these obstacles of conventional liposomes, and could serve as a local short-term delivery system for susceptible bioactive molecules in tissue engineering applications.

5.1.2.2.2 Liposomes with encapsulated growth factors adhered to PCL nanofibers stimulate MSC proliferation *in vitro*

It is necessary to develop effective drug delivery systems to protect labile synthetic growth factors and to extend their presence at the site of injury (Demidova-Rice et al. 2012). Labile synthetic growth factors were protected by incorporating them into liposomes, and PCL nanofibers were used as a model for fiber functionalization by liposomes. A preliminary study was made in order to evaluate the potential of the system as a nanoscale delivery system for synthetic growth factors. In a preliminary study, the adhesion and proliferation of MSCs on

functionalized scaffolds was confirmed by confocal microscopy and dsDNA amount determination. The cells were cultivated in a medium containing only 1% FBS, and in order to preserve the release of stimulating factors the medium was not refreshed during the cultivation period.

Adhesion of GF or LIPGF to the nanofiber mesh in the same location as the MSCs led to the localization of synthetic growth factors in the vicinity of the cells. Free growth factors and also growth factors incorporated into liposomes were immobilized on the nanofiber mesh, and were seeded together with MSCs on the nanofiber surface. Free growth factors that were adhered to the surface of the PCL nanofibers stimulated cell proliferation fitfully in the early stages of the experiment, mainly up to day 7, and subsequently their effect was significantly lower. By contrast, sustained release of growth factors from the liposomes to the neighboring cells resulted in gradual proliferation of MSCs during the study period.

Various *in vitro* studies have demonstrated the effects of IGF, TGF-beta and bFGF in stimulating the production of chondrocyte-specific ECM tissue (Luyten 1995). In the preliminary study, the induction of chondrocyte-specific ECM production and the expression of type II collagen were confirmed. The marker protein was produced on PCL scaffolds with growth factors, and also on PCL scaffolds with adhered liposomes containing growth factors. The results indicate that growth factors stimulate qualitatively superior matrix production and thus induce differentiation of MSCs even in 1% FBS. The advantage of nanofibers with adhered liposome-enriched growth factors is that there is slower, sustained release of growth factors. This system is therefore promising for the development of a controlled drug delivery system in tissue engineering, with shorter time scales.

High levels of free growth factors are correlated with an increased cancer risk. The possible use of lower concentrations and protection of growth factors from the surrounding

environment would minimize any potential risks. However, in order to optimize the system it will be necessary to carry out a more complex study showing in detail the influence of the dosage and the release kinetics of growth factors from liposomes adhered to nanofibers on MSC viability, proliferation and differentiation.

5.2 Incorporating bioactive substances into nanofibers by the blend electrospinning technique

5.2.1 Results

5.2.1.1 Encapsulating phosphatidylcholine liposomes into nanofibers by blend electrospinning

Blend electrospinning was employed to encapsulate liposomes into nanofibers to produce functionalized nanofibers. Unilamellar liposomes were dispersed in a 12% aqueous solution of PVA, and nanofibers with liposomes were electrospun using needleless electrospinning. In order to demonstrate that the blended nanofibers contained lipids, the total amount of incorporated phospholipids was determined (Table 5.1). The incorporation ratio of phospholipids into nanofibers prepared by blend electrospinning was 57.1 ± 5.8% (w/w).

Table 5.1 Determining and calculating the phospholipids incorporated into PVA nanofibers prepared by blend electrospinning
The phosphorus concentration was determined quantitatively. The total phospholipid concentration was >50%.

Samples	concentration of phospholipids (mg/mg)	total sample weight	phospholipids/total sample (mg)	Incorporation of phospholipids (%)
1	0,20	91,29	0,33	60,9
2	0,19	91,29	0,33	57,8
3	0,20	91,29	0,33	60,9
4	0,16	91,29	0,33	48,7
Arithmetic mean				57,1 ± 5,8

Nanofibers with liposomes containing FITC-dextran were visualized by means of scanning electron microscopy (SEM) (Figure 5.9a) and confocal microscopy (Figure 5.9c). These analyses did not show any intact liposomes; moreover, FITC-dextran was distributed in nonfibrous areas. The results indicate that the spinning technology caused the liposomes to break and release their encapsulated material.

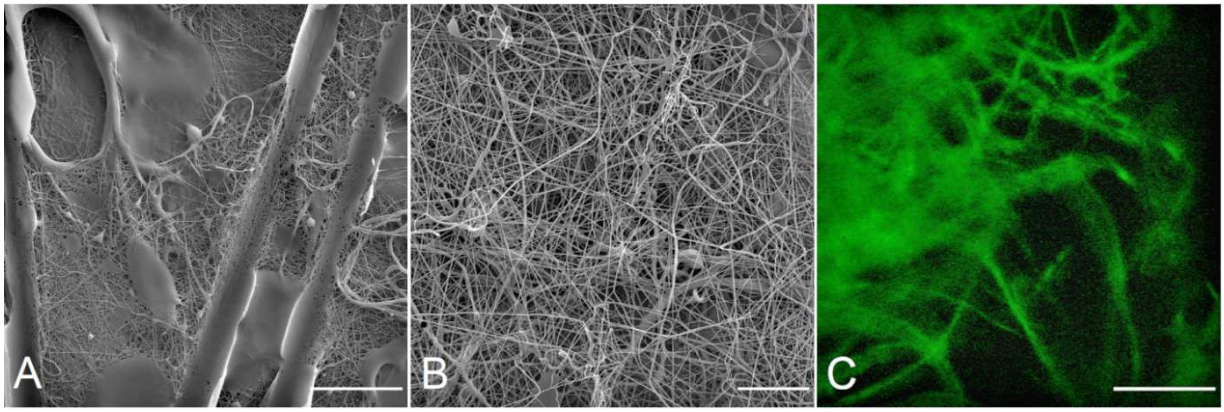

Figure 5.9 SEM and confocal microscopy analysis of blend electrospun PVA nanofibers with liposomes
SEM analysis of nanofibers with incorporated liposomes shows a large number of non-fibrous areas. The blend spinning technology causes the liposomes to break and consequently release their encapsulated material. The large non-fibrous areas are probably the result of the dissolution of PVA nanofibers caused by liposome breakage. (B) PVA nanofibers without liposomes as a control. (C) Visualization of liposomes containing FITC-dextran by confocal microscopy. Blend electrospinning of PVA nanofibers with liposomes does not keep the liposomes intact; consequently, FITC-dextran leaks from the liposomes and shows signals that are distributed throughout the sample. The scale bars indicate (A) 50 µm and (B, C) 20 µm.

5.2.1.2 Preservation of enzyme activity by blend electrospinning

The incorporation ratio and the enzymatic activity of HRP were tested in nanofibers prepared by blend electrospinning. Samples were prepared from a PVA solution containing HRP (B-HRP), or from a PVA solution containing HRP encapsulated in the liposomes (B-LIP; Figure 5.10). The sample concentration was correlated with the homogeneously distributed incorporation value to calculate the incorporation ratio. Proteins were encapsulated effectively, but the incorporation ratio of HRP was higher than the incorporation ratio of HRP encapsulated into the liposomes (Figure 5.10a). In addition, nanofibers prepared by blend electrospinning preserved the enzymatic activity of HRP at a very low level (Figure 5.10b).

Electrospun nanofibers prepared by blend electrospinning with liposomes were also tested for water content in a dry state. The highly sensitive and water-specific titration technique for water determination, i.e. coulometric Karl-Fisher titration, revealed that nanofibers prepared by blend electrospinning with liposomes contained 36.2 ± 0.9% water.

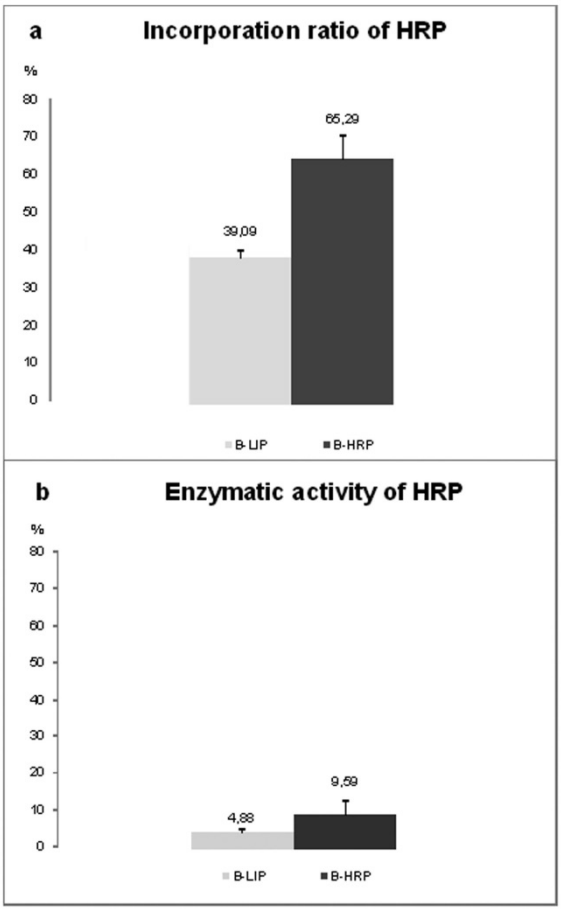

Figure 5.10 The incorporation ratio and enzymatic activity of HRP in nanofibers prepared by blend electrospinning
A comparison of HRP incorporation into nanofibers with (B-LIP) and without (B-HRP) liposomes prepared by blend electrospinning. The incorporation of HRP into the nanofibers was determined by the Bradford assay. (B) The enzyme activity in nanofibers prepared by blend electrospinning (B-LIP and B-HRP) was determined by converting the TMB substrate, and was correlated with the protein concentration.

5.2.1.3 The effect of the PVA polymer solution on liposome stability

In order to examine the effect of the PVA polymer solution on liposomes, the degradation ratio of liposomes in a 1–12% (w/v) PVA solution was determined. A higher degree of liposome degradation was observed with increasing polymer concentration (Figure 5.11). The degradation ratio of liposomes dissolved in 12% PVA, used for blend electrospinning, was (53.7 ± 8.7%). This indicated that more than one half of the liposomes were disintegrated before the electrospinning process started. For liposomes dissolved in 5% PVA, the

degradation ratio was lower (29.3 ± 2.5%), and approximately 70% of the liposomes remained intact.

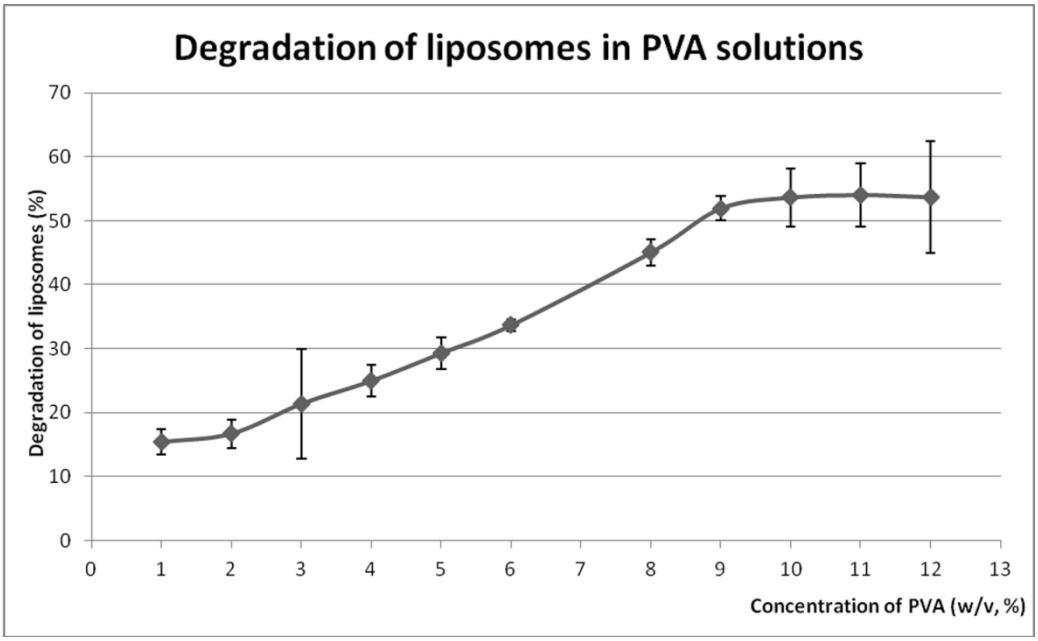

Figure 5.11 Degradation rate of liposomes in PVA solutions
The concentration of PVA was from 1–12% (w/v), and degradation was determined by fluorescence spectroscopy using ANTS as a fluorophore and DPX as a quencher. The degradation rate increased with the PVA concentration. All values represent the mean ± SD.

5.2.2 Discussion

5.2.2.1 Blend electrospinning does not conserve phosphatidylcholine liposomes intact

Functionalized nanofibers have been produced directly by electrospinning polymer blends/mixtures with various chemical agents (Zussman 2011). Progress in the preparation of protein-compatible nanofibers has improved the preservation of protein activity (Dahlin et al. 2011), but the proteins still remain in polymeric solutions and are not in their natural aqueous environment. This shortcoming could be solved by incorporating proteins into liposomes. Blend electrospinning was applied to encapsulate liposomes with FITC-dextran into PVA nanofibers. The results obtained by SEM and by confocal microscopy indicated that blend

electrospinning technology caused the liposomes to break and release their encapsulated material. This effect can be explained by the higher osmotic pressure of the blend PVA samples during the electrospinning process (Reznik et al. 2006). Osmotic pressure reportedly affects the viability of electrospun bacterial cells, indicating that this parameter may play a role in membrane systems, including liposomes (Salalha et al. 2006). A second factor affecting liposomal stability during the electrospinning process is shear stress (Reznik et al. 2006). The hypothesis is that during the process of blend electrospinning, the hydrodynamic forces disrupt the liposomal membrane and the large amount of water that evaporates during the fiber-forming process keeps the liposomes from reforming.

5.2.2.2 Blend electrospinning is not suitable for preserving HRP activity

The ability of nanofibers to maintain enzyme activity was demonstrated by the incorporation of natural proteins such as lipase and casein, HRP, alkaline phosphatase, and β-galactosidase (Dror et al. 2008; Patel et al. 2006; Xie and Hsieh 2003). Most proteins can only be dissolved in aqueous media. The polymers used for blend electrospinning of proteins are therefore required to be water soluble. PVA nanofibers were therefore used in the enzyme activity study. Blend electrospinning was applied for encapsulating HRP or liposomes with incorporated HRP into PVA nanofibers. The results confirmed that HRP was encapsulated very effectively into the nanofibers. However, the incorporation ratio of free HRP into the nanofibers was almost twice as high as the ratio of incorporated liposomes with embedded HRP. Moreover, the biological activity of the encapsulated protein was highly depressed in both samples and the measured water content in the dry nanofibers prepared by blend electrospinning with liposomes was less than 40%. One of the disadvantages caused by blend electrospinning is that the enzyme is not only encapsulated inside the fibers, but also resides on the surface of the nanofibers. Thus, loss of enzymes and their activity occur during measurement and storage. The loss of enzyme activity could be also explained by limited

mobility, as the accessibility of the substrate to the enzyme is confined (Wang et al. 2009). Fiber porosity also plays an important role in enzyme substrate interactions. To improve the accessibility of the substrate to the active centers of the enzyme, Patel et al. (2006) removed a template compound (glucose and PVA) after electrospinning silicate-PVA-glucose-HRP nanofibers, achieving fiber formation with pore sizes as large as 4 nm into fibers with average diameter around 150 nm. Another problem – release of the enzyme from the fibers – could be alleviated by polymer coatings to the prefabricated fibers, or by using coaxial electrospinning. Further disadvantages of using such scaffolds are low aqueous stability, burst release, and low adhesion of cells to the hydrophilic polymer surface (Ji et al. 2011). Thus there are several key challenges to be overcome before blended nanofibers can be implemented in practical applications as a sustained delivery system for bioactive factors in tissue engineering (Dahlin et al. 2011).

5.2.2.3 PVA polymer concentration has a significant effect on liposome stability

The effect of PVA polymer solution, with a concentration from 1-12%, on liposome stability was tested. Our results showed that the degradation rate increased with the PVA concentration. More than half of the liposomes were disintegrated in a 12% PVA solution before the electrospinning process started. The degradation rate was lower when 5% PVA was used, and ~70% of the liposomes remained intact before the electrospinning process. However, it is difficult to achieve stable electrospinning process parameters when a low concentration PVA polymer solution is used. When there is a low concentration, an electrospray occurs instead of electrospinning (Deitzel et al. 2001). Concentration and other solution parameters (e.g. viscosity, surface tension, conductivity, etc.) play an important role in fiber formation during the electrospinning process (Li and Wang 2013).

Successful incorporation of cerasomes - organic-inorganic lipid carriers - into blend nanofibers was reported recently (Zha et al. 2012). Cerasomes were shown to survive

encapsulation by blend electrospinning because they are more stable than conventional liposomes. A modification of the liposomal composition that promotes a more stable structure and more stable solution parameters, in combination with the processing parameters, could therefore enable the incorporation into nanofibers.

5.3 Core/shell nanofibers with embedded bioactive substances as a novel drug delivery system

5.3.1 Coaxial PVA/PCL nanofibers with embedded liposomes as a drug delivery system

5.3.2 Results

5.3.2.1 Incorporating liposomes into nanofibers by coaxial electrospinning

To overcome the problem with blend electrospinning of conventional liposomes, the coaxial electrospinning method was used to prepare PVA-core/PCL-shell nanofibers with embedded liposomes. The core medium contained liposomes dispersed in a 5% PVA solution. Two needles that were placed together coaxially to deliver the core and shell solutions, respectively, formed the main part of the coaxial spinneret apparatus. Cryo-FESEM was applied to visualize the outcome (Figure 5.12). Stereological measurements identified two main populations of nanofibers in the fibrous PVA/PCL mesh without liposomes. The first population had an average fiber diameter that peaked at 50 nm and second peaked at 150 nm. The sample also contained a fraction of microfibers. The mean porosity was 83%, and the most probable void space radius r_p, i.e. the most probable radius of a spherical pore, was 0.33 µm ± 0.07 µm. Stereological analysis of the PVA/PCL fiber mesh with embedded liposomes showed a similar radius distribution of nanofibers. Thin nanofibers with an average radius of

50 nm dominated, followed by nanofibers with an average radius of 150 nm and 350 nm. The mean porosity was 90%, and the most probable void space radius, r_p, was 0.17 ± 0.04 µm. Both samples also consisted of small fraction of microfibers.

When compared with control samples prepared without liposomes (Figure 5.12 Insert), the morphology of the fibers, with the presence of round bulges, indicated that the liposomes were encapsulated in the PVA/PCL nanofibers (Figure 5.12a). These bulges 233.4 ± 36.9 nm in size indicated the location of the embedded individual liposomes. The size of the liposomes prepared for the electrospinning process was characterized by dynamic light scattering measurements. It was confirmed that their size ranged from 100 nm to 1 µm (Figure 5.13). Detailed SEM micrograph observations using Ellipse software revealed nanofibers with embedded liposomes 835.5 ± 2.8 nm in size (Figure 5.12b).

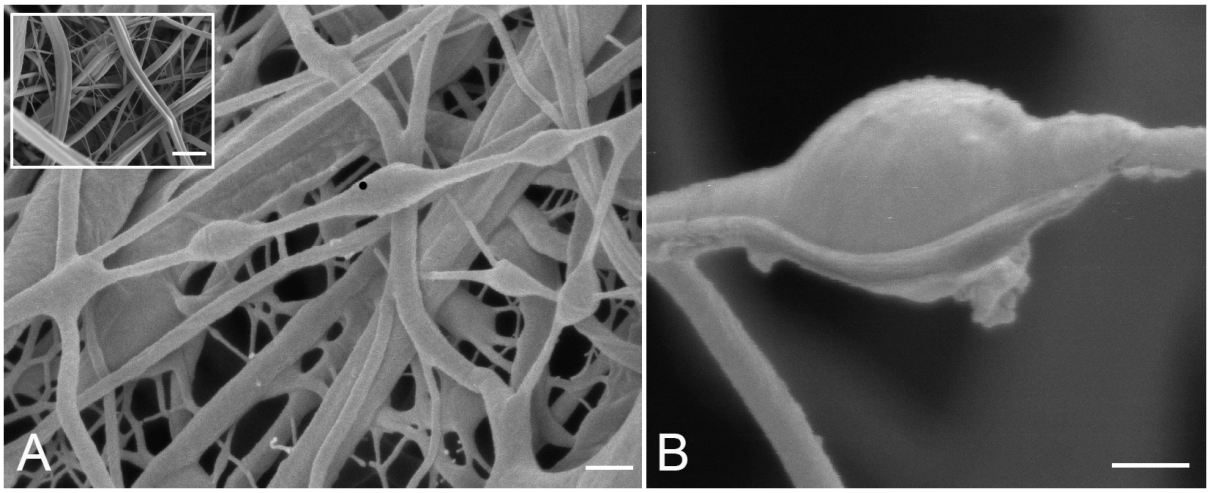

Figure 5.12 FESEM of coaxially electrospun PVA-core/PCL-shell nanofibers with encapsulated liposomes
(A) FESEM of liposomes embedded within PVA-core/PCL-shell nanofibers. (Insert) A pure PVA-core/PCL-shell nanofiber mesh without liposomes as a control. (B) Details of an incorporated intact liposome in a coaxially prepared nanofiber with a smaller nanofiber attached to the surface of the PCL nanofiber. The scale bars indicate (A, B) 300 nm and (Insert) 2 µm.

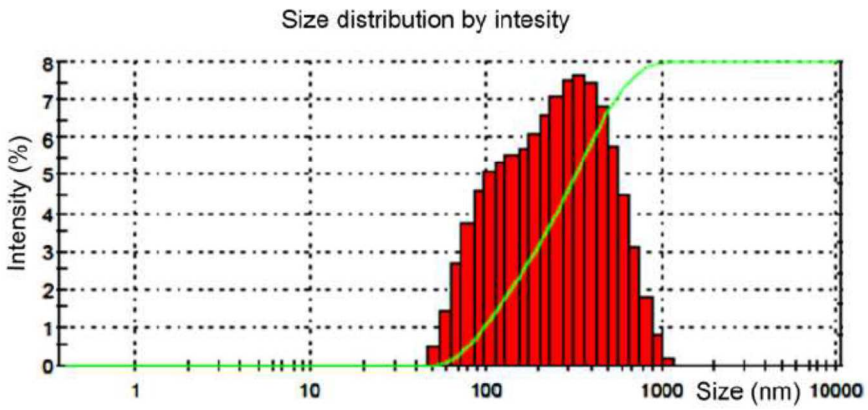

Figure 5.13 Size distribution of liposomes
The size distribution of the liposomes was detected by dynamic light scattering. The results were given in average mean diameters reported as a function of the size distribution and intensity.

Another batch of PVA/PCL nanofibers was prepared in order to investigate whether the embedded liposomes remained intact in the mesh. In this case, 10% PCL nanofibers were used as the shell solution, while the core solution consisted either of liposomes with encapsulated fluorescein dissolved in 5% PVA or of liposomes with encapsulated FITC-dextran dissolved in the same solution. The dry PVA/PCL nanofiber mesh with embedded liposomes was visualized by means of confocal microscopy (Figure 5.14), revealing distinct areas of liposomes containing either fluorescein (Figure 5.14a) or FITC-dextran (Figure 5.14c). In contrast, nanofibers prepared by coaxial electrospinning without liposomes, but with the addition of fluorescein (Figure 5.14b) or FITC-dextran (Figure 5.14d) in 5% PVA, showed a uniform distribution of the fluorescent substances throughout the nanofiber mesh. The localization of the fluorescent substances in the liposomes within a dry nanofiber mesh therefore suggests that the liposomes remained intact during and after the coaxial electrospinning process.

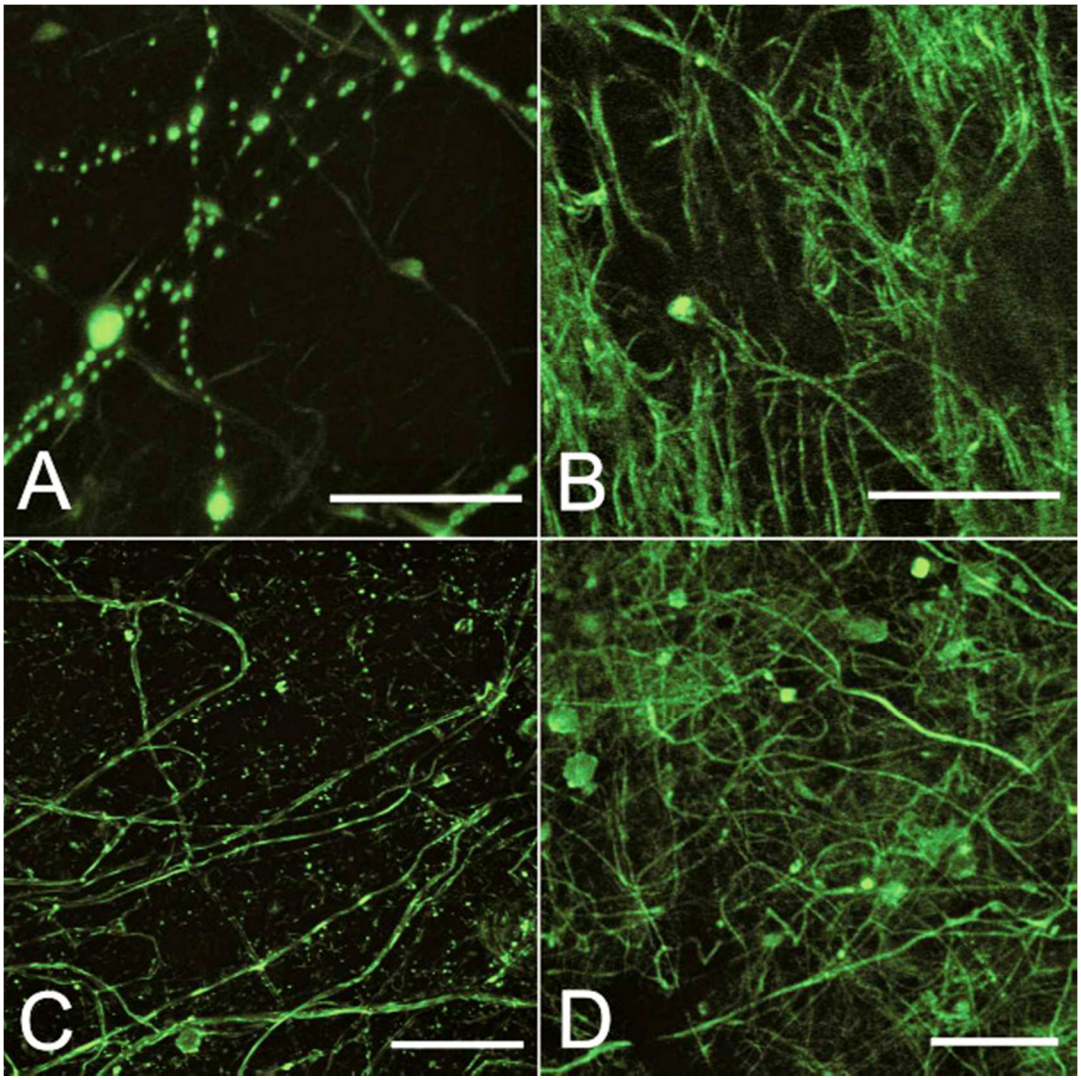

Figure 5.14 Confocal microscopy of PVA/PCL nanofibers prepared by coaxial electrospinning
A dry coaxially electrospun PVA/PCL nanofiber mesh with encapsulated liposomes containing either (A) fluorescein or (C) FITC-dextran with signals distributed inside the intact liposomes visualized by confocal microscopy. Coaxial nanofibers prepared without liposomes, but with the addition of either (B) fluorescein or (D) FITC-dextran show signals that are distributed throughout the fibers. The scale bars indicate (A, B) 20 µm and (C, D) 50 µm.

5.3.2.2 Cumulative release profile of FITC-dextran from coaxial nanofibers with intact liposomes

The system that had been developed was tested for drug release. To study the release profile from coaxially electrospun nanofiber meshes with or without liposomes, FITC-dextran incorporated into the nanofiber core was employed as the monitoring fluorescence probe. The

FITC-dextran samples were incubated at RT in TBS buffer, which was subsequently replaced by fresh buffer. The release profile of FITC-dextran was then obtained. The fractions that were collected were analyzed by fluorescence spectroscopy, and the cumulative release profile was calculated (Figure 5.15).

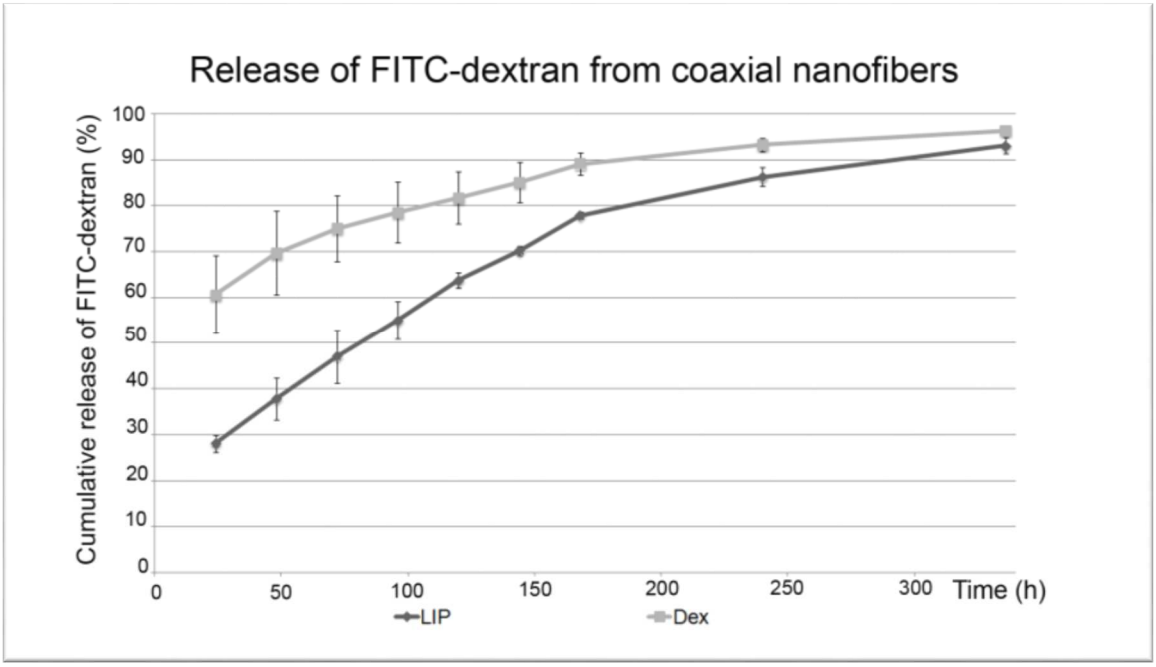

Figure 5.15 Cumulative release profile of FITC-dextran from nanofibers
A comparison of FITC-dextran release profiles from nanofibers prepared by coaxial electrospinning of PVA/PCL with (LIP) and without encapsulated liposomes (DEX). The release profile of the DEX sample showed an intensive burst release (60.6%) that was followed by a slow release. However, the release profile of the LIP sample showed a lower initial release (20%), which was followed by a sustained release. The release half-time (t_r) was 20 h for the DEX sample and 112 h for the LIP sample.

Core/shell nanofibers containing FITC-dextran (without liposomes) showed an intense burst release (60.6% of the FITC-dextran was released within 24 h), and the fluorescence in the collected TBS buffer was undetectable after 240 h. The release half-time was calculated as t_r = 20 h. Core/shell nanofibers with liposomes encapsulating FITC-dextran showed a slower initial release. Only ~20% of the FITC-dextran was detected after 24 h of incubation, which shows the protective function of the liposomes. The release half-time was shifted to t_r = 112 h for samples with FITC-dextran entrapped in liposomes. The wet (Figure 5.16a) and dry

(Figure 5.16b) coaxial nanofiber meshes were compared in order to explain the rapid FITC-dextran release from the nanofiber core.

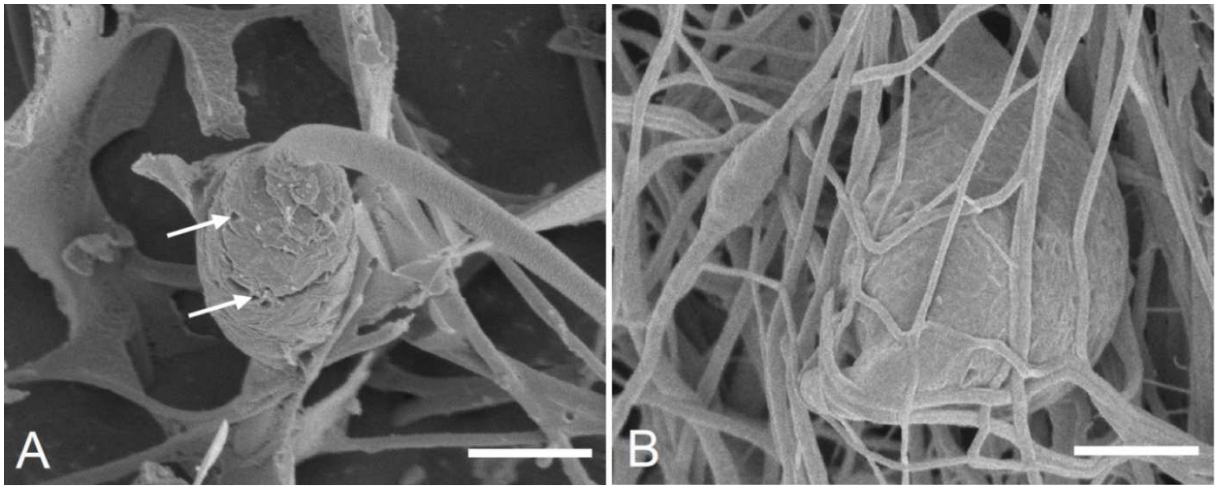

Figure 5.16 A comparison of dry and wet nanofibers indicates the formation of submicrometer pores in the nanofiber shell
Nanofibers prepared by coaxial electrospinning of PCL as a shell polymer with PVA and liposomes as the core polymer. (A) FESEM visualization of the wet nanofibers showed the formation of submicrometer pores on the nanofiber surface (see arrows). (B) The dry nanofibers visualized by FESEM microscopy exhibit smooth surfaces without pore structures. The scale bars indicate (A, B) 1 µm.

A comparison of the dry and wet coaxial nanofiber meshes indicated the formation of submicrometer pores in the PCL shell in the wet nanofiber samples (Figure 5.16a). These results indicate that the core content is released through newly-formed pores.

5.3.2.3 Preservation of enzyme activity by coaxial electrospinning

The enzyme activity of HRP was tested in order to verify the protective effect on enzymatic activity of liposomes in the nanofiber core. Nanofiber samples were prepared by coaxial electrospinning, where the shell solution was made from PVA and the core solution consisted either of PVA with HRP (K-HRP) or of PVA containing HRP encapsulated in the liposomes (K-LIP; Figure 5.17). The concentration of the sample was correlated with the homogeneously distributed incorporation value to calculate the incorporation ratio. Proteins were encapsulated effectively and the total amount of HRP in the nanofibers was comparable (Figure 5.17a). HRP activity was detected in both samples. However, the K-LIP samples

preserved HRP-specific activity (62.3 ± 7.9%) at a significantly higher level than the K-HRP samples (Figure 5.17b). In addition, nanofibers prepared with empty liposomes or without liposomes were tested for water content in a dry state. Interestingly, the samples prepared by coaxial electrospinning with liposomes showed 65.2 ± 0.8% water retention. These results indicate the preservation of intact liposomes filled with water, even in a dry state.

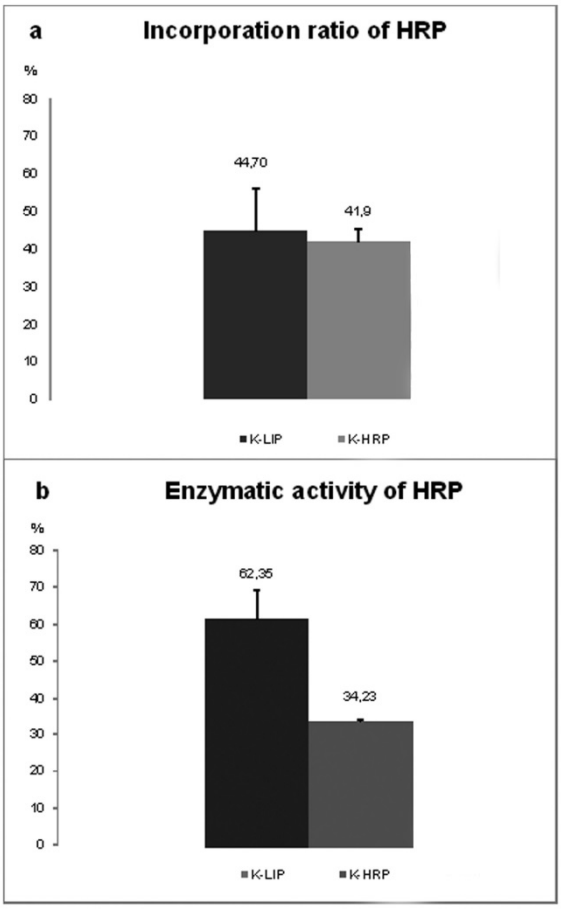

Figure 5.17 Incorporation ratio and enzymatic activity of HRP
A comparison of HRP incorporation into nanofibers with liposomes (K-LIP) and without liposomes (K-HRP) prepared by coaxial electrospinning. The incorporation of HRP into the nanofibers was determined by the Bradford assay. (B) The enzyme activity in nanofibers prepared by coaxial electrospinning (K-LIP and K-HRP) was determined by the conversion of the TMB substrate and was correlated with the protein concentration.

5.3.2.4 Mesenchymal stem cell culture studies on coaxial nanofibers with embedded liposomes for drug delivery of growth factors

The viability and proliferation of MSCs on prepared nanofibers was examined in order to demonstrate the potential of the coaxial system with embedded liposomes for drug delivery of growth factors. MSCs were seeded on PCL and PVA coaxial nanofibers with the addition of a mixture of growth factors (TGF-β, bFGF, and IGF-I) either dispersed in the core PVA solution (GF) or encapsulated in liposomes (LIP-GF). The concentrations of the released growth factors were detected by ELISA. The results showed controlled release of growth factors during the incubation period. The concentration of all three growth factors from the LIP-GF scaffold was lower than from the GF scaffold (Figure 5.18). From the scaffolds with embedded liposomes, 7.07 ± 0.65 ng of TGF-β, 420.02 ± 57.5 ng of IGF-I, and 131.37 ± 4.21 ng of bFGF were released during the 21-day study. By contrast, 11.69 ± 0.44 ng of TGF-β, 880.96 ± 10.27 ng of IGF-I, and 239.23 ± 7.83 ng of bFGF was released from the coaxial nanofibers without liposomes.

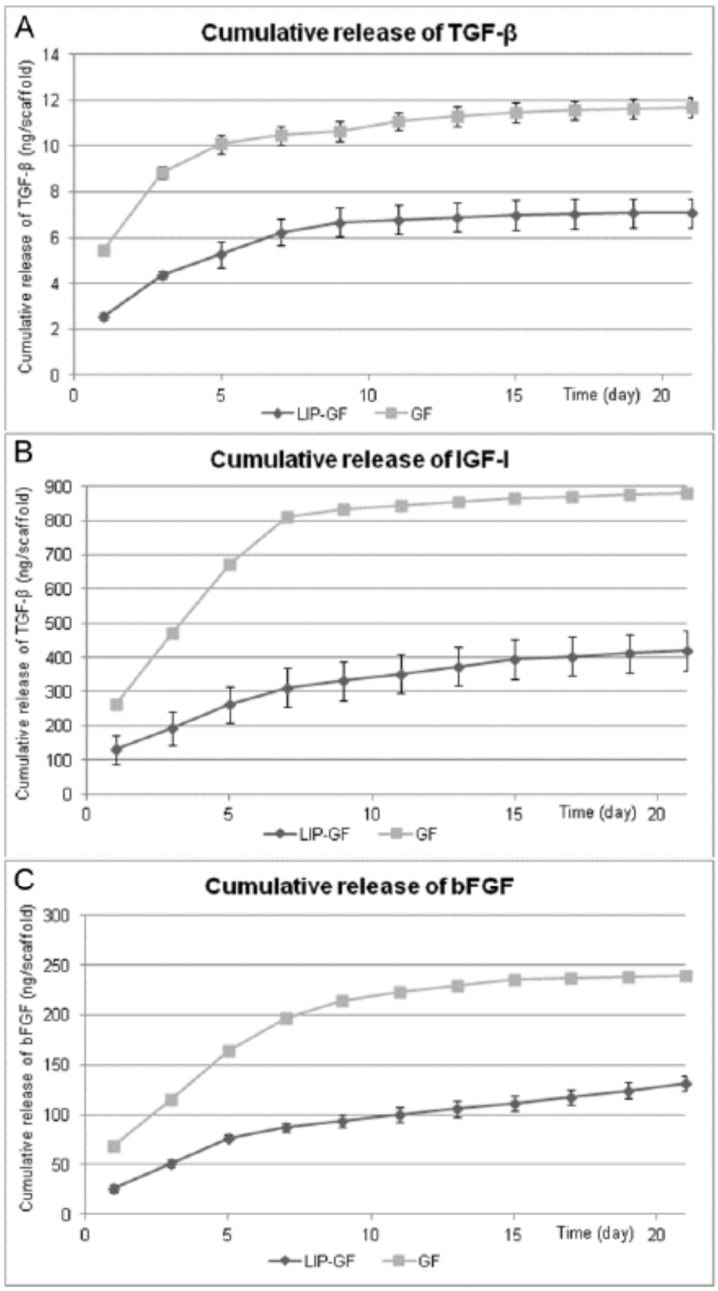

Figure 5.18 Cumulative release profile of growth factors
The release of growth factors was determined using ELISA. (A) Release profile of TGF-β released from coaxial nanofibers with liposomes (LIP-GF) and without liposomes (GF). (B) Release profile of IGF-I released from coaxial nanofibers with liposomes (LIP-GF) and without liposomes (GF). (C) Release profile of bFGF released from coaxial nanofibers with liposomes (LIP-GF) and without liposomes (GF).

To increase the effect of the delivered growth factors, the cells were cultivated in a cell culture medium containing only 1% fetal bovine serum, and the medium was not refreshed

during the cultivation period. The number of cells on the scaffolds was quantified using a dsDNA-specific assay on days 1, 3, 7 and 14 (Figure 5.19a). Statistically significant differences between scaffolds were detected on all days. To determine cell viability, an MTS assay was performed on days 1, 3, 7, and 14 (Figure 5.19b). On day 1, there was no difference in cell viability among the samples. However, the MTS assay showed significantly higher viability of MSCs cultured on LIP-GF scaffolds than on GF scaffolds on days 3 and 14, indicating that cells incubated on a sample with liposomes had greater viability. The MTS assay showed significantly higher MSC viability on LIP-GF scaffolds than on GF scaffolds. The increased DNA concentration of MSCs was indicative of higher rates of cell proliferation. Cell proliferation on the scaffolds was examined using a BrdU assay and confocal microscopy. The BrdU assay showed significantly higher proliferation rates on days 3 and 7 of cultivation on PVA/PCL scaffolds with embedded liposomes (Figure 5.19c).

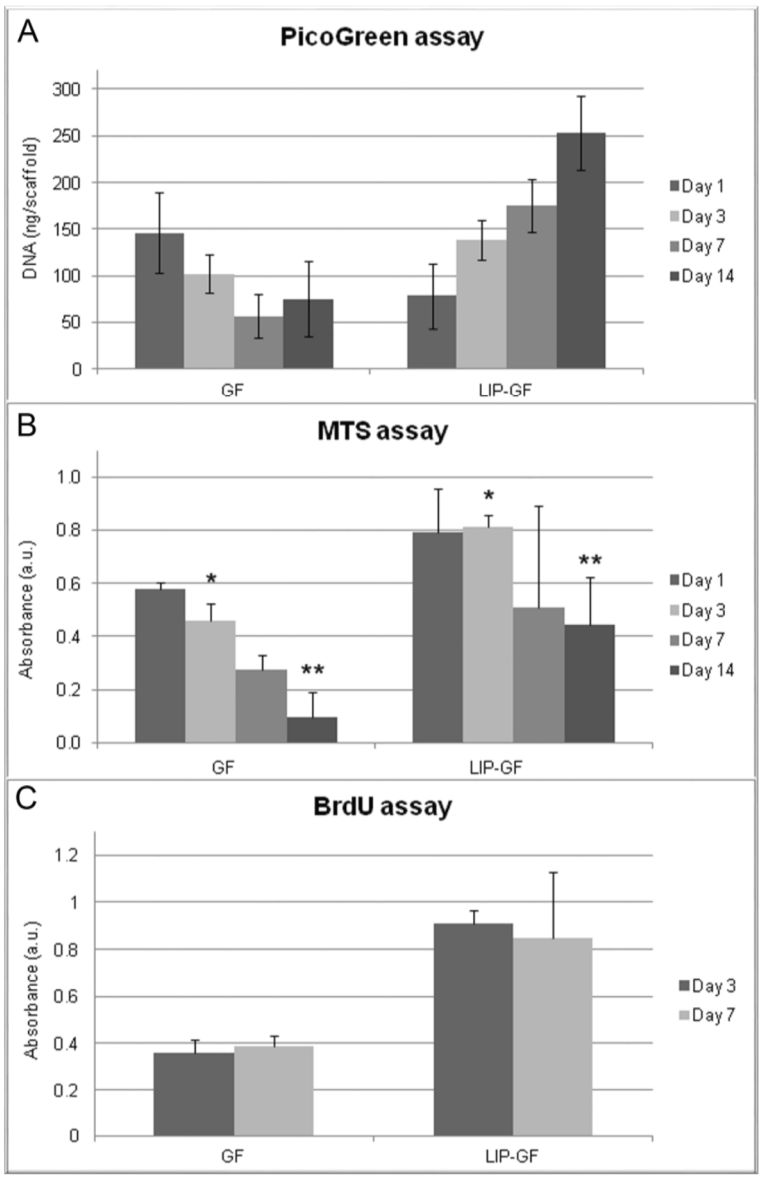

Figure 5.19 Viability and proliferation of MSCs on PVA/PCL coaxial nanofibers
Determination of the dsDNA content using the PicoGreen method showed that there were greater numbers of cells on the LIP-GF scaffolds than on the GF scaffolds. Statistically significant differences were detected between the scaffolds on all assayed days. (B) The MTS assay revealed significantly higher viability of MSCs on PVA/PCL coaxial scaffolds with liposomes (LIP-GF) on day 3 (indicated by *) and on day 14 (indicated by **) than on coaxial scaffolds without liposomes (GF). (C) The BrdU assay showed a significantly higher cell proliferation rate on the LIP-GF scaffolds than on the GF scaffolds on days 3 and 7. The level of statistical significance for the assay is indicated above the mean values (*$p < 0.05$, ** $p < 0.05$).

In addition, confocal microscopy showed that there was no difference between the GF and LIP-GF scaffolds on day 1, and that the cells were spread, isolated or in small groups, and were randomly distributed on the scaffold (Figure 5.20a,c). Low numbers of cells were

observed for the cells cultured on GF scaffolds, even on day 14. The cells were organized in small isolated groups, indicating poor cell growth on the scaffold (Figure 5.20b). By contrast, the LIP-GF scaffolds showed increased cell density (Figure 5.20d). The well-spread cells formed large groups, indicating increased cell proliferation. Confocal microscopy supported the results of the quantitative assays, and confirmed that core/shell nanofibers with embedded liposomes enhanced MSC proliferation and viability more than coaxial nanofibers without liposomes.

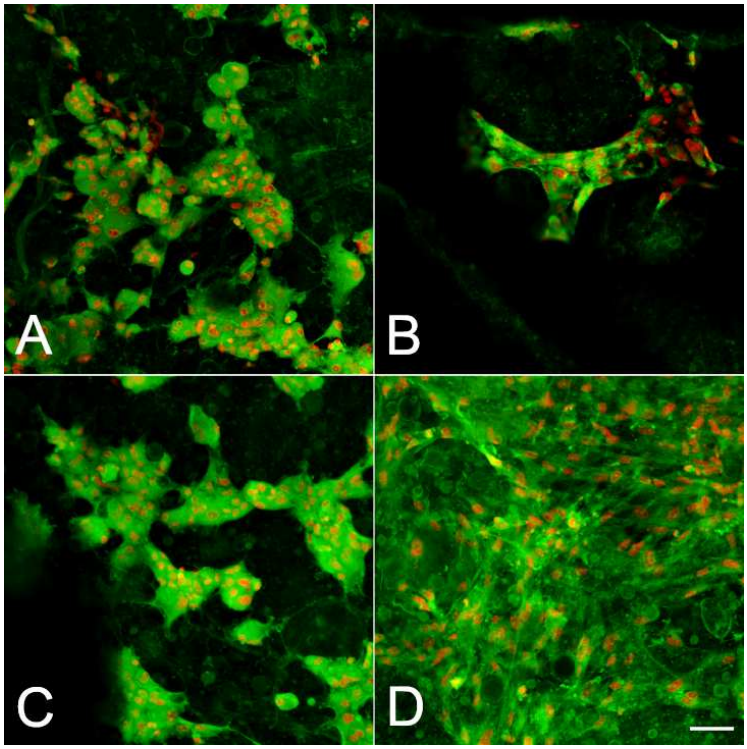

Figure 5.20 Confocal microscopy of MSCs on PVA/PCL coaxial scaffolds
Confocal microscopy on day 1 after seeding showed no difference between (A) PVA/PCL coaxial scaffolds containing a mixture of growth factors (GF), and (C) PVA/PCL coaxial scaffolds with liposomes containing growth factors (LIP-GF). The micrographs show increased proliferation of MSCs on (D) LIP-GF coaxial scaffolds 14 days after seeding in comparison with (B) GF coaxial scaffolds containing a growth factor solution in the core. Mitochondria and inner membranes of MSCs were detected using DiOC6 staining (green) and cell nuclei were detected using propidium iodide staining (red). The scale bar indicates 50 µm.

5.3.3 Discussion

5.3.3.1 Intact phosphatidylcholine liposomes can be incorporated into nanofibers by coaxial electrospinning

Coaxial electrospinning is an attractive strategy for delivering susceptible biomolecules, because the core/shell fibers that are produced have great potential for preserving proteins during the electrospinning process. The solvent system of the core and shell shows high interfacial tension and avoids mixing of the core and shell polymers, thus protecting bioactive molecules in the core from the solvents of the shell polymer. Electrospun coaxial nanofibers have been employed to deliver various bioactive substances, such as proteins, DNA, and siRNA (Cao et al. 2010; Li et al. 2010; Saraf et al. 2010). In addition proteins can be delivered in a controlled manner (Ji et al. 2011).

Liposomes have received widespread attention as carriers of therapeutically active compounds due to their unique characteristics. For example, they are able to incorporate hydrophilic and hydrophobic drugs, they show good biocompatibility and low toxicity, and they deliver bioactive compounds to the site of action in a targeted manner (Mufamadi et al. 2013). However, their short half-life, the low stability of conventional liposomes, and poor control of drug release over prolonged periods limit their use for long-term drug delivery (Sharma and Sharma 1997).

In this study, the limitation of conventional liposomes has been overcome by combining liposomes with polymeric scaffolds. A drug delivery system based on liposome-enriched nanofibers has been introduced. The morphology of the nanofibers has been examined using FESEM, and the morphology of intact embedded liposomes has been examined using confocal microscopy. The localization of the fluorescent substances in the liposomes within a dry nanofiber mesh suggested that the liposomes remained intact during and after coaxial electrospinning. As has been mentioned above, osmotic pressure and shear stress affect

liposomal stability during the electrospinning process. During coaxial electrospinning, the hydrodynamic forces in the core of the jet are lowered, thereby preventing disruption of the liposomal membrane (Reznik et al. 2006). The coaxial electrospinning process enables the incorporation of unilamellar phosphatidylcholine liposomes, and opens the way for their application in long-term drug delivery. The use of nanofibers of this kind as drug delivery systems can combine the unique advantages of nanofibers and liposomes.

5.3.3.2 FITC-dextran release is prolonged from coaxial nanofibers with intact liposomes

The system of coaxial nanofibers with embedded liposomes was tested for drug release. The release half-time from coaxial nanofibers was strongly dependent on the presence of a water-soluble core polymer (Jiang et al. 2006) - in our case, PVA. Rapid FITC-dextran release from the nanofiber core could be explained either by water sorption into the nanofiber core and/or by the formation of submicron pores in the nanofiber shell (Srikar et al. 2008; Tiwari et al. 2010). These results showed the protective activity of liposomes and the more sustained release of encapsulated FITC-dextran. A comparison between dry and wet coaxial nanofibers indicated the formation of submicrometer pores in the PCL shell in the wet nanofiber samples. The hypothesis is therefore that pore formation affected drug release from the nanofiber core. This observation supports the hypothesis introduced by Tiwari et al. (2010).

Interestingly, core/shell nanofibers with liposomes encapsulating FITC-dextran displayed slower initial release. Only ~20% of the FITC-dextran was detected after 24 h of incubation, and the release half-time was shifted to t_r = 112 h for samples with FITC-dextran entrapped in liposomes. These results showed the protective activity of liposomes and the sustained release of encapsulated FITC-dextran. This phenomenon can be explained by temporary stability of

the liposomes in the PVA core. The release half-time from nanofibers with encapsulated liposomes depends on many physical and chemical factors, especially on the chemical composition and the size of the liposomes (Chang and Yeh 2012). Nevertheless, the release from the system depends on the stability of the core and shell polymers and on the morphology of the fibers (Ji et al. 2011, Saraf et al. 2009). The observed results, however, demonstrated that nanofibers with liposomes in their core are appropriate means for controlled drug delivery. The design of coaxial nanofibers with the desired release kinetics for practical tissue engineering applications should be further examined.

5.3.3.3 Intact encapsulated liposomes preserve enzymatic activity

Coaxial electrospinning techniques have been widely used as drug delivery systems, mainly because of the possibility to control the drug release behavior, to modify the surface properties of the scaffold without disrupting the drug-embedded core, and to better preserve the activity of biomolecules (Zamani et al. 2013). In our study, the enzyme activity of HRP encapsulated into coaxial nanofibers was measured. Nanofiber samples with HRP incorporated into coaxial nanofibers were compared with samples containing liposomes with HRP dispersed within coaxial nanofibers. The highest potential was shown by intact liposomes incorporated into nanofibers by coaxial electrospinning. Enzymes encapsulated in liposomes can better survive the electrospinning process, probably because of the shielding effect of the lipid sphere. However, the preserved enzymatic activity either of HRP dispersed in the core of coaxial nanofibers or of HRP encapsulated into liposomes prepared by coaxial electrospinning was significantly higher than those prepared by blend electrospinning (see paragraph 5.2.1.2). The use of core/shell fiber structures with the enzyme entrapped in the core is a very effective strategy for alleviating the problem of loss of enzyme activity and leakage from electrospun nanofibers (Agarwal et al. 2008; Zhang et al. 2006). Silica

nanofibers were used to encapsulate HRP into the core of coaxial nanofibers and neither enzyme leakage nor fiber deformation was observed (Patel et al. 2006). Mesoporous silica nanofibers have also been widely used due to their large surface area, uniform pore distribution, tunable pore size and high adsorption capacity (Wang et al. 2011). Coaxial electrospinning enabled simultaneous entrapment of lipase and magnetite nanoparticles with biomimetic silica, which enhanced the enzyme activity in varying silane additives (Chen et al. 2011). Successful preservation of molecular bioactivity requires smaller amounts of delivered molecules to promote optimized tissue regeneration. In addition, reduced doses of biomolecules enable safe and cost-effective strategies for tissue engineering applications.

The water content in the dry nanofibers was measured in order to examine whether liposomes were able to maintain their internal aqueous environment. The study revealed that the liposomes entrapped in the nanofiber core maintained a water environment for several weeks of shelf storage; moreover, the system apparently did not leak water and could probably be used for even longer periods of storage (i.e. for periods of months). Thus, the nanofiber core appears in the dry state as a water-impermeable barrier, because of the interaction between the hydrophilic core polymer and the liposomes inside the core solution. This observation opens up new perspectives on the preservation of native enzymes. The coaxial electrospinning system appears suitable for enzyme immobilization, encapsulation and bioactivity preservation with wide-ranging applications in the field of fine chemistry, biomedicine biosensors and tissue engineering (Wang et al. 2009; Liao and Leong 2011).

5.3.3.4 Liposomes with encapsulated growth factors stimulate MSC proliferation and viability *in vitro*

Electrospun nanofibers were utilized for delivering various growth factors for the induction of MSC viability and proliferation. Sahoo et al. (2010) prepared nanofibrous scaffolds for

controlled delivery of bFGF, and showed that there was increased MSC proliferation on coaxial nanofibers. The potential of the coaxial system with embedded liposomes for drug delivery of growth factors for tissue engineering applications was evaluated by simple cell culture studies. We examined the viability and proliferation of MSCs on the prepared scaffolds. Interestingly, while the number of cells decreased on coaxial PVA/PCL scaffolds without liposomes during the study period, the concentration of DNA increased significantly in samples with embedded liposomes utilized as a growth factor delivery vehicle during cultivation. Confocal microscopy supported the results of the quantitative assays and confirmed that nanofibrous scaffolds containing embedded liposomes with encapsulated recombinant growth factors were more potent - they stimulated MSC proliferation and viability more than coaxial nanofibers without liposomes.

In addition, data from confocal microscopy showed poor cell infiltration into the scaffold. This result could be explained by the small pore size of the scaffold. Coaxial nanofibers with embedded liposomes had a mean pore size of 0.17 ± 0.04 µm, while coaxial nanofibers without liposomes had a mean pore size of 0.33 ± 0.07 µm. These pore sizes are insufficient for cell infiltration. If scaffolds made via electrospinning have a pore size of <10 µm, the cells cannot easily infiltrate the nanofibers and make a three-dimensional shape, such as exists in the ECM (Shabani et al. 2009). Thus the nanofiber mesh will essentially behave as a two-dimensional sheet, where the cells can only proliferate on its surface. Several approaches have been reported for overcoming this limitation. For example, systems combining insoluble fibers and sacrificial co-fibers have been reported (Guimaraes et al. 2010). In addition, pore size and cell infiltration of nanofibrous scaffolds can be regulated with the use of macromolecules, for example, hyaluronan (Li et al. 2012). Alternatively, pores can be introduced by salt particles that are subsequently leached out, or by introducing ice crystals (Laurencin and Nair 2008). After the removal of the sacrificial part of the system, void spaces

are introduced and the pore size of the scaffold increases. Other methods that can be used for adjusting the pore size are adjustment by regulating electrospinning processes or by using special collectors (Li et al. 2005; Pham et al. 2006). Approaches such as these can be combined with the proposed system; however further study is necessary to optimize their use for specific tissue engineering applications.

The results of the cell culture study showed that susceptible compounds can be protected by liposomes embedded in coaxial nanofibers. This drug delivery system seems to be a promising growth factor delivery strategy for use in regenerative medicine.

5.3.4 Coaxial nanofibers with incorporated platelet α-granules for biomedical use

5.3.4.1 Results

5.3.4.1.1 Isolation of α-granules from platelets

The aim of the investigation was to develop a novel drug delivery system using platelet α-granules as a source of natural growth factors. α-granules contain most of the platelet-secreted growth factors and are, thus, an ideal source for tissue engineering applications. The first task was therefore to isolate the α-granules from the platelets. Sonicated platelets were separated into three fractions by ultracentrifugation: the heaviest fraction ALPHA; FR1; and FR2. Dot blot analyses were performed to determine the α-granule content. The sonicated platelets were used as a positive control. P-selectin is expressed in the α-granules of platelets, so the protein was selected as a marker for their characterization. There was a significantly higher presence of P-selectin in ALPHA than that in the control (PRP) and in the FR1 and FR2 fractions. ALPHA assembled the vast majority of α-granules from the platelets, as the peak integral characterizing the PRP fraction represented approximately 50% of the ALPHA peak (Figure 5.21). The highest P-selectin

levels in ALPHA, in comparison with those in the sonicated platelets, may be explained by the higher absolute amount of P-selectin in ALPHA compared with other proteins when normalized to overall protein.

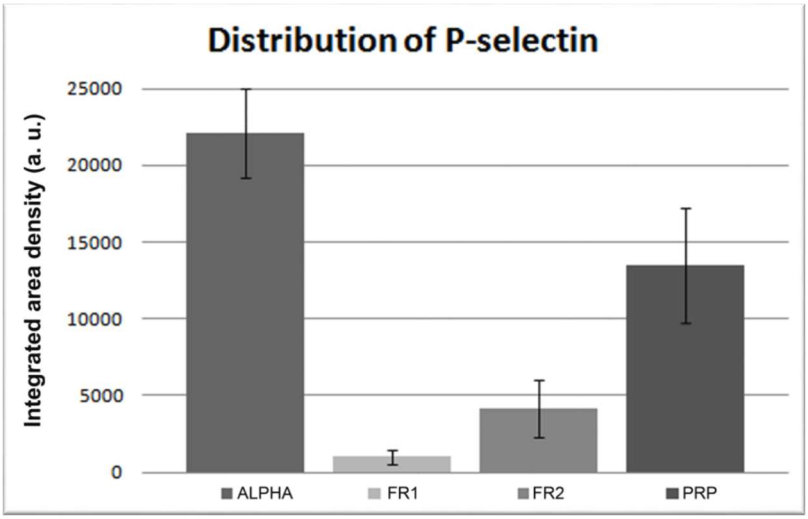

Figure 5.21 Distribution of P-selectin
The highest P-selectin content was measured in the α-granule-rich fraction (ALPHA), and a residual P-selectin content was observed in the lightest fraction (FR1) and in the middle fraction (FR2). Platelet-rich plasma lysate (PRP) was used as a positive control.

5.3.4.1.2 Incorporation of α-granules in the core of PVA/PCL nanofibers

Due to their small diameters, the isolated α-granules were ideal for encapsulation into the nanofiber core by coaxial electrospinning. The shell polymer consisted of 10% PCL, whereas the core consisted of 5% PVA and α-granules. The concentration of α-granules in the core (0.3 mg/ml of PVA) was selected as a balance between the maximal concentration of α-granules (1.2mg/ml) and the minimal volume (4ml) necessary for preparing a sufficient fiber mesh. FESEM analysis was applied to visualize the morphology of the electrospun nanofiber mesh (Figure 5.22). Two nanofiber populations were identified in the control PVA/PCL nanofiber samples: thin and thick. The mean diameter of the thin nanofibers was 222.32 ± 78.90 nm, and the mean diameter of the thick fibers was 613.28 ± 190.15 nm. In

addition, the sample contained a population of microfibers. The pore sizes differed, and were up to 3 µm; however, the majority of the pores were approximately 1 µm in diameter.

The morphology of the PVA/PCL nanofiber samples containing α-granules exhibited a similar fiber distribution. The mean diameter of the thin nanofiber population was 196.17 ± 99.60 nm, and the mean diameter of the thick fibers was 631.85 ± 190.25 nm. The sample contained only a small number of microfibers. Pore size analysis revealed pores with diameters of up to 10 µm; however, the majority of the pores had a diameter of < 5 µm. Detailed micrographs revealed a rough surface that could reflect the α-granules encapsulated in the nanofiber core (Figure 5.22a). The huge bundles had an average diameter of 4.52 ± 2.32 µm.

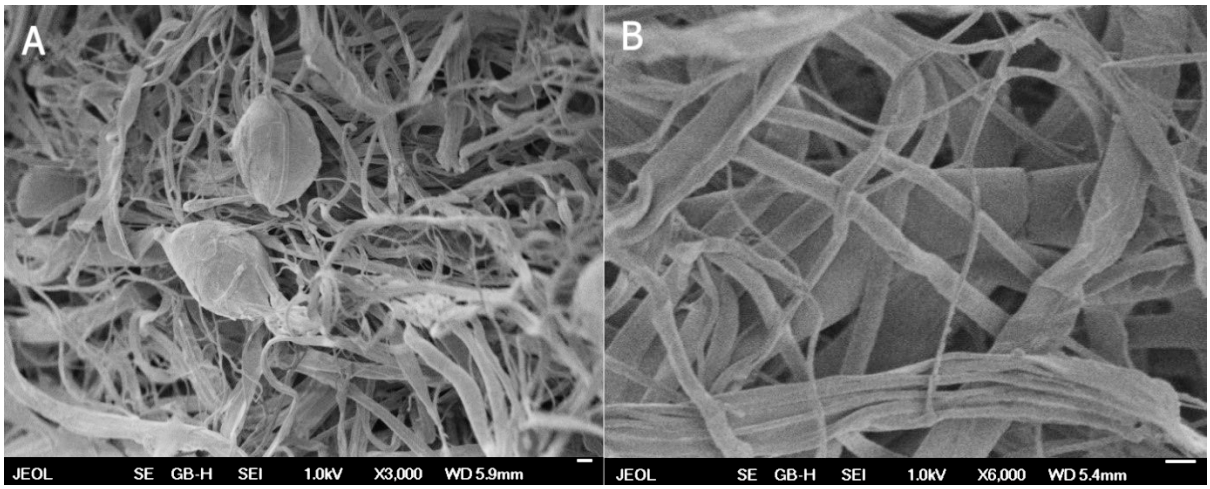

Figure 5.22 FESEM of coaxially electrospun PVA/PCL nanofibers with encapsulated α-granules

FESEM of α-granules encapsulated into coaxial PVA/PCL nanofibers. The micrograph depicts the nanofiber morphology and bundles with encapsulated α-granules. (B) Pure PVA/PCL nanofiber mesh as a control. The micrograph depicts the nanofiber morphology of the prepared nanofibers without bundle-like structures. The scale bars indicate (A, B) 2 µm.

The dry PVA/PCL nanofiber mesh with incorporated α-granules in the core of the coaxial nanofibers was visualized by means of confocal microscopy using fluorescent carboxyfluorescein succinimidyl ester (CFSE) labeled α-granules (Figure 5.23). The α-granules were assembled along the core of the fiber; however, the fluorescent signal

received by confocal microscopy and the phase contrast were shifted due to the differing optical thicknesses of the slides. Interestingly, the α-granules were incorporated into the core of the nanofibers either as single granules or as aggregates.

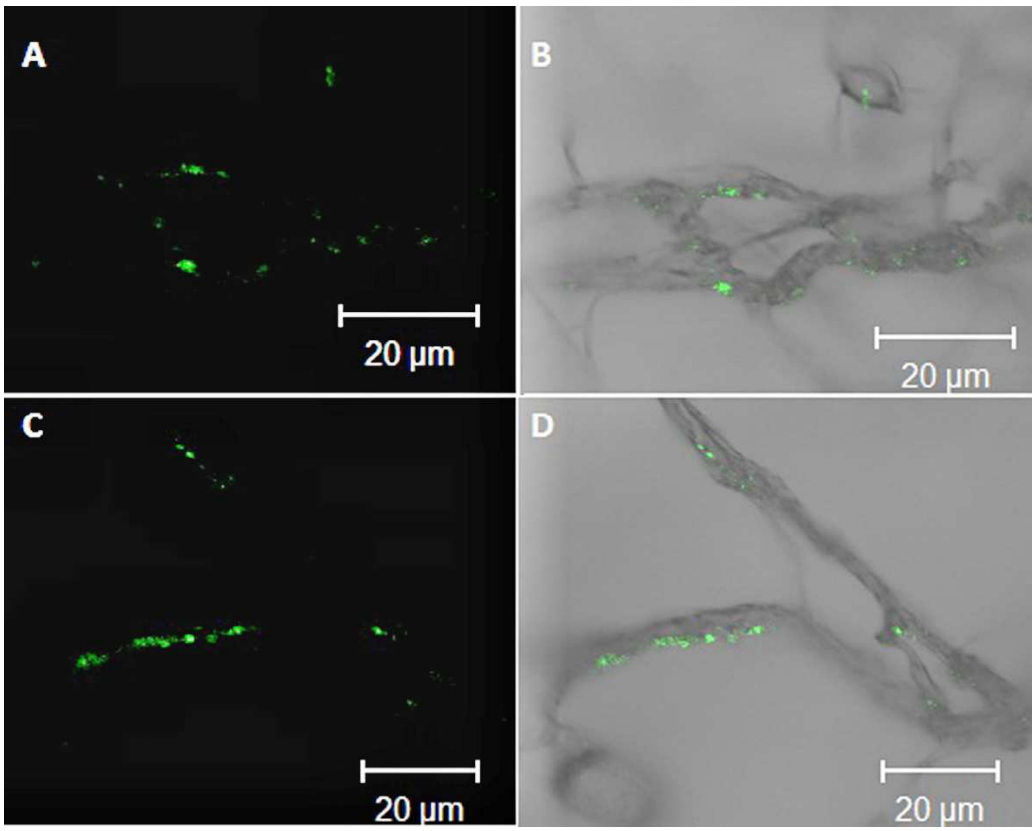

Figure 5.23 Confocal microscopy of encapsulated α-granules in PVA/PCL nanofibers prepared by coaxial electrospinning
(A, B) Localization of CFSE-labeled α-granules in nanofiber cores. (C, D) CFSE-labeled α-granules exhibiting the presence of single and aggregated α-granules in the fibers. The scale bars indicate 20 µm.

The efficiency of α-granule incorporation in our experiments was determined using overall protein quantification. The encapsulation was 43.1 ± 2.3%, due to material loss during the electrospinning process and chloroform extraction from the nanofibers.

5.3.4.1.3 Mesenchymal stem cell culture studies on coaxial nanofibers with incorporated alpha-granules

A preliminary study with MSCs was performed to demonstrate the potential of the coaxial system with encapsulated α-granules. MSCs were seeded on PVA/PCL nanofibers with encapsulated α-granules (ALF), and were compared with pure PVA/PCL nanofibers, as a control (PVA/PCL).

To determine cell viability, MTT assays were performed on days 1, 7 and 15 (Figure 5.24). On days 7 and 15, the MSCs showed significantly higher viability on the ALF scaffolds than on the control. Confocal microscopy was performed to visualize the cell adhesion to the scaffolds (Figure 5.25a,b). On day 1, cells adhered to both scaffold types and were well spread. Type II collagen was detected by immunofluorescence on days 7 and 15 to characterize chondrogenic differentiation (Figure 5.25c-f). On pure, coaxial PVA/PCL control nanofibers, type II procollagen and immature collagen production decreased between day 7 and day 15. The fluorescence signal had almost disappeared on the control scaffolds on day 15 (Figure 5.25f). However, the MSCs cultured on PVA/PCL coaxial nanofibers with encapsulated α-granules displayed high type II collagen production on day 7 and on day 15. The immunofluorescence results showed that MSCs cultured on a scaffold with encapsulated α-granules produced type II collagen as a marker molecule of chondrogenic differentiation.

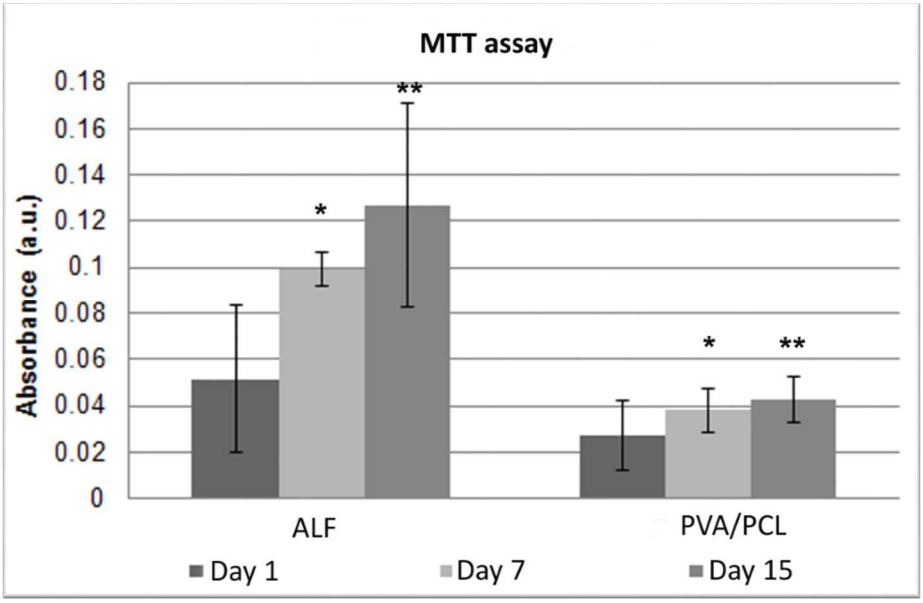

Figure 5.24 Cell viability of MSCs on PVA/PCL coaxial nanofibers with encapsulated α-granules

Cell viability was measured by a 3-(4,5-Dimethylthiazol-2-yl)-2,5-Diphenyltetrazolium Bromide (MTT) Assay. MSCs were cultivated on PVA/PCL scaffolds with encapsulated α-granules in the core of the nanofibers, and on pure PVA/PCL nanofibers as controls prepared by coaxial electrospinning. The level of statistical significance for the assay is indicated above the mean values (*$p < 0.05$, **$p < 0.05$).

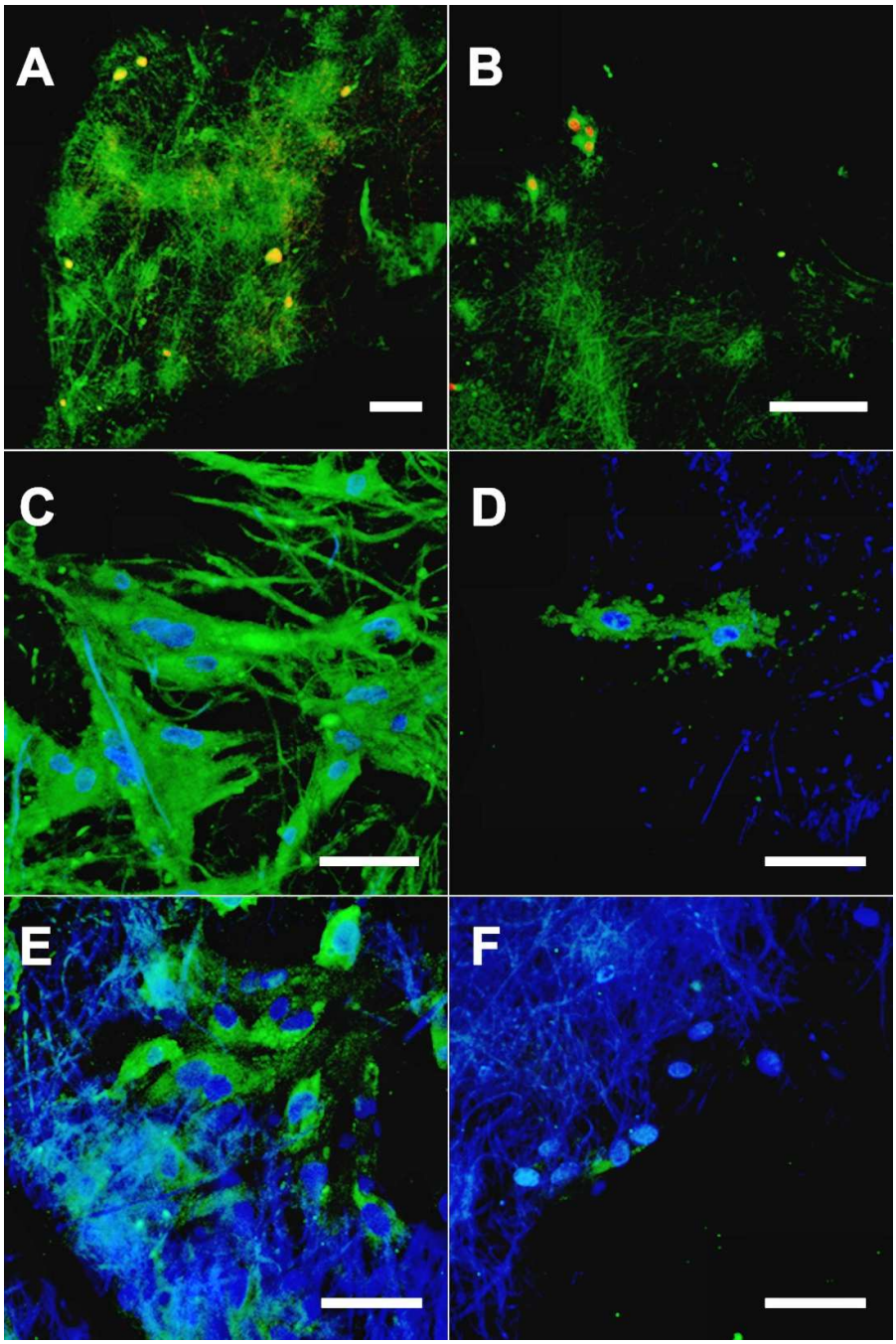

Figure 5.25 Confocal microscopy of MSCs on PVA/PCL coaxial scaffolds
Adhesion of MSCs on day 1 to (A) PVA/PCL coaxial scaffolds containing α-granules and (B) to pure PVA/PCL coaxial scaffolds, as a control. Nuclei were stained using propidium iodide (red) and membranes were detected using DIOC6 staining (green). Synthesis of type II collagen on day 7 on (C) PVA/PCL samples with encapsulated α-granules and (D) pure PVA/PCL control samples and on day 15 (E) PVA/PCL with encapsulated α-granules and (F) PVA/PCL control samples. Type II collagen was visualized by immunofluorescence (green), and cell nuclei were counterstained with Hoechst stain (blue). The scale bars indicate (A, B) 100 µm and (C-F) 50 µm.

5.3.4.2 Discussion

5.3.4.2.1 Isolated α-granules as a novel platelet derivative for tissue engineering applications

α-granules are platelet secretion organelles that contain most of the platelet-produced growth factors (Blair and Flaumenhaft 2009). These growth factors induce physiological tissue repair and play important roles in wound healing. Isolated α-granules have been used for biochemical and physiological applications and their molecular content is well characterized. The advantage of α-granules is that their fractions can be stored for several months at -80°C or in liquid nitrogen without losing their activation capacity (Niessen et al. 2007). By contrast, platelet concentrates can be conventionally stored for up to 1 week at 21°C, while some cryopreservation protocols enable longer shelf storage. However, these methods alter the platelet physiology, morphology and activation capacity (Nie et al. 2005).

In this study, isolated α-granules were introduced as a novel platelet derivative for tissue engineering applications.

5.3.4.2.2 PVA/PCL nanofibers containing alpha-granules in the core

α-granules in core/shell nanofibers prepared by coaxial electrospinning were introduced in this study. As has been mentioned above, coaxial electrospinning has been utilized successfully for encapsulating proteins, such as lysozyme, platelet-derived growth factor-bb (PDGF-bb), nerve growth factor (NGF), and basic fibroblast growth factor (bFGF) (Sahoo et al. 2010; Wang et al. 2012; Yang et al. 2008). This is the first time that a core/shell system incorporating α-granules has been introduced, and it combines the unique advantages of coaxial nanofibers with an autologous source of growth factors. An indisputable advantage of α-granules is that they contain concentrated amounts of growth factors in a relatively smaller size than that of platelets. The growth factors can be immobilized *in situ* and protected from

the environment, and the nanofibers can be further functionalized for cell adhesion. Briefly, this system is ideal for growth factor release in small regions.

In the present study, α-granules were incorporated into the core of coaxial nanofibers. Water-soluble PVA was shown to be an ideal core polymer that facilities the incorporation of intact α-granules. The solvent system of the core and shell shows high interfacial tension and avoids mixing of the core and shell polymers, thus protecting the bioactive molecules in the core from the solvents of the shell polymer. This is critical here, since the proteins would be denatured if they came into the contact with organic solvents such as chloroform, which was used as a solvent for the shell polymer. In addition, as a hydrophilic polymer, PVA stabilizes α-granule membranes via its hydroxy groups during the fiber-forming process. This hypothesis was supported by confocal microscopy visualization of the incorporation of intact α-granules into nanofibers. However, it is not clear from the confocal images whether the granules are localized in the core or are sequestered on the surface. Localization on the surface is not probable due to the high interfacial tension between PCL and PVA during the electrospinning process, and limited diffusion between the core and shell polymers. Moreover, α-granules would be unstable as membrane structures in a non-aqueous environment such as chloroform. Thus, it is convincing that α-granules are incorporated into the core of the nanofibers. In addition, the coaxial nanofiber mesh containing α-granules, enables long-term storage of α-granules in the form of a dry nanofiber mesh. The storage does not require an aqueous environment and thus simplifies their biomedical use.

Another important feature of the scaffold is the pore size, which affects cell penetration. The pore sizes of both PVA/PCL nanofibers as a control and PVA/PCL nanofibers with embedded α-granules were < 5 µm. However, as was mentioned above, scaffolds prepared by electrospinning with a pore size smaller than 10 µm are not suitable for cell infiltration

(Shabani et al. 2009). Further optimization of the proposed system will therefore be necessary in order to overcome the pore size limitations for better cell penetration.

5.3.4.2.3 Coaxial nanofibers with incorporated α-granules stimulate MSC proliferation and viability *in vitro*

The potential of the coaxial system with incorporated α-granules for cartilage tissue engineering was evaluated by a simple cell culture study of MSCs. Human chondrocytes have relatively low basal propensity for proliferation and ECM production. However, the proliferation capacity of chondrocytes decreases with age, the usage of stem cells is therefore believed to be a promising tool in tissue engineering. Platelet-released growth factors have been shown to induce chondrogenic differentiation of MSCs (Mishra et al. 2009).

The cell viability assay of MSCs showed that the viability on coaxial nanofibers with incorporated α-granules was significantly higher than the viability on the pure control PVA/PCL coaxial nanofibers on days 7 and 15. In addition, the differentiation and production of chondrocyte specific ECM and the expression of type II collagen were examined. Interestingly, the marker protein was produced on PVA/PCL scaffolds with and also without α-granules on day 7. This observation could be explained by the surface chemistry of PCL, which partially stimulates chondrogenic differentiation (Chastain et al. 2006). However, there was higher production of type II collagen on scaffolds containing α-granules. A high level of type II collagen production persisted until day 15. A low concentration of α-granules embedded into nanofibers was able to induce the production of chondrocyte-specific ECM, and is therefore a prospective system for targeting MSCs into a chondrogenic phenotype. The importance of sustained delivery of growth factors for cartilage tissue engineering has been demonstrated (Catelas et al. 2008). Buzgo et al. revealed that the release of growth factors from coaxial nanofibers incorporating α-granules were slower than from scaffolds containing

adhered platelets. Moreover, the concentration of relelased TGF-β1 from the samples with adhered platelets was nearly six-times higher on day 1 than from coaxial scaffolds with encapsulated α-granules. This observation further supported the delayed relelase of growth factors from encapsulated α-granules (data not presented here, Buzgo et al. 2012). The advantage of a nanofiber system is the stable release of growth factors, independent from the composition of the surrounding environment.

High levels of applied growth factors are correlated with an increased risk of cancer (Stattin et al. 2004). Although the use of platelet derivatives has not been correlated with any cell transformation to date, the use of a lower concentration of growth factors would minimize any potential risk.

α-granules incorporated into nanofibers stimulated MSC viability and the production of extracellular proteins specific for chondrogenesis. However, it is necessary to carry out a more complex study pointing to the detailed influence of the dosage and the release kinetics of α-granule growth factors on chondrogenic differentiation in order to optimize the system.

6 Conclusion

Platelets were successfully immobilized on the surface of PCL nanofiber scaffolds for tissue engineering applications. Biocompatible and biodegradable PCL nanofiber scaffolds prepared by an electrospinning technique efficiently immobilized platelets after 2 hours of pre-incubation in a platelet-rich plasma solution. Results have proved that functionalized PCL nanofibers provide a suitable matrix for chondrocyte cultivation. A proliferative effect of platelet functionalized nanofibers on chondrocytes *in vitro* has been demonstrated. Functionalized PCL nanofibers with adhered platelets appear to be suitable for drug delivery of growth factors, and for tissue engineering applications with comparatively short time scales. (attachements Jakubová et al. 2011; Buzgo et al. 2012).

A tight interaction between liposomes and PCL nanofibers has been clearly demonstrated. A preliminary *in vitro* study showed that liposomes with encapsulated growth factors adhered to PCL nanofiber scaffolds provides a suitable system for adhesion and proliferation of MSCs. The release of growth factors from liposomes to the neighboring cells resulted in gradual proliferation of MSCs during the study period. In addition, type II collagen production was observed in samples with adhered liposomes on PCL nanofibers, and also in samples with adhered free growth factors on PCL nanofibers. A preliminary study has indicated that growth factor-enriched liposomes adhered to a PCL nanofiber system could be useful as a drug delivery tool in applications with a comparatively short time scale, and could find broader use in tissue engineering. However, in order to optimize the system, a more complex study is needed to specify the influence of the dosage and release kinetics of growth factors from liposomes adhered to nanofibers on MSC viability, proliferation and differentiation (preliminary results).

Blend electrospinning was applied to encapsulate liposomes with FITC-dextran into PVA nanofibers. However, the blend electrospinning technology caused the liposomes to break and release their encapsulated material. The incorporation ratio and the preservation of enzyme activity in PVA nanofibers were also tested. The results confirmed that HRP was encapsulated effectively into the nanofibers. However, the biological activity of the encapsulated protein was highly depressed in nanofibers with incorporated HRP, and also in PVA nanofibers with HRP encapsulated into the liposomes. The results indicated that the PVA polymer solution has a significant effect on liposome stability. More than 50% of the liposomes were disintegrated in a 12% PVA polymer solution before the electrospinning process started. By contrast, approximately 70% of the liposomes dissolved in a 5% PVA polymer solution remained intact. The results showed that blend electrospinning technology does not conserve phosphatidylcholine liposomes intact, and is not suitable for preserving HRP activity (attachement Mickova et al. 2012).

Core/shell nanofibers with embedded liposomes have been produced. Coaxial electrospinning enabled the retention of an aqueous environment inside intact liposomes embedded in nanofibers for several weeks of shelf storage. Nanofibrous scaffolds containing embedded liposomes with encapsulated recombinant growth factors were more potent at stimulating MSC proliferation than coaxial nanofibers without liposomes. Finally, enzymes encapsulated in liposomes can better survive the electrospinning process, probably because of the shielding effect of the lipid sphere. The results presented in the current study show the potential of this drug delivery system using intact liposomes embedded in coaxial nanofibers in various fields of tissue engineering and regenerative medicine (attachement Mickova et al. 2012).

Finally, α-granules were introduced as an autologous source of growth factors. α-granules were isolated from platelets and were incorporated into nanofibers by coaxial electrospinning. The prepared scaffold was tested *in vitro* by cultivation with MSCs. The tested system preserved the biological activity of the delivered growth factors and stimulated the viability, production of type II collagen and chondrogenic differentiation of MSCs. Successful preservation of molecular bioactivity required a low concentration of the delivered growth factors in order to promote optimized tissue regeneration. The results showed that coaxial nanofibers with embedded α-granules are a promising system for applications in tissue engineering with comparatively prolonged time scales (attachement Buzgo et al. 2012).

7 Future perspectives

In order to preserve molecular bioactivity encapsulated into intact liposomes in coaxial nanofibers, it is necessary to limit the amounts of molecules delivered to promote optimized tissue regeneration. In addition, reduced doses of biomolecules such as growth factors enable safe and cost-effective strategies in various fields of tissue engineering and in regenerative medicine. However, only a limited number of growth factors have been approved for clinical use in regenerative medicine, and their use is limited to a specific type of application. It is believed that the solution to this problem is to use natural growth factors. Platelet-based preparations probably have the highest clinical potential, due to the high content of growth factors, reduced cost, simple collection from donors and the lack of an immune response when they are applied autologically. The potential of platelets in combination with nanofibers as a suitable delivery system for natural growth factors has been confirmed *in vitro* in this thesis. Moreover, these results have already been confirmed *in vivo* by our research team (Prosecka 2015). It is believed that a combination of natural growth factors in α-granules embedded in coaxial nanofibers could lead to the production of an efficient drug delivery system for tissue engineering in a clinical setting. The release of bioactive molecules from core/shell fibers is prolonged, and can be controlled by changing the composition of the polymer. For proper regulation of the release half-life, however, a more complex mechanism is necessary. It is therefore considered critical to develop a drug delivery system that enables time-resolved sequential release of multiple growth factors in order to promote better and more reproducible tissue regeneration outcomes. Further research can overcome this challenge, and core/shell nanofibers releasing a defined cocktail of clinically-approved bioactive molecules may form the next generation of nanofibrous scaffolds, and may soon enter into clinical use.

8 Summary

Electrospinning is an attractive method for producing nanofibrous scaffolds for tissue engineering and for controlled drug delivery.

The aim of this thesis was to develop functionalized nanofibers as a controlled delivery system for growth factors. Nanofibers were functionalized by simple adhesion of bioactive agents to the nanofiber surface, and incorporating them into the nanofiber mesh using a blend or coaxial electrospinning technique.

Within the framework of this thesis, poly-ε.caprolactone (PCL) nanofibers were functionalized with platelets, and also with synthetic growth factors and with growth factors incorporated into liposomes adhered to the nanofiber surface. Functionalized PCL nanofibers with adhered bioactive agents appear to be suitable for drug delivery of growth factors, and for tissue engineering applications with comparatively short time scales. In the second set of experiments, we focused on prolonging the release time of growth factors by incorporating them into the liposome-nanofiber system using blend or coaxial electrospinning. It was found that liposomes are not preserved intact during the blend electrospinning process. Moreover, loss of protein activity was observed. However, coaxial electrospinning enabled liposomes to be incorporated into nanofibers and thus to preserve the protein activity. The importance of activity protection was further emphasized by more potent stimulation of mesenchymal stem cells (MSCs). Finally, nanofiber scaffolds containing alpha-granules as a natural source of growth factors were prepared by coaxial electrospinning. Successful preservation of molecular bioactivity required a low concentration of the growth factors that were delivered in order to stimulate cell viability and also chondrogenic differentiation of MSCs.

In conclusion, core/shell nanofibers with incorporated liposomes and incorporated alpha granules are promising systems for applications in tissue engineering with comparatively prolonged time scales.

9 Souhrn

Elektrostatické zvlákňování je perspektivní metoda, kterou lze vyrábět nanovlákenné nosiče pro aplikace tkáňového inženýrství a řízeného dodávání léčiv.

Cílem práce bylo vyvinout funkcionalizované nanovlákenné nosiče pro řízené dodávání bioaktivních látek. Funkcionalizace nanovláken byla provedena fyzikální adsorpcí na povrch nanovláken a inkorporací do nanovlákenných nosičů metodou směsného a koaxiálního zvlákňování.

Byly vyvinuty funkcionalizované nanovlákenné nosiče PCL s adherovanými trombocyty, rekombinantními růstovými faktory a růstovými faktory inkorporovanými do liposomů. Funkcionalizace pomocí fyzikální adsorpce na povrch PCL nanovláken se ukázala jako vhodná metoda pro aplikace v tkáňovém inženýrství, v kterých je potřeba rychlé a krátkodobé dodání látek. Další set experimentů byl zaměřen na vytvoření nosiče s prodlouženou dobou uvolňování bioaktivních látek. Byly připraveny systémy „nanovlákna-liposomy“ metodou směsného a koaxiálního elektrostatického zvlákňovaní. U zvlákňování ze směsi došlo k rozbití liposomů a ke ztrátě enzymatické aktivity modelového proteinu. Metoda koaxiálního zvlákňování umožnila inkorporaci liposomů do nanovláken a intaktnost liposomů byla prokázána zachováním enzymatické aktivity inkorporovaného modelového proteinu. Potenciál systému pro aplikace v tkáňovém inženýrství byl potvrzen stimulací proliferace mesenchymálních kmenových buněk (MSC). Na závěr byl pomocí koaxiálního zvlákňování vyvinut nanovlákenný nosič s inkorporovanými α-granulemi. Podařilo se zachovat bioaktivitu inkorporovaných růstových faktorů a jejich postupným uvolňováním z koaxiálních nanovláken byla zajištěna stimulace viability a chondrogenní diferenciace MSC.

Nanovlákenné systémy s inkorporovanými liposomy i s α-granulemi připravené pomocí koaxiálního zvlákňování mají vysoký potenciál pro využití v tkáňovém inženýrství a to zejména v aplikacích, kde je potřeba zajistit dlouhodobé uvolňování bioaktivních látek.

10 References

1 AGARWAL, S. AND A. GREINER On the way to clean and safe electrospinning-green electrospinning: emulsion and suspension electrospinning. Polymers for Advanced Technologies, Mar 2011, 22(3), 372-378.

2 AGARWAL, S., J. H. WENDORFF AND A. GREINER Use of electrospinning technique for biomedical applications. Polymer, 2008, 49(26), 5603-5621.

3 AGGARWAL, S. AND M. F. PITTENGER Human mesenchymal stem cells modulate allogeneic immune cell responses. Blood, 2005, 105(4), 1815-1822.

4 AKEDA, K., H. S. AN, M. OKUMA, M. ATTAWIA, et al. Platelet-rich plasma stimulates porcine articular chondrocyte proliferation and matrix biosynthesis. Osteoarthritis and cartilage / OARS, Osteoarthritis Research Society, 2006, 14(12), 1272-1280.

5 ALBERTS, B., A. JOHNSON, J. LEWIS, M. RAFF, et al. Molecular Biology of the Cell, 2007.

6 ALSOUSOU, J., M. THOMPSON, P. HULLEY, A. NOBLE, et al. The biology of platelet-rich plasma and its application in trauma and orthopaedic surgery: a review of the literature. J Bone Joint Surg Br, Aug 2009, 91(8), 987-996.

7 ANGELES, M., H.-L. CHENG AND S. S. VELANKAR Emulsion electrospinning: composite fibers from drop breakup during electrospinning. Polymers for Advanced Technologies, 2008, 19(7), 728-733.

8 ANITUA, E., M. SANCHEZ, G. ORIVE AND I. ANDIA The potential impact of the preparation rich in growth factors (PRGF) in different medical fields. Biomaterials, Nov 2007, 28(31), 4551-4560.

9 ANITUA, E., M. SANCHEZ, G. ORIVE AND I. ANDIA. Delivering growth factors for therapeutics. In *Trends Pharmacol Sci.* England, 2008, vol. 29, p. 37-41.

10 ANITUA, E., M. SÁNCHEZ, M. M. ZALDUENDO, M. DE LA FUENTE, et al. Fibroblastic response to treatment with different preparations rich in growth factors. Cell proliferation, 2009, 42(2), 162-170.

11 ASRAN, A. S., K. RAZGHANDI, N. AGGARWAL, G. H. MICHLER, et al. Nanofibers from blends of polyvinyl alcohol and polyhydroxy butyrate as potential scaffold material for tissue engineering of skin. Biomacromolecules, 2010, 11(12), 3413-3421.

12 BAENZIGER, N. L., G. N. BRODIE AND P. W. MAJERUS A thrombin-sensitive protein of human platelet membranes. Proc Natl Acad Sci U S A, Jan 1971, 68(1), 240-243.

13 BALAZS, D. A. AND W. T. GODBEY Liposomes for use in gene delivery. Journal of drug delivery, 2010, 2011.

14 BANGHAM, A. D., M. M. STANDISH AND J. C. WATKINS Diffusion of univalent ions across the lamellae of swollen phospholipids. J Mol Biol, Aug 1965, 13(1), 238-252.

15 BARENHOLZ, Y. Cholesterol and other membrane active sterols: from membrane evolution to “rafts”. Progress in lipid research, 2002, 41(1), 1-5.

16 BARENHOLZ, Y. Relevancy of drug loading to liposomal formulation therapeutic efficacy. Journal of liposome research, 2003, 13(1), 1-8.

17 BARRIENTOS, S., O. STOJADINOVIC, M. S. GOLINKO, H. BREM, et al. Growth factors and cytokines in wound healing. Wound Repair and Regeneration, 2008, 16(5), 585-601.

18 BAZILEVSKY, A. V., A. L. YARIN AND C. M. MEGARIDIS Co-electrospinning of Core−Shell Fibers Using a Single-Nozzle Technique. Langmuir, 2007/02/01 2007, 23(5), 2311-2314.

19 BEANES, S. R., C. DANG, C. SOO AND K. TING Skin repair and scar formation: the central role of TGF-[beta]. Expert reviews in molecular medicine, 2003, 5(08), 1-22.
20 BEENKEN, A. AND M. MOHAMMADI. The FGF family: biology, pathophysiology and therapy. In *Nat Rev Drug Discov*. England, 2009, vol. 8, p. 235-253.
21 BEI, D., J. MENG AND B. B. YOUAN Engineering nanomedicines for improved melanoma therapy: progress and promises. Nanomedicine (Lond), Nov 2010, 5(9), 1385-1399.
22 BLAIR, P. AND R. FLAUMENHAFT Platelet alpha-granules: basic biology and clinical correlates. Blood Rev, Jul 2009, 23(4), 177-189.
23 BLANES, M., M. J. GISBERT, B. MARCO, M. BONET, et al. Influence of glyoxal in the physical characterization of PVA nanofibers. Textile Research Journal, 2010, 80(14), 1465-1472.
24 BOCHET, C. G. Photolabile protecting groups and linkers. Journal of the Chemical Society, Perkin Transactions 1, 2002, (2), 125-142.
25 BRITTBERG, M. AND W. GERSOFF *Cartilage Surgery: An Operative Manual, with Expert Consult*. Edtion ed.: Elsevier Health Sciences, 2010. ISBN 143773622X.
26 BRODKIN, K. R., A. J. GARCIA AND M. E. LEVENSTON Chondrocyte phenotypes on different extracellular matrix monolayers. Biomaterials, 2004, 25(28), 5929-5938.
27 BUENO, D. F., I. KERKIS, A. M. COSTA, M. T. MARTINS, et al. New source of muscle-derived stem cells with potential for alveolar bone reconstruction in cleft lip and/or palate patients. Tissue Engineering Part A, 2008, 15(2), 427-435.
28 BURNOUF, T., H. A. GOUBRAN, T.-M. CHEN, K.-L. OU, et al. Blood-derived biomaterials and platelet growth factors in regenerative medicine. Blood reviews, 2013, 27(2), 77-89.
29 BUZGO, M., R. JAKUBOVA, A. MICKOVA, M. RAMPICHOVA, et al. Time-regulated drug delivery system based on coaxially incorporated platelet alpha-granules for biomedical use. Nanomedicine (Lond), Dec 2 2012.
30 CAO, H. Q., X. JIANG, C. CHAI AND S. Y. CHEW RNA interference by nanofiber-based siRNA delivery system. Journal of Controlled Release, Jun 1 2010, 144(2), 203-212.
31 CASPER, C. L., J. S. STEPHENS, N. G. TASSI, D. B. CHASE, et al. Controlling surface morphology of electrospun polystyrene fibers: Effect of humidity and molecular weight in the electrospinning process. Macromolecules, Jan 27 2004, 37(2), 573-578.
32 CATELAS, I., J. F. DWYER AND S. HELGERSON Controlled Release of Bioactive Transforming Growth Factor Beta-1 from Fibrin Gels In Vitro. Tissue Engineering Part C: Methods, 2008, 14(2), 119-28.
33 CHANG, H.-I. AND M.-K. YEH Clinical development of liposome-based drugs: formulation, characterization, and therapeutic efficacy. International journal of nanomedicine, 2012a, 7, 49.
34 CHANG, H. I. AND M. K. YEH Clinical development of liposome-based drugs: formulation, characterization, and therapeutic efficacy. Int J Nanomedicine, 2012b, 7, 49-60.
35 CHASTAIN, S. R., A. K. KUNDU, S. DHAR, J. W. CALVERT, et al. Adhesion of mesenchymal stem cells to polymer scaffolds occurs via distinct ECM ligands and controls their osteogenic differentiation. Edtion ed. ISBN 1.
36 CHEN, F. M., M. ZHANG AND Z. F. WU Toward delivery of multiple growth factors in tissue engineering. Biomaterials, Aug 2010, 31(24), 6279-6308.
37 CHEN, G.-C., I. C. KUAN, J.-R. HONG, B.-H. TSAI, et al. Activity enhancement and stabilization of lipase from Pseudomonas cepacia in polyallylamine-mediated biomimetic silica. Biotechnology Letters, Mar 2011, 33(3), 525-529.

38 CHOWDHURY, M. AND G. STYLIOS Effect of experimental parameters on the morphology of electrospun Nylon 6 fibres. International Journal of Basic & Applied Sciences, 2010, 10(6), 116.
39 CHUNG, C. AND J. A. BURDICK Engineering cartilage tissue. Advanced drug delivery reviews, 2008, 60(2), 243-262.
40 CHUNG, H. J. AND T. G. PARK Surface engineered and drug releasing pre-fabricated scaffolds for tissue engineering. Advanced Drug Delivery Reviews, 5/30/ 2007, 59(4–5), 249-262.
41 CIPITRIA, A., A. SKELTON, T. R. DARGAVILLE, P. D. DALTON, et al. Design, fabrication and characterization of PCL electrospun scaffolds-a review. Journal of Materials Chemistry, 2011 2011, 21(26), 9419-9453.
42 COLE, B. J., C. PASCUAL-GARRIDO AND R. C. GRUMET Surgical management of articular cartilage defects in the knee. The Journal of Bone & Joint Surgery, 2009, 91(7), 1778-1790.
43 COPLAND, M. J., T. RADES, N. M. DAVIES AND M. A. BAIRD. Lipid based particulate formulations for the delivery of antigen. In *Immunol Cell Biol.* Australia, 2005, vol. 83, p. 97-105.
44 CUI, W., Y. ZHOU AND J. CHANG Electrospun nanofibrous materials for tissue engineering and drug delivery. Science and Technology of Advanced Materials, Feb 2010, 11(1).
45 DAHLIN, R. L., F. K. KASPER AND A. G. MIKOS Polymeric nanofibers in tissue engineering. Tissue Eng Part B Rev, Oct 2011, 17(5), 349-364.
46 DANISOVIC, L., I. VARGA, S. POLAK, M. ULICNA, et al. Comparison of in vitro chondrogenic potential of human mesenchymal stem cells derived from bone marrow and adipose tissue. General physiology and biophysics, 2009, 28(1), 56-62.
47 DARAIN, F., W. Y. CHAN AND K. S. CHIAN PERFORMANCE OF SURFACE-MODIFIED POLYCAPROLACTONE ON GROWTH FACTOR BINDING, RELEASE, AND PROLIFERATION OF SMOOTH MUSCLE CELLS. Soft Materials, 2011 2011, 9(1), 64-78.
48 DARLING, E. M. AND K. A. ATHANASIOU Retaining zonal chondrocyte phenotype by means of novel growth environments. Tissue engineering, 2005, 11(3-4), 395-403.
49 DAVE, R., P. JAYARAJ, P. K. AJIKUMAR, H. JOSHI, et al. Endogenously triggered electrospun fibres for tailored and controlled antibiotic release. Journal of Biomaterials Science, Polymer Edition, 2013, 24(11), 1305-1319.
50 DE BOER, J., C. VAN BLITTERSWIJK, P. THOMSEN, J. HUBBELL, et al. *Tissue Engineering*. Edtion ed.: Elsevier Science, 2008. ISBN 9780080559193.
51 DEITZEL, J. M., J. KLEINMEYER, D. HARRIS AND N. C. B. TAN The effect of processing variables on the morphology of electrospun nanofibers and textiles. Polymer, Jan 2001, 42(1), 261-272.
52 DEMIDOVA-RICE, T. N., M. R. HAMBLIN AND I. M. HERMAN. Acute and impaired wound healing: pathophysiology and current methods for drug delivery, part 2: role of growth factors in normal and pathological wound healing: therapeutic potential and methods of delivery. In *Adv Skin Wound Care.* United States, 2012, vol. 25, p. 349-370.
53 DHANDAYUTHAPANI, B., Y. YOSHIDA, T. MAEKAWA AND D. S. KUMAR Polymeric scaffolds in tissue engineering application: a review. International Journal of Polymer Science, 2011, 2011.
54 DING, B., E. KIMURA, T. SATO, S. FUJITA, et al. Fabrication of blend biodegradable nanofibrous nonwoven mats via multi-jet electrospinning. Polymer, Mar 15 2004, 45(6), 1895-1902.

55 DING, Z., A. SALIM AND B. ZIAIE Selective nanofiber deposition through field-enhanced electrospinning. Langmuir, Sep 1 2009, 25(17), 9648-9652.
56 DOSHI, J. AND D. H. RENEKER Electrospinning Process and Applications of Electrospun Fibers. Journal of Electrostatics, Aug 1995, 35(2-3), 151-160.
57 DRENGK, A., A. ZAPF, E. K. STUERMER, K. M. STUERMER, et al. Influence of Platelet-Rich Plasma on Chondrogenic Differentiation and Proliferation of Chondrocytes and Mesenchymal Stem Cells. Cells Tissues Organs, 2009 2009, 189(5), 317-326.
58 DROR, Y., J. KUHN, R. AVRAHAMI AND E. ZUSSMAN Encapsulation of enzymes in biodegradable tubular structures. Macromolecules, Jun 24 2008, 41(12), 4187-4192.
59 DUNCAN, R. The dawning era of polymer therapeutics. Nature Reviews Drug Discovery, 2003, 2(5), 347-360.
60 DVIR, T., B. P. TIMKO, D. S. KOHANE AND R. LANGER Nanotechnological strategies for engineering complex tissues. Nat Nanotechnol, Jan 2011, 6(1), 13-22.
61 EDA, G. AND S. SHIVKUMAR Bead-to-fiber transition in electrospun polystyrene. Journal of Applied Polymer Science, Oct 5 2007, 106(1), 475-487.
62 EHRENFEST, D. M., L. RASMUSSON AND T. ALBREKTSSON Classification of platelet concentrates: from pure platelet-rich plasma (P-PRP) to leucocyte- and platelet-rich fibrin (L-PRF). Trends Biotechnol, Mar 2009, 27(3), 158-167.
63 FENG, J. J. The stretching of an electrified non-Newtonian jet: A model for electrospinning. Physics of Fluids, Nov 2002, 14(11), 3912-3926.
64 FERRETTI, C. AND M. MATTIOLI-BELMONTE Periosteum derived stem cells for regenerative medicine proposals: boosting current knowledge. World journal of stem cells, 2014, 6(3), 266.
65 FILOVA, E., Z. BURDIKOVA, M. RAMPICHOVA, P. BIANCHINI, et al. Analysis and three-dimensional visualization of collagen in artificial scaffolds using nonlinear microscopy techniques. J Biomed Opt, Nov-Dec 2010, 15(6), 066011.
66 FILOVA, E., M. RAMPICHOVA, A. LITVINEC, M. DRZIK, et al. A cell-free nanofiber composite scaffold regenerated osteochondral defects in miniature pigs. Int J Pharm, Apr 15 2013, 447(1-2), 139-149.
67 FISER, R. AND I. KONOPASEK Different modes of membrane permeabilization by two RTX toxins: HlyA from Escherichia coli and CyaA from Bordetella pertussis. Biochimica Et Biophysica Acta-Biomembranes, Jun 2009, 1788(6), 1249-1254.
68 Process and apparatus for preparing artificial thread. FORMHALS, A.
69 FORWARD, K. M., A. FLORES AND G. C. RUTLEDGE Production of core/shell fibers by electrospinning from a free surface. Chemical Engineering Science, 12/18/ 2013, 104(0), 250-259.
70 GARG, K. AND G. L. BOWLIN Electrospinning jets and nanofibrous structures. Biomicrofluidics, Mar 2011, 5(1).
71 GOMES, D. S., A. N. R. DA SILVA, N. I. MORIMOTO, L. T. F. MENDES, et al. Characterization of an electrospinning process using different PAN/DMF concentrations. Polimeros, 2007, 17(3), 206-211.
72 GOMES, S. R., G. RODRIGUES, G. G. MARTINS, M. A. ROBERTO, et al. In vitro and in vivo evaluation of electrospun nanofibers of PCL, chitosan and gelatin: A comparative study. Materials Science and Engineering: C, 2015, 46, 348-358.
73 GOOCH, K. J., T. BLUNK, D. L. COURTER, A. L. SIEMINSKI, et al. IGF-I and mechanical environment interact to modulate engineered cartilage development. Biochemical and biophysical research communications, 2001, 286(5), 909-915.
74 GREPLOVA, J. Využití imunoliposomů pro tansport a řízené uvolňování léčiv Universita Karlova, 2009.

75 GUILAK, F. Compression-induced changes in the shape and volume of the chondrocyte nucleus. Journal of biomechanics, 1995, 28(12), 1529-1541.
76 GUIMARAES, A., A. MARTINS, E. D. PINHO, S. FARIA, et al. Solving cell infiltration limitations of electrospun nanofiber meshes for tissue engineering applications. Nanomedicine (Lond), Jun 2010, 5(4), 539-554.
77 GUNATILLAKE, P., R. MAYADUNNE AND R. ADHIKARI Recent developments in biodegradable synthetic polymers. Biotechnology annual review, 2006, 12, 301-347.
78 HAMMOUCHE, S., D. HAMMOUCHE AND M. MCNICHOLAS Biodegradable bone regeneration synthetic scaffolds: in tissue engineering. Current stem cell research & therapy, 2012, 7(2), 134-142.
79 HARASHIMA, H., K. SAKATA, K. FUNATO AND H. KIWADA Enhanced hepatic uptake of liposomes through complement activation depending on the size of liposomes. Pharmaceutical research, 1994, 11(3), 402-406.
80 HAYES, M., G. CURLEY, B. ANSARI AND J. G. LAFFEY. Clinical review: Stem cell therapies for acute lung injury/acute respiratory distress syndrome - hope or hype? In *Crit Care.* England, 2012, vol. 16, p. 205.
81 HE, W., T. YONG, W. E. TEO, Z. MA, et al. Fabrication and endothelialization of collagen-blended biodegradable polymer nanofibers: potential vascular graft for blood vessel tissue engineering. Tissue Eng, Sep-Oct 2005, 11(9-10), 1574-1588.
82 HOKUGO, A., M. OZEKI, O. KAWAKAMI, K. SUGIMOTO, et al. Augmented bone regeneration activity of platelet-rich plasma by biodegradable gelatin hydrogel. Tissue Engineering, Jul-Aug 2005, 11(7-8), 1224-1233.
83 HOMAYONI, H., S. A. H. RAVANDI AND M. VALIZADEH Electrospinning of chitosan nanofibers: Processing optimization. Carbohydrate Polymers, Jul 11 2009, 77(3), 656-661.
84 HOWARD, D., L. D. BUTTERY, K. M. SHAKESHEFF AND S. J. ROBERTS Tissue engineering: strategies, stem cells and scaffolds. Journal of anatomy, 2008, 213(1), 66-72.
85 HU, X., S. LIU, G. ZHOU, Y. HUANG, et al. Electrospinning of polymeric nanofibers for drug delivery applications. Journal of Controlled Release, 2014, 185, 12-21.
86 HUANG, C., H. NIU, C. WU, Q. KE, et al. Disc-electrospun cellulose acetate butyrate nanofibers show enhanced cellular growth performances. Journal of Biomedical Materials Research Part A, 2013, 101(1), 115-122.
87 HUANG, C. B., S. L. CHEN, C. L. LAI, D. H. RENEKER, et al. Electrospun polymer nanofibres with small diameters. Nanotechnology, Mar 28 2006a, 17(6), 1558-1563.
88 HUANG, X.-J., D. GE AND Z.-K. XU Preparation and characterization of stable chitosan nanofibrous membrane for lipase immobilization. European Polymer Journal, 2007, 43(9), 3710-3718.
89 HUANG, X.-J., Z.-K. XU, L.-S. WAN, C. INNOCENT, et al. Electrospun Nanofibers Modified with Phospholipid Moieties for Enzyme Immobilization. Macromolecular Rapid Communications, 2006b, 27(16), 1341-1345.
90 IGNATIUS, R., K. MAHNKE, M. RIVERA, K. HONG, et al. Presentation of proteins encapsulated in sterically stabilized liposomes by dendritic cells initiates CD8+ T-cell responses in vivo. Blood, 2000, 96(10), 3505-3513.
91 IMMORDINO, M. L., F. DOSIO AND L. CATTEL Stealth liposomes: review of the basic science, rationale, and clinical applications, existing and potential. International journal of nanomedicine, 2006, 1(3), 297.
92 ISOGAI, N., T. MOROTOMI, S. HAYAKAWA, H. MUNAKATA, et al. Combined chondrocyte–copolymer implantation with slow release of basic fibroblast growth factor for tissue engineering an auricular cartilage construct. Journal of Biomedical Materials Research Part A, 2005, 74A(3), 408-418.

93 ITALIANO, J. E., JR, J. L. RICHARDSON, S. PATEL-HETT, E. BATTINELLI, et al. Angiogenesis is regulated by a novel mechanism: pro- and antiangiogenic proteins are organized into separate platelet {alpha} granules and differentially released. Blood, February 1, 2008 2008, 111(3), 1227-1233.
94 JACOBS, V., R. D. ANANDJIWALA AND M. MAAZA The Influence of Electrospinning Parameters on the Structural Morphology and Diameter of Electrospun Nanofibers. Journal of Applied Polymer Science, Mar 5 2010, 115(5), 3130-3136.
95 JAKOB, M., O. DEMARTEAU, D. SCHÄFER, B. HINTERMANN, et al. Specific growth factors during the expansion and redifferentiation of adult human articular chondrocytes enhance chondrogenesis and cartilaginous tissue formation in vitro. Journal of cellular biochemistry, 2001, 81(2), 368-377.
96 JELEN, K., F. LOPOT, S. BUDKA, V. NOVACEK, et al. Rheological properties of myometrium: experimental quantification and mathematical modeling. Neuro endocrinology letters, 2008, 29(4), 454-460.
97 JESORKA, A. AND O. ORWAR Liposomes: technologies and analytical applications. Annu. Rev. Anal. Chem., 2008, 1, 801-832.
98 JEUN, J-P., Y.-K. JEON, Y.-C. NHO AND P.-H. KANG Effects of gamma irradiation on the thermal and mechanical properties of chitosan/PVA nanofibrous mats. Journal of Industrial and Engineering Chemistry, 2009, 15(3), 430-433.
99 JI, W., Y. SUN, F. YANG, J. J. J. P. VAN DEN BEUCKEN, et al. Bioactive electrospun scaffolds delivering growth factors and genes for tissue engineering applications. Pharmaceutical research, 2011, 28(6), 1259-1272.
100 JIANG, G. AND X. QIN An improved free surface electrospinning for high throughput manufacturing of core–shell nanofibers. Materials Letters, 8/1/ 2014, 128(0), 259-262.
101 JIANG, H., Y. HU, P. ZHAO, Y. LI, et al. Modulation of protein release from biodegradable core-shell structured fibers prepared by coaxial electrospinning. J Biomed Mater Res B Appl Biomater, Oct 2006, 79(1), 50-57.
102 A method of nanofibres production from a polymer solution using electrostatic spinning and a device for carrying out the method. JIRSAK, O., J. CHALOUPEK, K. KOTEK, D. LUKAS, et al. 2009, Patent US7585437 B2
103 JIRSAK, O., P. SYSEL, F. SANETRNIK, J. HRUZA, et al. Polyamic Acid Nanofibers Produced by Needleless Electrospinning. Journal of Nanomaterials, 2010 2010.
104 KARUPPUSWAMY, P., J. R. VENUGOPAL, B. NAVANEETHAN, A. L. LAIVA, et al. Polycaprolactone nanofibers for the controlled release of tetracycline hydrochloride. Materials Letters, 2015, 141, 180-186.
105 KEUN KWON, I., S. KIDOAKI AND T. MATSUDA Electrospun nano- to microfiber fabrics made of biodegradable copolyesters: structural characteristics, mechanical properties and cell adhesion potential. Biomaterials, 2005, 26(18), 3929-3939.
106 KHAJAVI, R. AND M. ABBASIPOUR Electrospinning as a versatile method for fabricating coreshell, hollow and porous nanofibers. Scientia Iranica, 12// 2012, 19(6), 2029-2034.
107 KI, C. S., J. W. KIM, J. H. HYUN, K. H. LEE, et al. Electrospun three-dimensional silk fibroin nanofibrous scaffold. Journal of applied polymer science, 2007, 106(6), 3922-3928.
108 KIM, C.-K., B.-S. KIM, F. A. SHEIKH, U.-S. LEE, et al. Amphiphilic poly (vinyl alcohol) hybrids and electrospun nanofibers incorporating polyhedral oligosilsesquioxane. Macromolecules, 2007, 40(14), 4823-4828.
109 KIM, G., Y.-S. CHO AND W. D. KIM Stability analysis for multi jets electrospinning process modified with a cylindrical electrode. European Polymer Journal, Sep 2006, 42(9), 2031-2038.

110 KIM, Y. S., H. J. LEE, J. E. YEO, Y. I. KIM, et al. Isolation and Characterization of Human Mesenchymal Stem Cells Derived From Synovial Fluid in Patients With Osteochondral Lesion of the Talus. The American journal of sports medicine, 2014, 0363546514559822.
111 KNUTSEN, G., J. O. DROGSET, L. ENGEBRETSEN, T. GRØNTVEDT, et al. A Randomized Trial Comparing Autologous Chondrocyte Implantation with Microfracture. The Journal of Bone & Joint Surgery, 2007, 89(10), 2105-2112.
112 KOCER, A. A remote controlled valve in liposomes for triggered liposomal release. In *J Liposome Res*. United States, 2007, vol. 17, p. 219-225.
113 KRAMER, J., C. HEGERT, K. GUAN, A. M. WOBUS, et al. Embryonic stem cell-derived chondrogenic differentiation in vitro: activation by BMP-2 and BMP-4. Mechanisms of development, 2000, 92(2), 193-205.
114 KUMAR, V. V. Complementary molecular shapes and additivity of the packing parameter of lipids. Proc Natl Acad Sci U S A, Jan 15 1991, 88(2), 444-448.
115 LACCI, K. M. AND A. DARDIK Platelet-rich plasma: support for its use in wound healing. Yale J Biol Med, Mar 2010, 83(1), 1-9.
116 LANA, J. F., A. WEGLEIN, E. VICENTE, A. G. M. PEREZ, et al. Platelet Rich Plasma and Its Growth Factors: The State of the Art. In *Platelet-Rich Plasma*. Springer, 2014, p. 1-59.
117 LANGER, R. AND J. P. VACANTI Tissue engineering. Science, May 14 1993, 260(5110), 920-926.
118 LAURENCIN, C. T. AND L. S. NAIR *Nanotechnology and tissue engineering: the scaffold*. Edtion ed.: CRC Press, 2008. ISBN 1420051830.
119 LEE, G. H., J.-C. SONG AND K.-B. YOON Controlled wall thickness and porosity of polymeric hollow nanofibers by coaxial electrospinning. Macromolecular Research, 2010, 18(6), 571-576.
120 LI, D., G. OUYANG, J. T. MCCANN AND Y. XIA Collecting electrospun nanofibers with patterned electrodes. Nano Letters, May 2005, 5(5), 913-916.
121 LI, D. AND Y. XIA Direct Fabrication of Composite and Ceramic Hollow Nanofibers by Electrospinning. Nano Letters, 2004/05/01 2004, 4(5), 933-938.
122 LI, H., C. ZHAO, Z. WANG, H. ZHANG, et al. Controlled release of PDGF-bb by coaxial electrospun dextran/poly(L-lactide-co-epsilon-caprolactone) fibers with an ultrafine core/shell structure. J Biomater Sci Polym Ed, 2010a, 21(6), 803-819.
123 LI, J., R. SHI AND S. CONNELL *Biomimetic architectures for tissue engineering*. Edtion ed.: INTECH Open Access Publisher, 2010b. ISBN 9533070250.
124 LI, P., D. LIU, X. SUN, C. LIU, et al. A novel cationic liposome formulation for efficient gene delivery via a pulmonary route. Nanotechnology, 2011, 22(24), 245104.
125 LI, Z. AND C. WANG. One-Dimensional nanostructures: Electrospinning Technique and Unique Nanofibers. In.: Springer, 2013.
126 LIAO, I. C., S. Y. CHEW AND K. W. LEONG Aligned core-shell nanofibers delivering bioactive proteins. Nanomedicine (Lond), Dec 2006, 1(4), 465-471.
127 LIAO, I. C. AND K. W. LEONG Efficacy of engineered FVIII-producing skeletal muscle enhanced by growth factor-releasing co-axial electrospun fibers. Biomaterials, Feb 2011, 32(6), 1669-1677.
128 LIMA, A. C., P. SHER AND J. F. MANO Production methodologies of polymeric and hydrogel particles for drug delivery applications. Expert opinion on drug delivery, 2012, 9(2), 231-248.
129 LIN, J. S., L. CHEN, Y. LIU AND Y. Z. WANG Flame-retardant and physical properties of poly (vinyl alcohol) chemically modified by diethyl chlorophosphate. Journal of Applied Polymer Science, 2012, 125(5), 3517-3523.

130 LIU, X. AND P. X. MA Polymeric scaffolds for bone tissue engineering. Annals of biomedical engineering, 2004, 32(3), 477-486.
131 LOSCERTALES, I. G., A. BARRERO, M. MÁRQUEZ, R. SPRETZ, et al. Electrically forced coaxial nanojets for one-step hollow nanofiber design. Journal of the American Chemical Society, 2004, 126(17), 5376-5377.
132 LOWERY, A., H. ONISHKO, D. E. HALLAHAN AND Z. HAN Tumor-targeted delivery of liposome-encapsulated doxorubicin by use of a peptide that selectively binds to irradiated tumors. Journal of Controlled Release, 2011, 150(1), 117-124.
133 LUKAS, D., A. SARKAR AND J. CHALOUPEK. Principles of Electrospinning In *V.K. KOTHARI* ed. *Nonwoven Fabrics. New Delhi, India* IAFL Publications, 2008a, vol. 4.
134 LUKAS, D., A. SARKAR, L. MARTINOVÁ, K. VODSEĎÁLKOVÁ, et al. Physical principles of electrospinning (Electrospinning as a nano-scale technology of the twenty-first century). Textile progress, 2009, Vol.41(No.2), 59-140.
135 LUKAS, D., A. SARKAR AND P. POKORNY Self-organization of jets in electrospinning from free liquid surface: A generalized approach. Journal of Applied Physics, Apr 15 2008b, 103(8).
136 LUTTENBERGER, T., A. SCHMID-KOTSAS, A. MENKE, M. SIECH, et al. Platelet-derived growth factors stimulate proliferation and extracellular matrix synthesis of pancreatic stellate cells: implications in pathogenesis of pancreas fibrosis. Laboratory investigation, 2000, 80(1), 47-55.
137 LUYTEN, F. P. Cartilage-derived morphogenetic proteins - Key regulators in chondrocyte differentiation? Acta Orthopaedica Scandinavica, Oct 1995, 66, 51-54.
138 MA, Z., M. KOTAKI, R. INAI AND S. RAMAKRISHNA Potential of Nanofiber Matrix as Tissue-Engineering Scaffolds. Tissue Engineering, 2005/01/01 2005, 11(1-2), 101-109.
139 MAKRIS, E. A., A. H. GOMOLL, K. N. MALIZOS, J. C. HU, et al. Repair and tissue engineering techniques for articular cartilage. Nature Reviews Rheumatology, 2014.
140 MARTINS, A., A. R. DUARTE, S. FARIA, A. P. MARQUES, et al. Osteogenic induction of hBMSCs by electrospun scaffolds with dexamethasone release functionality. In *Biomaterials.* England: 2010 Elsevier Ltd, 2010, vol. 31, p. 5875-5885.
141 MARX, R. E., E. R. CARLSON, R. M. EICHSTAEDT, S. R. SCHIMMELE, et al. Platelet-rich plasma: Growth factor enhancement for bone grafts. Oral Surg Oral Med Oral Pathol Oral Radiol Endod, Jun 1998, 85(6), 638-646.
142 MASOUNAVE, J., A. L. ROLLIN AND R. DENIS Prediction of permeability of non-woven geotextiles from morphometry analysis. Journal of Microscopy, 1981, 121(1), 99-110.
143 MASUOKA, K., T. ASAZUMA, H. HATTORI, Y. YOSHIHARA, et al. Tissue engineering of articular cartilage with autologous cultured adipose tissue-derived stromal cells using atelocollagen honeycomb-shaped scaffold with a membrane sealing in rabbits. Journal of Biomedical Materials Research Part B: Applied Biomaterials, 2006, 79(1), 25-34.
144 MATLOCK-COLANGELO, L. AND A. J. BAEUMNER Biologically Inspired Nanofibers for Use in Translational Bioanalytical Systems. Annual Review of Analytical Chemistry, 2014, 7, 23-42.
145 MATTANAVEE, W., O. SUWANTONG, S. PUTHONG, T. BUNAPRASERT, et al. Immobilization of biomolecules on the surface of electrospun polycaprolactone fibrous scaffolds for tissue engineering. ACS Appl Mater Interfaces, May 2009, 1(5), 1076-1085.
146 MATTEUCCI, M. L. AND D. E. THRALL THE ROLE OF LIPOSOMES IN DRUG DELIVERY AND DIAGNOSTIC IMAGING: A REVIEW. Veterinary Radiology & Ultrasound, 2000, 41(2), 100-107.

147 MAYER, L. D., M. B. BALLY, M. J. HOPE AND P. R. CULLIS Techniques for encapsulating bioactive agents into liposomes. Chem Phys Lipids, 1986, 40(2-4):333-45.
148 MIOT, S., P. SCANDIUCCI DE FREITAS, D. WIRZ, A. U. DANIELS, et al. Cartilage tissue engineering by expanded goat articular chondrocytes. Journal of orthopaedic research, 2006, 24(5), 1078-1085.
149 MISHRA, A., P. TUMMALA, A. KING, B. LEE, et al. Buffered platelet-rich plasma enhances mesenchymal stem cell proliferation and chondrogenic differentiation. Tissue Eng Part C Methods, Sep 2009, 15(3), 431-435.
150 MIT-UPPATHAM, C., M. NITHITANAKUL AND P. SUPAPHOL Ultratine electrospun polyamide-6 fibers: Effect of solution conditions on morphology and average fiber diameter. Macromolecular Chemistry and Physics, Nov 26 2004, 205(17), 2327-2338.
151 MOURITSEN, O. G. *Life-as a matter of fat: the emerging science of lipidomics*. Edtion ed.: Springer Science & Business Media, 2005. ISBN 3540232486.
152 MROSS, K., B. NIEMANN, U. MASSING, J. DREVS, et al. Pharmacokinetics of liposomal doxorubicin (TLC-D99; Myocet) in patients with solid tumors: an open-label, single-dose study. Cancer Chemother Pharmacol, Dec 2004, 54(6), 514-524.
153 MUFAMADI, M. S., Y. E. CHOONARA, P. KUMAR, G. MODI, et al. Ligand-functionalized nanoliposomes for targeted delivery of galantamine. International journal of pharmaceutics, 2013, 448(1), 267-281.
154 MUIR, H. The chondrocyte, architect of cartilage. Biomechanics, structure, function and molecular biology of cartilage matrix macromolecules. Bioessays, 1995, 17(12), 1039-1048.
155 NEVES, N. M., R. CAMPOS, A. PEDRO, J. CUNHA, et al. Patterning of polymer nanofiber meshes by electrospinning for biomedical applications. International journal of nanomedicine, 2007, 2(3), 433.
156 NEW, R. R. C. *Liposomes: A Practical Approach*. edited by D. RICKWOOD AND B.D. JAMES. Edtion ed.: IRL Press at Oxford University Press, 1990, 1990. 301 p.
157 NIE, H., B. W. SOH, Y. C. FU AND C. H. WANG Three-dimensional fibrous PLGA/HAp composite scaffold for BMP-2 delivery. Biotechnol Bioeng, Jan 1 2008, 99(1), 223-234.
158 NIE, Y., J. J. DE PABLO AND S. P. PALECEK Platelet cryopreservation using a trehalose and phosphate formulation. Biotechnology and Bioengineering, 2005, 92(1), 79-90.
159 NIESSEN, J., G. JEDLITSCHKY, M. GRUBE, S. BIEN, et al. Subfractionation and purification of intracellular granule-structures of human platelets: an improved method based on magnetic sorting. J Immunol Methods, Dec 1 2007, 328(1-2), 89-96.
160 NISHIKAWA, K., H. ARAI AND K. INOUE Scavenger receptor-mediated uptake and metabolism of lipid vesicles containing acidic phospholipids by mouse peritoneal macrophages. Journal of Biological Chemistry, 1990, 265(9), 5226-5231.
161 NIU, H., T. LIN AND X. WANG Needleless electrospinning. I. A comparison of cylinder and disk nozzles. Journal of Applied Polymer Science, 2009, 114(6), 3524-3530.
162 NIU, H., X. WANG AND T. LIN Upward Needleless Electrospinning of Nanofibers. Journal of Engineered Fibers and Fabrics, 2012 2012, 7, 17-22.
163 O'BYRNE, K. J., A. L. THOMAS, R. A. SHARMA, M. DECATRIS, et al. A phase I dose-escalating study of DaunoXome, liposomal daunorubicin, in metastatic breast cancer. Br J Cancer, Jul 1 2002, 87(1), 15-20.
164 PAN, N. AND G. PHIL Thermal and moisture transport in fibrous materials. Edtion ed., 2006.

165 PARK, J.-C., T. ITO, K.-O. KIM, K.-W. KIM, et al. Electrospun poly(vinyl alcohol) nanofibers: effects of degree of hydrolysis and enhanced water stability. Polymer Journal, Mar 2010, 42(3), 273-276.
166 PATEL, A. C., S. LI, J. M. YUAN AND Y. WEI In situ encapsulation of horseradish peroxidase in electrospun porous silica fibers for potential biosensor applications. Nano Letters, May 2006, 6(5), 1042-1046.
167 PATEL, H., M. BONDE AND G. SRINIVASAN Biodegradable polymer scaffold for tissue engineering. Trends Biomater Artif Organs, 2011, 25(1), 20-29.
168 PERESIN, M. S., Y. HABIBI, J. O. ZOPPE, J. J. PAWLAK, et al. Nanofiber composites of polyvinyl alcohol and cellulose nanocrystals: manufacture and characterization. Biomacromolecules, 2010, 11(3), 674-681.
169 PERSANO, L., A. CAMPOSEO, C. TEKMEN AND D. PISIGNANO Industrial Upscaling of Electrospinning and Applications of Polymer Nanofibers: A Review. Macromolecular Materials and Engineering, May 2013, 298(5), 504-520.
170 PHAM, Q. P., U. SHARMA AND A. G. MIKOS Electrospun Poly(ε-caprolactone) Microfiber and Multilayer Nanofiber/Microfiber Scaffolds: Characterization of Scaffolds and Measurement of Cellular Infiltration. Biomacromolecules, 2006/10/01 2006, 7(10), 2796-2805.
171 PITTENGER, M. F., A. M. MACKAY, S. C. BECK, R. K. JAISWAL, et al. Multilineage potential of adult human mesenchymal stem cells. science, 1999, 284(5411), 143-147.
172 PROSECKA, E., M. RAMPICHOVA, L. VOJTOVA, D. TVRDIK, et al. Optimized conditions for mesenchymal stem cells to differentiate into osteoblasts on a collagen/hydroxyapatite matrix. Journal of Biomedical Materials Research Part A, Nov 2011, 99A(2), 307-315.
173 PROSECKÁ, E., M. RAMPICHOVÁ, A. LITVINEC, Z. TONAR, et al. Collagen/hydroxyapatite scaffold enriched with polycaprolactone nanofibers, thrombocyte-rich solution and mesenchymal stem cells promotes regeneration in large bone defect in vivo. Journal of Biomedical Materials Research Part A, 2015, 103(2), 671-682.
174 PURI, A. Phototriggerable Liposomes: Current Research and Future Perspectives. Pharmaceutics, Mar 2014, 6(1), 1-25.
175 QU, H., S. WEI AND Z. GUO Coaxial electrospun nanostructures and their applications. Journal of Materials Chemistry A, 2013, 1(38), 11513-11528.
176 RAMOS-TORRECILLAS, J., E. DE LUNA-BERTOS, O. GARCIA-MARTINEZ AND C. RUIZ Clinical Utility of Growth Factors and Platelet-Rich Plasma in Tissue Regeneration: A Review. WOUNDS-A COMPENDIUM OF CLINICAL RESEARCH AND PRACTICE, 2014, 26(7), 207-213.
177 RAMPICHOVA, M., J. CHVOJKA, M. BUZGO, E. PROSECKA, et al. Elastic three-dimensional poly (epsilon-caprolactone) nanofibre scaffold enhances migration, proliferation and osteogenic differentiation of mesenchymal stem cells. Cell Prolif, Feb 2013, 46(1), 23-37.
178 RAMPICHOVA, M., L. MARTINOVA, E. KOSTAKOVA, E. FILOVA, et al. A simple drug anchoring microfiber scaffold for chondrocyte seeding and proliferation. Journal of Materials Science-Materials in Medicine, Feb 2012, 23(2), 555-563.
179 RAYLEIGH, F. R. S. XX. On the equilibrium of liquid conducting masses charged with electricity. In Philosophical Magazine Series 5. Taylor & Francis Group 1882, vol. 14, p. 184-186.
180 RENEKER, D. H. AND I. CHUN Nanometre diameter fibres of polymer, produced by electrospinning. Nanotechnology, Sep 1996, 7(3), 216-223.

181 REZNIK, S. N., A. L. YARIN, A. THERON AND E. ZUSSMAN Transient and steady shapes of droplets attached to a surface in a strong electric field. Journal of Fluid Mechanics, Oct 10 2004, 516, 349-377.
182 REZNIK, S. N., A. L. YARIN, E. ZUSSMAN AND L. BERCOVICI Evolution of a compound droplet attached to a core-shell nozzle under the action of a strong electric field. Phys. Fluids, 2006, 18(6), 062101.
183 RNJAK-KOVACINA, J. AND A. S. WEISS Increasing the pore size of electrospun scaffolds. Tissue Engineering Part B: Reviews, 2011, 17(5), 365-372.
184 RODOPLU, D. AND M. MUTLU Effects of Electrospinning Setup and Process Parameters on Nanofiber Morphology Intended for the Modification of Quartz Crystal Microbalance Surfaces. Journal of Engineered Fibers and Fabrics, 2012 2012, 7(2), 118-123.
185 RUGGERI, F., A. AKESSON, P.-Y. CHAPUIS, C. A. SKRZYNSKI NIELSEN, et al. The dendrimer impact on vesicles can be tuned based on the lipid bilayer charge and the presence of albumin. Soft Matter, 2013, 9(37), 8862-8870.
186 SAHOO, S., L. T. ANG, J. C.-H. GOH AND S.-L. TOH Growth factor delivery through electrospun nanofibers in scaffolds for tissue engineering applications. Journal of Biomedical Materials Research Part A, 2010, 93A(4), 1539-1550.
187 SALALHA, W., J. KUHN, Y. DROR AND E. ZUSSMAN Encapsulation of bacteria and viruses in electrospun nanofibres. Nanotechnology, 2006, 17(18), 4675.
188 SAMAD, A., Y. SULTANA AND M. AQIL Liposomal drug delivery systems: an update review. Current drug delivery, 2007, 4(4), 297-305.
189 SANTO, V. E., M. E. GOMES, J. F. MANO AND R. L. REIS From nano- to macro-scale: nanotechnology approaches for spatially controlled delivery of bioactive factors for bone and cartilage engineering. Nanomedicine (Lond), Jul 2012, 7(7), 1045-1066.
190 SANTOS, C., C. J. SILVA, Z. BÜTTEL, R. GUIMARÃES, et al. Preparation and characterization of polysaccharides/PVA blend nanofibrous membranes by electrospinning method. Carbohydrate polymers, 2014, 99, 584-592.
191 SAPRA, P. AND T. M. ALLEN Improved outcome when B-cell lymphoma is treated with combinations of immunoliposomal anticancer drugs targeted to both the CD19 and CD20 epitopes. Clinical Cancer Research, Apr 1 2004, 10(7), 2530-2537.
192 SARAF, A., L. S. BAGGETT, R. M. RAPHAEL, F. K. KASPER, et al. Regulated non-viral gene delivery from coaxial electrospun fiber mesh scaffolds. Journal of Controlled Release, Apr 2 2010, 143(1), 95-103.
193 SARAF, A., G. LOZIER, A. HAESSLEIN, F. K. KASPER, et al. Fabrication of nonwoven coaxial fiber meshes by electrospinning. Tissue Engineering Part C: Methods, 2009, 15(3), 333-344.
194 SCHNABEL, M., S. MARLOVITS, G. ECKHOFF, I. FICHTEL, et al. Dedifferentiation-associated changes in morphology and gene expression in primary human articular chondrocytes in cell culture. In *Osteoarthritis Cartilage*. England: 2002 OsteoArthritis Research Society International., 2002, vol. 10, p. 62-70.
195 SCHROEDER, A., J. KOST AND Y. BARENHOLZ Ultrasound, liposomes, and drug delivery: principles for using ultrasound to control the release of drugs from liposomes. Chemistry and physics of lipids, 2009, 162(1), 1-16.
196 SCHULDINER, M., O. YANUKA, J. ITSKOVITZ-ELDOR, D. A. MELTON, et al. Effects of eight growth factors on the differentiation of cells derived from human embryonic stem cells. Proceedings of the National Academy of Sciences of the United States of America, Oct 2000, 97(21), 11307-11312.

197 SCHULZE-TANZIL, G., P. DE SOUZA, H. V. CASTREJON, T. JOHN, et al. Redifferentiation of dedifferentiated human chondrocytes in high-density cultures. Cell and tissue research, 2002, 308(3), 371-379.
198 SCHULZE-TANZIL, G., A. MOBASHERI, P. DE SOUZA, T. JOHN, et al. Loss of chondrogenic potential in dedifferentiated chondrocytes correlates with deficient Shc–Erk interaction and apoptosis. Osteoarthritis and cartilage, 2004, 12(6), 448-458.
199 SCOTT, R. A., K. PARK AND A. PANITCH Water soluble polymer films for intravascular drug delivery of antithrombotic biomolecules. European Journal of Pharmaceutics and Biopharmaceutics, 2013, 84(1), 125-131.
200 SENIOR, J. H. Fate and behavior of liposomes in vivo: a review of controlling factors. Critical reviews in therapeutic drug carrier systems, 1986, 3(2), 123-193.
201 SHABANI, I., V. HADDADI-ASL, E. SEYEDJAFARI, F. BABAEIJANDAGHI, et al. Improved infiltration of stem cells on electrospun nanofibers. Biochem Biophys Res Commun, Apr 24 2009, 382(1), 129-133.
202 SHALUMON, K. T., K. H. ANULEKHA, C. M. GIRISH, R. PRASANTH, et al. Single step electrospinning of chitosan/poly (caprolactone) nanofibers using formic acid/acetone solvent mixture. Carbohydrate Polymers, 2010, 80(2), 413-419.
203 SHANMUGARAJAN, T. S., B.-S. KIM, H. LEE AND G.-I. IM Growth Factors and Signaling Pathways in the Chondrogenic Differentiation of Mesenchymal Stem Cells. Tissue Engineering and Regenerative Medicine, Jun 2011, 8(3), 292-299.
204 SHARMA, A. AND U. S. SHARMA Liposomes in drug delivery: progress and limitations. International Journal of Pharmaceutics, Aug 26 1997, 154(2), 123-140.
205 SILL, T. J. AND H. A. VON RECUM Electrospinning: applications in drug delivery and tissue engineering. Biomaterials, 2008, 29(13), 1989-2006.
206 SONG, T., Y. ZHANG, T. ZHOU, C. T. LIM, et al. Encapsulation of self-assembled FePt magnetic nanoparticles in PCL nanofibers by coaxial electrospinning. Chemical Physics Letters, 11/11/ 2005, 415(4–6), 317-322.
207 SRIKAR, R., A. L. YARIN, C. M. MEGARIDIS, A. V. BAZILEVSKY, et al. Desorption-limited mechanism of release from polymer nanofibers. Langmuir, Feb 5 2008, 24(3), 965-974.
208 STATTIN, P., S. RINALDI, C. BIESSY, U.-H. STENMAN, et al. High Levels of Circulating Insulin-Like Growth Factor-I Increase Prostate Cancer Risk: A Prospective Study in a Population-Based Nonscreened Cohort. Journal of Clinical Oncology, August 1, 2004 2004, 22(15), 3104-3112.
209 STEADMAN, J. R., K. K. BRIGGS, J. J. RODRIGO, M. S. KOCHER, et al. Outcomes of microfracture for traumatic chondral defects of the knee: average 11-year follow-up. Arthroscopy: The Journal of Arthroscopic & Related Surgery, 2003, 19(5), 477-484.
210 SUKIGARA, S., M. GANDHI, J. AYUTSEDE, M. MICKLUS, et al. Regeneration of Bombyx mori silk by electrospinning - part 1: processing parameters and geometric properties. Polymer, Sep 2003, 44(19), 5721-5727.
211 SUN, Z., E. ZUSSMAN, A. L. YARIN, J. H. WENDORFF, et al. Compound Core–Shell Polymer Nanofibers by Co-Electrospinning. Advanced Materials, 2003, 15(22), 1929-1932.
212 SUNDARAY, B., V. SUBRAMANIAN, T. S. NATARAJAN, R.-Z. XIANG, et al. Electrospinning of continuous aligned polymer fibers. Applied physics letters, 2004, 84(7), 1222-1224.
213 TAY, A. G., J. FARHADI, R. SUETTERLIN, G. PIERER, et al. Cell yield, proliferation, and postexpansion differentiation capacity of human ear, nasal, and rib chondrocytes. Tissue engineering, 2004, 10(5-6), 762-770.

214 TAYLOR, D. W., M. PETRERA, M. HENDRY AND J. S. THEODOROPOULOS A systematic review of the use of platelet-rich plasma in sports medicine as a new treatment for tendon and ligament injuries. Clinical journal of sport medicine, 2011, 21(4), 344-352.
215 TAYLOR, G. E. *Math.Phys.Sci. 280* Edtion ed., 1964.
216 TEMENOFF, J. S. AND A. G. MIKOS Review: tissue engineering for regeneration of articular cartilage. Biomaterials, 2000, 21(5), 431-440.
217 TEO, W.-E., R. INAI AND S. RAMAKRISHNA Technological advances in electrospinning of nanofibers. Science and Technology of Advanced Materials, Feb 2011, 12(1).
218 THERON, S. A., A. L. YARIN, E. ZUSSMAN AND E. KROLL Multiple jets in electrospinning: experiment and modeling. Polymer, Apr 15 2005, 46(9), 2889-2899.
219 THOMSON, J. A., J. ITSKOVITZ-ELDOR, S. S. SHAPIRO, M. A. WAKNITZ, et al. Embryonic stem cell lines derived from human blastocysts. science, 1998, 282(5391), 1145-1147.
220 TIWARI, S. K., R. TZEZANA, E. ZUSSMAN AND S. S. VENKATRAMAN Optimizing partition-controlled drug release from electrospun core-shell fibers. International Journal of Pharmaceutics, 2010, 392(1-2), 209-217.
221 TOMIC-CANIC, M., E. A. AYELLO, O. STOJADINOVIC, M. S. GOLINKO, et al. Using gene transcription patterns (bar coding scans) to guide wound debridement and healing. Advances in skin & wound care, 2008, 21(10), 487.
222 TONTI, G. A. AND F. MANNELLO From bone marrow to therapeutic applications: different behaviour and genetic/epigenetic stability during mesenchymal stem cell expansion in autologous and foetal bovine sera? International Journal of Developmental Biology, 2008, 52(8), 1023-1032.
223 TRIVANOVIĆ, D., J. KOCIĆ, S. MOJSILOVIĆ, A. KRSTIĆ, et al. Mesenchymal stem cells isolated from peripheral blood and umbilical cord Wharton's jelly. Srpski arhiv za celokupno lekarstvo, 2013, 141(3-4), 178-186.
224 TULI, R., S. TULI, S. NANDI, X. X. HUANG, et al. Transforming growth factor-beta-mediated chondrogenesis of human mesenchymal progenitor cells involves N-cadherin and mitogenactivated protein kinase and Wnt signaling cross-talk. Journal of Biological Chemistry, Oct 2003, 278(42), 41227-41236.
225 UCCELLI, A., L. MORETTA AND V. PISTOIA Mesenchymal stem cells in health and disease. Nature Reviews Immunology, 2008, 8(9), 726-736.
226 UWE, M. AND H. HEINRICH. Targeting of Cationic Liposomes to Endothelial Tissue. In *Liposome Technology, Volume III*. Informa Healthcare, 2006, p. 151-170.
227 VACANTI, C. A. AND J. P. VACANTI Functional Organ Replacement: The New Technology of Tissue Engineering. Surgical Technology International, 1991, 43.
228 VAQUETTE, C. AND J. J. COOPER-WHITE Increasing electrospun scaffold pore size with tailored collectors for improved cell penetration. Acta biomaterialia, 2011, 7(6), 2544-2557.
229 VARESANO, A., R. A. CARLETTO AND G. MAZZUCHETTI Experimental investigations on the multi-jet electrospinning process. Journal of Materials Processing Technology, Jun 21 2009, 209(11), 5178-5185.
230 VASITA, R. AND D. S. KATTI Nanofibers and their applications in tissue engineering. Int J Nanomedicine, Mar 2006, 1(1), 15-30.
231 VON HUNDELSHAUSEN, P. AND C. WEBER Platelets as Immune Cells: Bridging Inflammation and Cardiovascular Disease. Circ Res, January 5, 2007 2007, 100(1), 27-40.
232 WANG, B., T. J. SIAHAAN AND R. A. SOLTERO *Drug delivery: principles and applications*. Edtion ed.: John Wiley & Sons, 2005. ISBN 0471475718.

233 WANG, C. Y., J. J. LIU, C. Y. FAN, X. M. MO, et al. The effect of aligned core-shell nanofibres delivering NGF on the promotion of sciatic nerve regeneration. In *J Biomater Sci Polym Ed*. Netherlands, 2012, vol. 23, p. 167-184.
234 WANG, H., D. WU, D. LI, Z. NIU, et al. Fabrication of continuous highly ordered mesoporous silica nanofibre with core/sheath structure and its application as catalyst carrier. Nanoscale, 2011, 3(9), 3601-3604.
235 WANG, Y. Y., L. X. LU, Z. Q. FENG, Z. D. XIAO, et al. Cellular compatibility of RGD-modified chitosan nanofibers with aligned or random orientation. In *Biomed Mater*. England, 2010, vol. 5, p. 054112.
236 WANG, Z.-G., L.-S. WAN, Z.-M. LIU, X.-J. HUANG, et al. Enzyme immobilization on electrospun polymer nanofibers: An overview. Journal of Molecular Catalysis B-Enzymatic, Apr 2009, 56(4), 189-195.
237 WASUNGU, L. AND D. HOEKSTRA Cationic lipids, lipoplexes and intracellular delivery of genes. Journal of Controlled Release, 2006, 116(2), 255-264.
238 WATT, F. M. Effect of seeding density on stability of the differentiated phenotype of pig articular chondrocytes in culture. Journal of cell science, 1988, 89(3), 373-378.
239 WEISS, D. J., I. BERTONCELLO, Z. BOROK, C. KIM, et al. Stem cells and cell therapies in lung biology and lung diseases. Proceedings of the American Thoracic Society, 2011, 8(3), 223-272.
240 WENGUO, C. AND ET AL. Electrospun nanofibrous materials for tissue engineering and drug delivery. Science and Technology of Advanced Materials, 2010, 11(1), 014108.
241 WHITE, J. G. An overview of platelet structural physiology. Scanning Microsc, Dec 1987, 1(4), 1677-1700.
242 WOODWARD, S. C., P. S. BREWER, F. MOATAMED, A. SCHINDLER, et al. The intracellular degradation of poly(epsilon-caprolactone). J Biomed Mater Res, Apr 1985, 19(4), 437-444.
243 XIE, J. B. AND Y. L. HSIEH Ultra-high surface fibrous membranes from electrospinning of natural proteins: casein and lipase enzyme. Journal of Materials Science, May 15 2003, 38(10), 2125-2133.
244 YANG, D.-Z., Y.-H. LONG AND J. NIE Release of lysozyme from electrospun PVA/lysozyme-gelatin scaffolds. Frontiers of Materials Science in China, 2008/09/01 2008, 2(3), 261-265.
245 YANG, H., S. LANG, Z. ZHAI, L. LI, et al. Fibrinogen is required for maintenance of platelet intracellular and cell-surface P-selectin expression. Blood, Jul 9 2009, 114(2), 425-436.
246 YANG, Q. B., Z. Y. LI, Y. L. HONG, Y. Y. ZHAO, et al. Influence of solvents on the formation of ultrathin uniform poly(vinyl pyrrolidone) nanofibers with electrospinning. Journal of Polymer Science Part B-Polymer Physics, Oct 15 2004, 42(20), 3721-3726.
247 YARIN, A. L. Coaxial electrospinning and emulsion electrospinning of core–shell fibers. Polymers for Advanced Technologies, 2011, 22(3), 310-317.
248 YARIN, A. L., S. KOOMBHONGSE AND D. H. RENEKER Bending instability in electrospinning of nanofibers. Journal of Applied Physics, Mar 1 2001, 89(5), 3018-3026.
249 YARIN, A. L. AND E. ZUSSMAN Upward needleless electrospinning of multiple nanofibers. Polymer, Apr 27 2004, 45(9), 2977-2980.
250 YEGANEGI, M., R. A. KANDEL AND J. P. SANTERRE Characterization of a biodegradable electrospun polyurethane nanofiber scaffold: mechanical properties and cytotoxicity. Acta biomaterialia, 2010, 6(10), 3847-3855.
251 YOERDEM, O. S., M. PAPILA AND Y. Z. MENCELOGLU Effects of electrospinning parameters on polyacrylonitrile nanofiber diameter: An investigation by response surface methodology. Materials & Design, 2008 2008, 29(1), 34-44.

252 YOSHIMOTO, H., Y. M. SHIN, H. TERAI AND J. P. VACANTI A biodegradable nanofiber scaffold by electrospinning and its potential for bone tissue engineering. Biomaterials, 2003, 24(12), 2077-2082.
253 YU, J. H., S. V. FRIDRIKH AND G. C. RUTLEDGE Production of Submicrometer Diameter Fibers by Two-Fluid Electrospinning. Advanced Materials, 2004, 16(17), 1562-1566.
254 ZAMANI, M., M. P. PRABHAKARAN AND S. RAMAKRISHNA Advances in drug delivery via electrospun and electrosprayed nanomaterials. International journal of nanomedicine, 2013, 8, 2997.
255 ZELENY, J. *Phys. Rev. 3*. Edtion ed., 1914.
256 ZELENY, J. *Phys. Rev. 10*. Edtion ed., 1917.
257 ZENG, J., A. AIGNER, F. CZUBAYKO, T. KISSEL, et al. Poly(vinyl alcohol) nanofibers by electrospinning as a protein delivery system and the retardation of enzyme release by additional polymer coatings. Biomacromolecules, May-Jun 2005, 6(3), 1484-1488.
258 ZHA, Z., S. L. LEUNG, Z. DAI AND X. WU Centering of organic-inorganic hybrid liposomal cerasomes in electrospun gelatin nanofibers. Applied Physics Letters, 2012, 100(3), 033702-033702-033703.
259 ZHANG, N., Y.-P. WU, S.-J. QIAN, C. TENG, et al. Research progress in the mechanism of effect of PRP in bone deficiency healing. The Scientific World Journal, 2013, 2013.
260 ZHANG, Y. Z., X. WANG, Y. FENG, J. LI, et al. Coaxial electrospinning of (fluorescein isothiocyanate-conjugated bovine serum albumin)-encapsulated poly(epsilon-caprolactone) nanofibers for sustained release. Biomacromolecules, Apr 2006, 7(4), 1049-1057.
261 ZHAO, Y. Y., Q. B. YANG, X. F. LU, C. WANG, et al. Study on correlation of morphology of electrospun products of polyacrylamide with ultrahigh molecular weight. Journal of Polymer Science Part B-Polymer Physics, Aug 15 2005, 43(16), 2190-2195.
262 ZHOU, Y., D. YANG, X. CHEN, Q. XU, et al. Electrospun water-soluble carboxyethyl chitosan/poly (vinyl alcohol) nanofibrous membrane as potential wound dressing for skin regeneration. Biomacromolecules, 2007, 9(1), 349-354.
263 ZUK, P. A., M. ZHU, P. ASHJIAN, D. A. DE UGARTE, et al. Human adipose tissue is a source of multipotent stem cells. Molecular biology of the cell, 2002, 13(12), 4279-4295.
264 ZUSSMAN, E. Encapsulation of cells within electrospun fibers. Polymers for Advanced Technologies, 2011, 22(3), 366-371.

11 Reprints of papers published by the author

Papers with impact factor:

Míčková A, Buzgo M, Benada O, Rampichová M, Fišar Z, Filová E, Tesařová M, Lukáš D, Amler E. Core/Shell Nanofibers with Embedded Liposomes as a Drug Delivery System. *Biomacromolecules* 2012, 13(4), 952-962. IF 5.371

Buzgo M, Jakubová R, Míčková A, Rampichová M, Prosecká E, Kochová P, Lukáš D, Amler E. Time-regulated drug delivery system based on coaxially incorporated platelet α-granules for biomedical use. *Nanomedicine (Lond), 2013; 8(7): 1137-54. IF 5.824* Time-regulated drug delivery system based on coaxially incorporated platelet α-granules for biomedical use. *Nanomedicine* (Lond), 2013, 8(7), 1137-54. IF 5.824

Jakubová R, Míčková A, Buzgo M, Rampichová M, Prosecká E, Tvrdík D, Amler E. Immobilization of thrombocytes on PCL nanofibers enhances chondrocytes proliferation *in vitro*. *Cell proliferation*., 2011, 44, 183-191. IF 2.521

Review:

Amler E, Míčková A, Buzgo M. Electrospun core/shell nanofibers: a promising system for cartilage and tissue engineering? *Nanomedicine*, 2013, 8(4), 509-512. IF 5.824

Articles not directly related to the topic of this thesis

Papers with impact factor:

Rampichová M, Martinová L, Košťáková E, Filová E, Míčková A, Buzgo M, Michálek J, Přádný M, Nečas A, Lukáš D, Amler E. A simple drug anchoring microfiber scaffold for chondrocyte seeding and proliferation. *Journal of Materials Science: Materials in Medicine* 2012, 23(2), 555-563. DOI: 10.1007/s10856-011-4518-x. IF 2.163

Filová E, Rampichová M,Litvinec A, Držík M, Míčková A, Buuzgo M, Košťáková E, Martinová L, Usvald D, prosecká E, Uhlík J, Motlík J, Vajner L, Amler E. A cell-free nanofiber composite scaffold regenerated osteochondral defects in miniature pigs. *International Journal of Pharmaceutics.* 2013, 447(1-2), 139-149. DOI: 10.1016/j.ijpharm.2013.02.056. IF 3.785

Knotek P, Pouzar M, Buzgo M, Křížková B, Vlček M, Míčková A, Plencner M, Návěsník P, Amler E, Bělina P. Cryogenic grinding of electrospun poly-ε-caprolactone mesh submerged in liquid media. *Materials Science and Engineering: C.* 2012, 32(6), 1366-1374 DOI: 10.1016/j.msec.2012.04.012. IF 2.736

Plencner M, East B, Tonar Z, M, Otáhal M, Prosecká E, Rampichová M, Krejčí T, Litvinec A, Buzgo M, Míčková A, Nečas A, Hoch J, Amler E. Abdominal closure reinforcement by using polypropylene mesh functionalized with poly-ε-caprolactone nanofibers and growth factors for prevention of incisional hernia formation. *International Journal of Nanomedicine*, 2014, 9, 3263–3277. IF 4.195

Prosecká E, Rampichová M, Litvinec A, Tonar Z, Králíčková M,Vojtová L, Kochová P, Plencner M, Buzgo M, Míčková A, Jančář J, Amler E. Collagen/hydroxyapatite scaffold enriched with polycaprolactone nanofibres, thrombocyte-rich solution and MSCs accelerates regeneration in large bone defect *in vivo*. *Journal of Biomedical Materials Research- Part A,* 2015, 103(2), 671-682. IF 2,88

Míčková A, Tománková K, Kolářová H, Bajgar R, Kolář P, Šunka P, Plencner M, Jakubova R, Beneš J, Koláčná L, Plánka L, Nečas A, Amler E. Ultrasonic shock-wave as a control mechanism for liposome drug delivery system for possible use in scaffold implanted to animals with iatrogenic articular cartilage defects. *Acta Veterinaria Brno*. 2008, 77(2), 285-296. IF 0,448

Papers without impact factor:

Vocetkova K, Míčková A, Rosina J, Handl M, Amler E. Liposomy, jejich charakterizace, příprava a inkorporace do nanovlákenných nosičů. *Lékař a technika - Clinician and Technology* 2014, 2(44), 11-17.

Textbook:

Amler E, Buzgo M, Filová E, Jakubová R, Koláčná L, Kotyk A, Míčková A, Plencner M, Prosecká E, Rampichová M, Varga F, Zavřelová T. Lékařské textilie – 1. díl.; Centrum pro podporu konkurenceschopnosti v biomedicínských technologiích; Amler E (ed) Ústav experimentální medicíny AV ČR, v.v.i., Praha, 2008.

12 Appendix

The Council of Research, Development and Innovation Office of the Government of the Czech Republic published a list of the top 20% of results for year 2014, which qualify for a special bonus under Pillar II. Methodologies 2013. The paper "*Míčková A, Buzgo M, Benada O, Rampichová M, Fišar Z, Filová E, Tesařová M, Lukáš D, Amler E.* Core/Shell Nanofibers with Embedded Liposomes as a Drug Delivery System. *Biomacromolecules* 2012, 13(4), 952-962 (IF 5.371)" was classified in the published list under panel EP-11, A-class results, with the commendation: Exceptionally high-quality results in original pharmaceutical research with excellent publication output.

http://www.vyzkum.cz/FrontAktualita.aspx?aktualita=737422

Rada pro výzkum, vývoj a inovace Úřadu vlády ČR zveřejnila seznam 20% nejlepších výsledků za rok 2014, které si zaslouží zvláštní bonifikaci dle Pilíře II. Metodiky 2013. Článek "*Míčková A, Buzgo M, Benada O, Rampichová M, Fišar Z, Filová E, Tesařová M, Lukáš D, Amler E.* Core/Shell Nanofibers with Embedded Liposomes as a Drug Delivery System. *Biomacromolecules* 2012, 13(4), 952-962 (IF 5.371)" byl zařazen do uvedeného seznamu v panelu EP-11, výsledky třídy A s odůvodněním: Mimořádné kvalitní výsledky originálního farmaceutického výzkumu s výborným publikačním výstupem.

http://www.vyzkum.cz/FrontAktualita.aspx?aktualita=737422

13 Acknowledgements

This study has been supported by the Academy of Sciences of the Czech Republic (institutional research plans AV0Z50390703 and AV0Z50390512), the Grant Agency of the Czech Republic (Grants Nos. P304/10/1307, 106/09/P226 and GA202/09/1151), the Grant Agency of the Academy of Sciences (Grant No. IAA500390702), the Grant Agency of Charles University (Grants Nos. 96610, 330611, 384311, 626012, 119209 and 648112), the Ministry of Education of the Czech Republic – project ERA–NET CARSILA no. ME 10145, the Grant Agency of the Czech Ministry of Health (project No. NT12156), the Ministry of Education, Youth, and Sports of the Czech Republic (Research Programs NPV II 2B06130 and 1M0510, Grant No. MSM0021620849, and Project MSM Grant No. 4977751303) and the University Centre for Energy Efficient Buildings (UCEEB) support IPv6.